

The official bi-monthly publication of Bhabha Atomic Research Centre



BARC newsletter

March-April 2023 ISSN: 0976-2108

▲ Radiation Metrology ▲ Antiproton Radiotherapy ▲ Industrial Hygiene & Safety ▲ Ionizing Radiations



Editor

Dr. S. Adhikari

Associate Editors

Dr. B.K. Sapra

Dr. Rosaline Mishra

Editorial Assistant

Shri Madhav N

Design & Creative Work

Shri Dinesh J. Vaidya

Shri Madhav N

Newsletter Committee

Chairman

Dr. A.P. Tiwari

Members

Dr. A.K. Nayak

Dr. G. Sugilal

Dr. V.H. Patankar

Dr. (Smt.) B.K. Sapra

Dr. L.M. Pant

Dr. Ranjan Mittal

Dr. (Smt.) S. Mukhopadhyay

Dr. K.P. Muthe

Dr. V. Sudarsan

Dr. A.V.S.S.N. Rao

Dr. S.R. Shimjith

Dr. Sandip Basu

Dr. Pranesh Sengupta

Dr. R. Tripathi

Member Secretary &

Coordination

Shri Madhav N




BARC Newsletter

March-April 2023

ISSN: 0976-2108





HEALTH, SAFETY and ENVIRONMENT

Relook into the Radiation Protection Philosophy

This thematic issue of BARC Newsletter encapsulates the vivid domain of basic research, in-house development and services executed by Health Safety & Environment Group (HS&EG) of BARC. By regular surveillance, Environmental Survey Laboratories of HS&EG ensure that the environments around the various nuclear facilities are safe and the radiation levels due to the operation of these facilities are negligible. Director, HS&EG also has a very important role as Emergency Response Director, to ensure proper monitoring and management of any radiological emergency in the country with support of the twenty six DAE Emergency Response Centres established in the country.

Over decades, HS&EG has gathered adequate scientific data to show that the radiation protection regulations are being adequately complied, so as to ensure that the risks due to radiation are negligible. However, it is to be pondered upon that the concept of Linear No Threshold Model (LNT) that is applied in radiation protection as a conservative measure, has resulted in undue efforts towards ALARA, thereby leading to increased financial implications at every stage. Additionally, the LNT model propagates the misconception that the risk of detrimental effects increases proportionately with increasing radiation dose, even at very low doses that are equivalent to the naturally occurring levels. This has made the public overly concerned and fearful about the biological effects of radiation, the recent example being the uncalled-for levels of panic in the event of Fukushima nuclear accident.

Data from many research studies have shown a lack of increased cancer rates in populations residing in high natural background-radiation areas (e.g., Kerala, India; Yangjiang China). On the contrary, there is an indication of the existence of hormesis. However, these are presently ignored by the policy making international bodies of radiation protection. Such preconceived concepts result in substantial medical, economic, and other societal impediments. Hence, it is important that radiation professionals and biologists should constantly review and publish research related to effects at low doses of radiation with a view of aiding a revisit to the concept of LNT.


Hearty congratulations to all the authors for their precious contributions that amplify the scientific and technological contents of the current issue. I also appreciate the focused approach of the Editorial Team members that has resulted in a time-bound compilation of this special HS&EG thematic issue which will be very informative for the readers.

Dr. D. K. Aswal


Director
Health, Safety and Environment Group
Bhabha Atomic Research Centre

This page intentionally left blank


Health and Safety at the core of Nuclear Programmes



We are delighted to bring out this issue on Health Safety & Environment Group (HS&EG), which has the service mandate of providing radiological and environmental surveillance for all radiation facilities in the realm of Department of Atomic Energy, and at times, other non-governmental institutions as well. This calls for constant upgradations in systems, techniques and computations that are utilized to meet the ever-increasing requirements of the radiation related applications. During the journey spanning over six decades, the Group has become self-reliant in achieving its goals. BARC, being the designated institute for ionizing radiation in the country, provides services related to standardization of radiation sources and calibration of radiation measuring equipments, by way of in-house developed primary and secondary standards. We have a completely indigenous personnel monitoring programme based on the $\text{CaSO}_4(\text{Dy})$ thermoluminescent phosphor, that includes the development of material, reading system and setting up of laboratories to cater to provide services to non-DAE institutions engaged in radiation related work. The important element of quality assurance is inbuilt at each stage of this programme. Several need based experimental analytical techniques have been established for assessment of radioactivity in various types of matrices. The internal monitoring assays and biosimetric techniques are at par with those available at well-established international institutes. These are not only used for routine monitoring of radiation workers, but also can be geared up for monitoring of personnel involved in radiation/nuclear emergency scenarios.



This compendium of twelve articles encapsulates the activities that are being undertaken in HS&EG with a view to give a flavor of the advancements being pursued towards technological developments, capacity building, and human resource development. Ongoing research and development studies towards medical applications such as radiotherapy and cytogenetics based clinical diagnosis have been touched upon. Interesting news snippets from around the world, based on published peer reviewed work, related to the theme of the issue have been included.



We are thankful to the members of HS&EG for their contribution to this thematic issue and appreciative of the meticulous effort put in by the reviewers in ensuring the quality of the contents. We are optimistic that the contents showcase a vivid state-of-art activities that will inspire the young researchers to come up with innovations to address the gap areas and contribute positively.

Dr. B. K. Sapra
RP&AD, BARC

Dr. Rosaline Mishra
RP&AD, BARC

- **FOREWORD:** Dr. D. K. Aswal **3**
- **ASSOCIATE EDITORS' MESSAGE:** Dr. B. K. Sapra and Dr. Rosaline Mishra **5**

RESEARCH AND DEVELOPMENT IN HEALTH, SAFETY AND ENVIRONMENT

- 1 Ionising Radiation Metrology: Role of BARC as a "Designated Institute" 9**
S. K. Singh, V. Sathian, Probal Chaudhury and D. K. Aswal
- 2 Improving TLD Personnel Dosimetry of Occupational Workers 14**
Munir S. Pathan, S. M. Pradhan and T. Palani Selvam
- 3 Self Reliance in Personnel Monitoring of Radiation Workers in India 18**
Kshama Srivastava, Rupali Pal and, A. K. Bakshi
- 4 Integrated Environmental Radiation Monitor with Autonomous Profiler for Underwater Radiation Monitoring 22**
Pratip Mitra, S. S. Salunkhe, T. Mukundan, Anisha Kumari, S. G. Gavas, P. R. Ninawe, Saurabh Srivastava, G. Priyanka Reddy, S. Garg, and A. Vinod Kumar
- 5 Programs Deploying Indigenous DTPS and DRPS 24**
Rosaline Mishra, R. Prajith, R. P. Rout, Jalaluddin S., A. T. Khan and B. K. Sapra
- 6 Antiproton Radiotherapy: A Monte Carlo-based Microdosimetric Approach 29**
Arghya Chattaraj and T. Palani Selvam
- 7 Classical & Molecular Cytogenetics as a Tool for Clinical Investigation of Genetic/Acquired Abnormalities 32**
Rajesh K. Chaurasia, Nagesh N. Bhat and B. K. Sapra
- 8 Dosimetry in Nanoparticles-aided Radiotherapy 37**
Nitin Kakade, Rajesh Kumar, S. D. Sharma, Rajesh K. Chaurasia, N. N. Bhat and B. K. Sapra
- 9 Nuclear Forensics Approach to Address Nuclear Emergencies & Radiological Preparedness 40**
S. Mishra, R. S. Sathyapriya, Amar Pant, Sukanta Maity, Sandeep Police, Amit Kumar Verma, R. K. Prabhath, Jis Romal Jose, Anilkumar S. Pillai and A. Vinod Kumar
- 10 Emergency Radio-bioassay Methodologies for First Responders & Public Approach 46**
Supreetha P. Prabhu, Priyanka J. Reddy, Sonal M. Wankhede, Soumitra Panda, Nanda Raveendran, Pramilla D. Sawant, Probal Chaudhury and M. S. Kulkarni
- 11 Overview of Activities Related to Industrial Hygiene and Safety 50**
Munish Kumar, Garima Singh, Praveen Dubey, Nitin V. Choughule and Alok Srivastava
- 12 Beryllium: Associated Hazards, Safety Evolution & Safety Limits 52**
Ankur Chauhan, Mahesh K. Kamble, Munish Kumar and Alok Srivastava
- 13 Certification Courses on Radiation Safety 55**
B. K. Sapra

NEWS & EVENTS

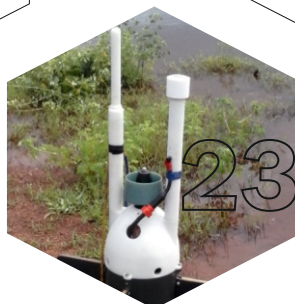
- **Reporting on Latest Global Developments in Health, Safety and Environment 57**
- **From Vision to Realization: The Success Story of 'APURVA' 58**
Vivek Shrivastav, Harish, Rajit Kumar, P. K. Mishra and Joe Mohan

RESEARCH HIGHLIGHTS

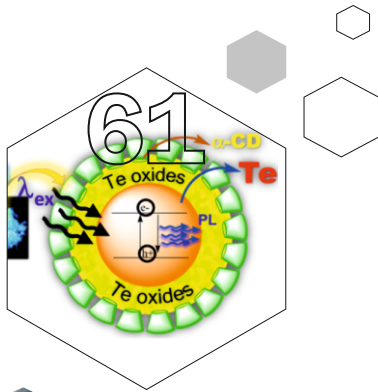
- **Tapping the Potential of Ionizing Radiations 61**
Apurav Guleria and S. Adhikari
- **A New Quantum-cosmological Model: The Source of Energy for Creation of the Universe 62**
Biswaranjan Dikshit

CONNECT

- **Reports from Conferences, Theme Meetings & Workshops 64**



C O N T E N T S



FORTHCOMING ISSUE

Applications of CFD

⁽ⁱⁱ⁾ Chemical Engineering, Materials Science and Safety

- Hydrogen Recombiner - Benchmarking & Performance Evaluation.
- Artificial Compressibility Method for Incompressible Flow Solver.
- Safety Evaluation for Nisargruna Biogas Plant - Fire, Explosion & Toxicity.
- Numerical Simulations to Understand & Evaluate Spread of Aerosols.
- Short notes on journal articles published in CFD domain by BARC.



This page intentionally left blank

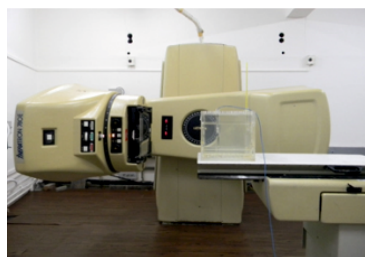
Radiation Metrology

1

Ionizing Radiation Metrology: Role of BARC as a "Designated Institute"

S. K. Singh¹, V. Sathian¹, Probal Chaudhury*¹ and D. K. Aswal²

¹Radiation Safety Systems Division; ²Health, Safety and Environment Group, Bhabha Atomic Research Centre, Trombay – 400085, INDIA



Tele-cobalt calibration facility

ABSTRACT

BARC is the DI for ionizing radiation and represents India in the consultative committee of CIPM, IAEA and APMP. It realizes, establishes, maintains, and upgrades the national measurement standards & calibration facilities for ionizing radiation measurements which has applications in medical, environmental, radiation protection, industrial and scientific research. The activities carried out at BARC are related to dosimetry for radiotherapy, brachytherapy, nuclear medicine, radiation processing, radiation protection, calibration of radiology instruments etc. BARC is in the process of implementing Quality Management System as per ISO/IEC:17025 and progressing for an international peer review.

KEYWORDS: Dosimetry, Radiotherapy, Radiation protection, Radiopharmaceutical, Nuclear medicine, Radiation metrology

Introduction

Metrology is the science of measurement which ensures that measurements are consistent, comparable, accurate and have stated level of uncertainty, in any field of science and technology. Metrology assures the measurement results, required in the important areas like national/international trade, health, safety, environmental monitoring, food safety, regulatory and law enforcement. These measurement results are linked to a national standard (primary/reference measurement standards) through a documented unbroken chain of calibrations, each contributing to the measurement uncertainty. The responsibility of maintaining measurement standards and its dissemination lies with the National Metrology Institute (NMI) or Designated Institute (DI) of that country. In India, CSIR-NPL is the NMI whereas Bhabha Atomic Research Centre (BARC) is the DI for Ionizing Radiation (IR). Similarly, responsibility of maintaining international measurement standards and its dissemination lies with International Bureau of Weights and Measures (BIPM) which is an international organization established by the Metre Convention, through which Member States act together on matters related to measurement science and measurement standards. The activities of BIPM are supervised by International Committee for Weights and Measures (CIPM).

As the "Designated Institute" (DI) for ionizing radiation, BARC represents India in the consultative committee of CIPM, International Atomic Energy Agency (IAEA) and regional metrology organization i.e., Asia Pacific Metrology Programme (APMP). Additionally, BARC is also recognized as Secondary Standards Dosimetry Laboratory (SSDL) for India by IAEA, in collaboration with World Health Organization (WHO). Therefore, as the DI, the statutory obligation of BARC is to realize, establish, maintain, and augment the national measurement standards & calibration facilities for ionizing radiation measurements which has applications in medical,

environmental, radiation protection, industrial and scientific research. Accordingly, BARC has developed, established, and is maintaining various standards (primary, secondary, working and field standards) for ionizing radiation, covering the measurements of alpha, beta, gamma, X rays and neutrons. The degree of equivalence of these measurement standards are established through participation in international intercomparisons conducted by Consultative Committee for Ionizing Radiation (CCRI), BIPM, Asia Pacific Metrology Program (APMP) and IAEA. Participating in these comparisons (i) demonstrates the international equivalence of national measurement standards, (ii) enables exchange of knowledge, information, and experience at the international level and (iii) contributes to global decision-making concerning metrological developments. BARC also participates in the postal quality audit, conducted by IAEA, for assessment of the quality of service provided by it.

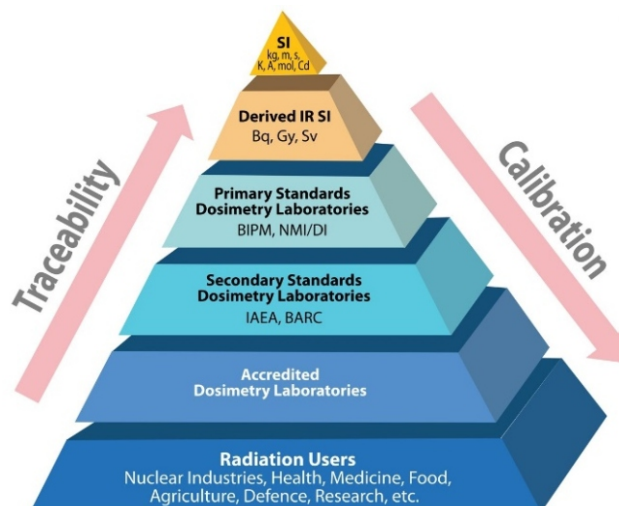


Fig.1: Hierarchy of traceability chain (present status of radiation dosimetry in India).

*Author for Correspondence: Probal Chaudhury
E-mail: probal@barc.gov.in



Fig.2: a) Tele-cobalt calibration facility, b) Typical cylindrical ionization chamber, c) Parallel plate ionization chamber.

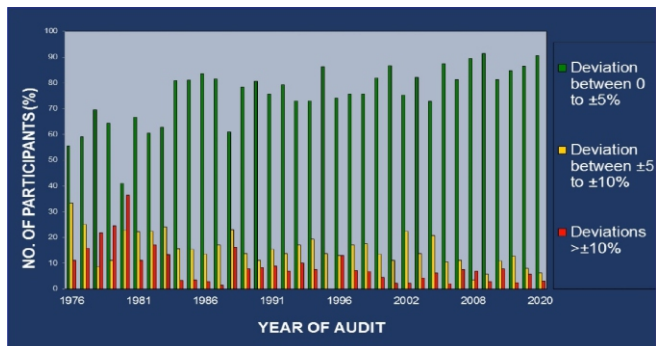


Fig.3: Dosimetric Quality Audit Programme conducted by SSDL-BARC.

BARC disseminates the ionizing radiation measurements to the end users in the country by means of providing traceable calibration services. The traceability chain of radiation measurement is a vertical concept (as shown in Fig.1: present status of radiation dosimetry in India, as per IAEA terminology). In the hierarchy, the SI units of a measurement have highest accuracy and are realized by international measurement standards. National measurement standards, maintained in a National Metrology Institute (NMI) or the DI is compared with these international standards. The result of such comparisons, together with the degree of equivalence and uncertainty of the national standard are stated and available in the BIPM key comparison database at www.bipm.org/kcdb. The national standards serve as a reference for calibration of users standards with lower precision or higher uncertainty. At each stage in the traceability chain, a certain degree of precision is lost.

The activities carried out at BARC are synonymous to the activities of CCRI which is distributed in three sections of CCRI namely CCRI Section I (Dosimetry): X- and gamma rays, charged particles; CCRI Section II (Radioactivity Measurement): Measurement of radionuclides and CCRI Section III (Neutron): Neutron measurements. In BARC, the responsibility of looking after the activities of the DI lies with Radiation Standards Section (RSS), Radiation Safety Systems Division (RSSD), Health Safety & Environment Group (HS&EG). Some of the important activities of BARC as the DI, are discussed here.

Activities related to ionizing radiation dosimetry

Dosimetry of ionizing radiation deals with application related to medicine (treatment of cancer and diagnostic radiology), radiation protection and radiation processing. In medicine (radiotherapy and brachytherapy), accurate dosimetry is very important for optimization of cancer treatment. It is also important for radiation protection of occupational workers (working in various radiological and nuclear facilities) and patients undergoing diagnostics examinations (radiology). Similarly, dosimetry is also important for radiation processing like blood irradiation, sterilization of health care products, processing of food & agriculture products, etc.

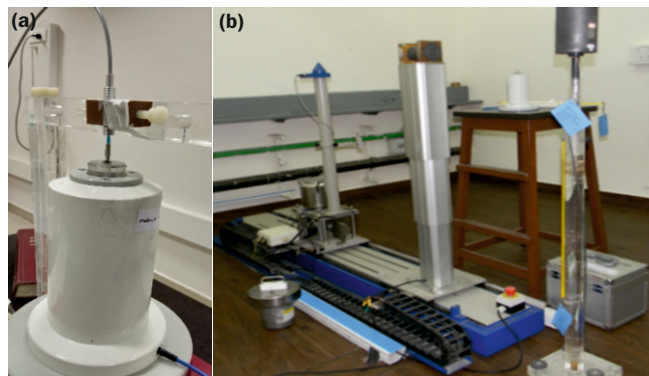


Fig.4: a) Well type ionization chamber, b) BARC brachytherapy calibration facility.

Dosimetry for radiotherapy

Radiotherapy, an important tool for cancer cure, requires the highest level of accuracy (within $\pm 5\%$) to optimize the absorbed doses delivered to the tumour, sparing surrounding normal tissues. In India, currently, there are over 500 radiotherapy institutes having more than 230 telecobalt and 350 accelerator units. To ascertain the stated level of accuracy of dose delivery in India, SSDL-BARC has established a telecobalt facility (Fig.2a), that maintains measurement standards (ionization chamber, Fig.2b), calibrates dosimeters of hospitals and conducts TLD postal dose quality audit for radiotherapy centres. Cylindrical ionization chambers (Fig.2b) and parallel plate ionization chambers (Fig.2c) of nominal volume about 0.6 cc are generally used in dosimetry of external beam therapy. SSDL-BARC maintains a reference standards ionization chamber for absorbed dose to water which is calibrated at BIPM with a relative standard uncertainty of 0.2%. The user (hospitals) chambers are calibrated against this standard, in terms of absorbed dose to water as per the IAEA TRS 398 [1] protocol. This calibrated chamber is used by hospitals/radiotherapy centres to perform dosimetry of their beam qualities, used for radiotherapy. Annually, ~ 300 such chambers (Secondary Standard Dosimeters) are calibrated at SSDL-BARC. SSDL-BARC also maintains reference standard ionization chamber for air Kerma at ^{60}Co energy and provides calibration against this standard.

An independent verification of the quality of the dosimetry practices in hospitals / radiotherapy centres is also carried out by RSS, RSSD, BARC through postal dose quality audits. Since 1976, SSDL-BARC has been conducting TLD postal dose quality audits leading to improvement in the accuracy of the dose delivery capability at radiotherapy centers over a period of 5 decades (Fig.3).

Dosimetry for Brachytherapy

Brachytherapy dosimetry generally involves use of Well type ionization chambers (Fig. 4a) of nominal volume of around 200 cc to determine the brachytherapy source strength. Calibrations of these dosimeters are carried out in terms of

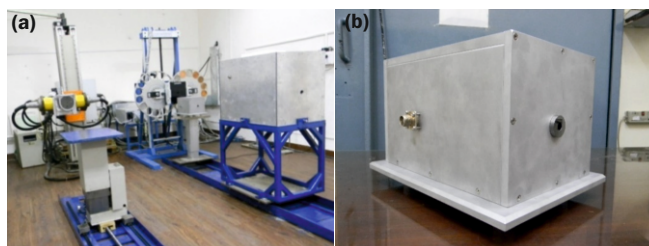


Fig.5: a) X-ray calibration facility, b) Free air ionization chamber for 20-150 kV X-rays.

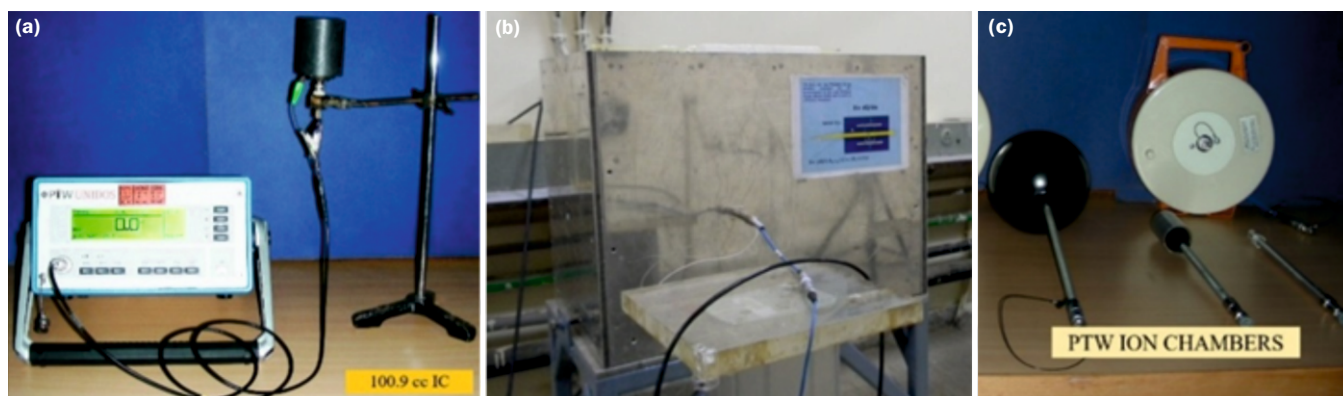


Fig.6: a) 100.9cc graphite ion chamber, b) Free air ionization chamber (upto 300 kV), c) Working standards for radiation protection.

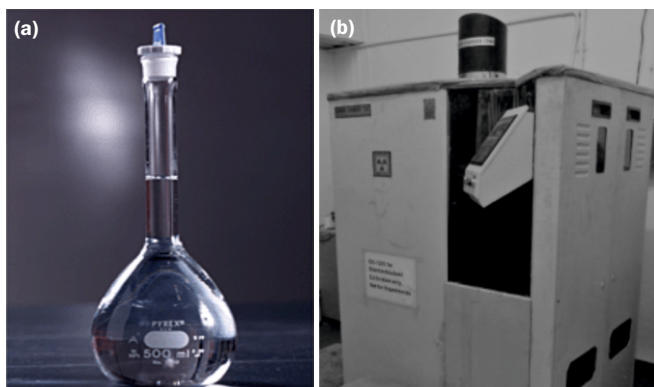


Fig.7: a) Fricke solution in a standard volumetric flask; b) Gamma Chamber 1200.

reference air Kerma rate (RAKR) for ^{192}Ir and ^{60}Co energy as per IAEA TECDOC 1274 recommended procedure [2]. BARC has developed a reference standard (graphite walled ionization chamber having a nominal volume of 1000 cc, Fig.4b) for RAKR measurement and calibration of well type ionization chambers. Annually around 100 well type ion chambers are calibrated at ^{192}Ir based brachytherapy calibration facility (Fig.4b) of BARC. In addition, onsite well type chamber calibration is also carried out for ^{60}Co HDR brachytherapy sources based on the request from institutions.

Dosimetry for calibration of radiology instruments (20-150 kV X-ray diagnostic beam qualities)

SSDL-BARC has established nineteen diagnostic beam qualities at its X-ray calibration facility (Fig.5a), as per recommendations of IEC 61267 [3] and the IAEA protocol TRS-457 [4]. These beam qualities are established using the free air ionization chamber (Fig.5b), a primary standard. Traceable calibration is provided at these beam qualities for users.

Dosimetry for Radiation Protection

Radiation monitors (radiation survey meters, area gamma monitors, environmental monitors, and pocket dosimeters) are backbone for all the radiological and nuclear installations, for the safety of radiation workers. Periodic calibration of these radiation monitors is required to ensure that they are working properly and are suitable for their intended use/purpose. BARC has developed and is maintaining a cavity ionization chamber (Fig.6a) and a Free air ionization chamber (Fig.6b) as national standard for gamma and X-ray dosimetry, respectively. Commercially available PTW ion chambers (Fig.6c) are calibrated against reference standards and are used routinely for calibration of users radiation monitors and radiation fields. Radiation monitors, installed in almost all the radiological facilities of BARC, are calibrated for dose rate range $1 \mu\text{Gy/h}$ ($\sim 1 \mu\text{Sv/h}$) to 100 Gy/h

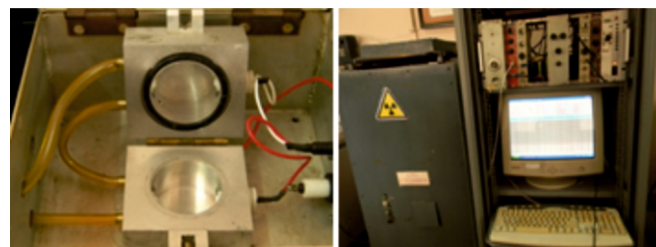


Fig.8: Photograph of $4\pi\beta$ (PC) - γ coincidence counting system.

($\sim 100 \text{ Sv/h}$). Annually, more than 300 radiation monitors are calibrated at RSS, BARC.

Role of BARC in establishment of calibration laboratories and their traceability

BARC provides measurement traceability, technical support, and guidance for establishment of radiation monitors calibration laboratories by government bodies and private agencies. Currently, more than 10 NABL accredited/AERB recognized calibration laboratories are established with the help from BARC which are spread across the country. Three of them are within DAE (IGCAR, Kalpakkam, ECIL, Hyderabad and BRIT, Vashi), one in defence (Defence Laboratory, Jodhpur) and the remaining from the private sectors.

Dosimetry for Radiation Processing

Now a days, radiation processing technologies are very widely used in medical (blood irradiation) and industrial applications like sterilization of health care products, processing of food & agriculture products (for disinfection, shelf-life extension, sprout inhibition, pest control, sterilization, etc.) and materials modification (such as polymer cross linking, chain scission and gemstone colorization, etc). Proper dosimetry is the backbone of success of these high dose applications (few Gy to kGy range). BARC maintains Fricke dosimeter (Fig.7a) as a primary reference standard, according to ISO/ASTM 51026 [5], in this field.

Gamma chamber (Fig.7b), used for irradiation and other R&D applications in this field, are calibrated using the Fricke dosimetry system; as per ISO/ASTM 52116 standard [6]. BARC also maintains and uses other dosimeters like Alanine ESR, glutamine (indigenously developed), etc. for dosimetry in the field of radiation processing. These standards provide results with uncertainty better than 3-4% at coverage factor $k=1$.

Activities related to Radionuclide measurements (CCRI Section II):

Metrology in Nuclear Medicine

There has been a tremendous surge of usage of radioisotopes in medical applications especially in the field of

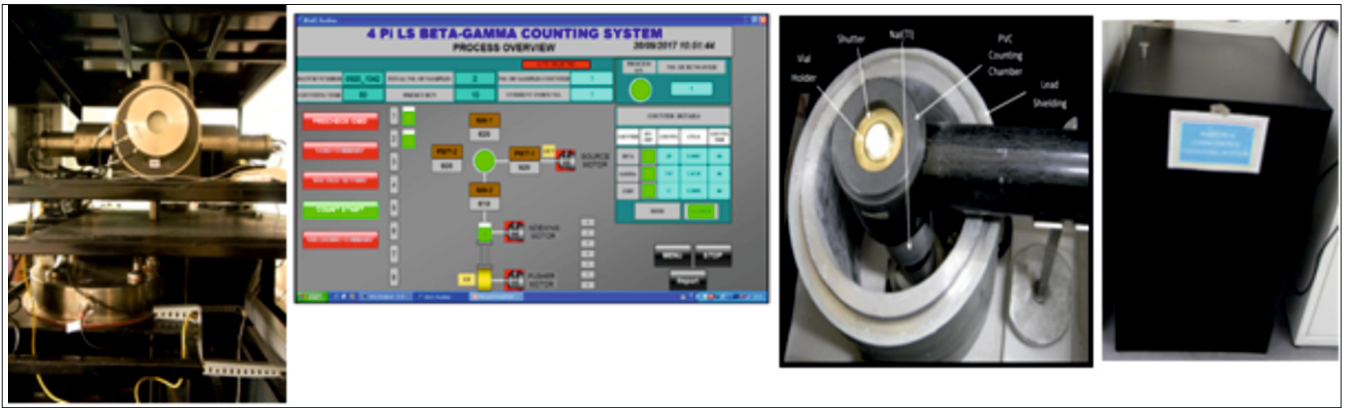


Fig.9: Photograph of 4πβ (LS) - γ coincidence counting system.

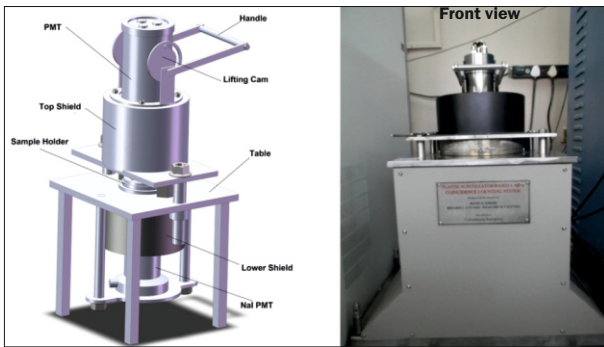


Fig.10: 4πβ (PS) - γ coincidence counting system.

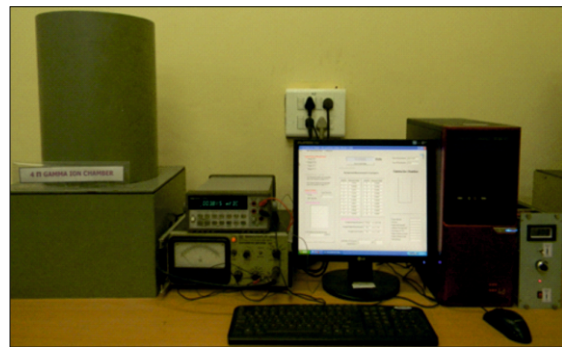


Fig.11: Photograph of 4π re-entrant pressurized gamma ionization chamber.

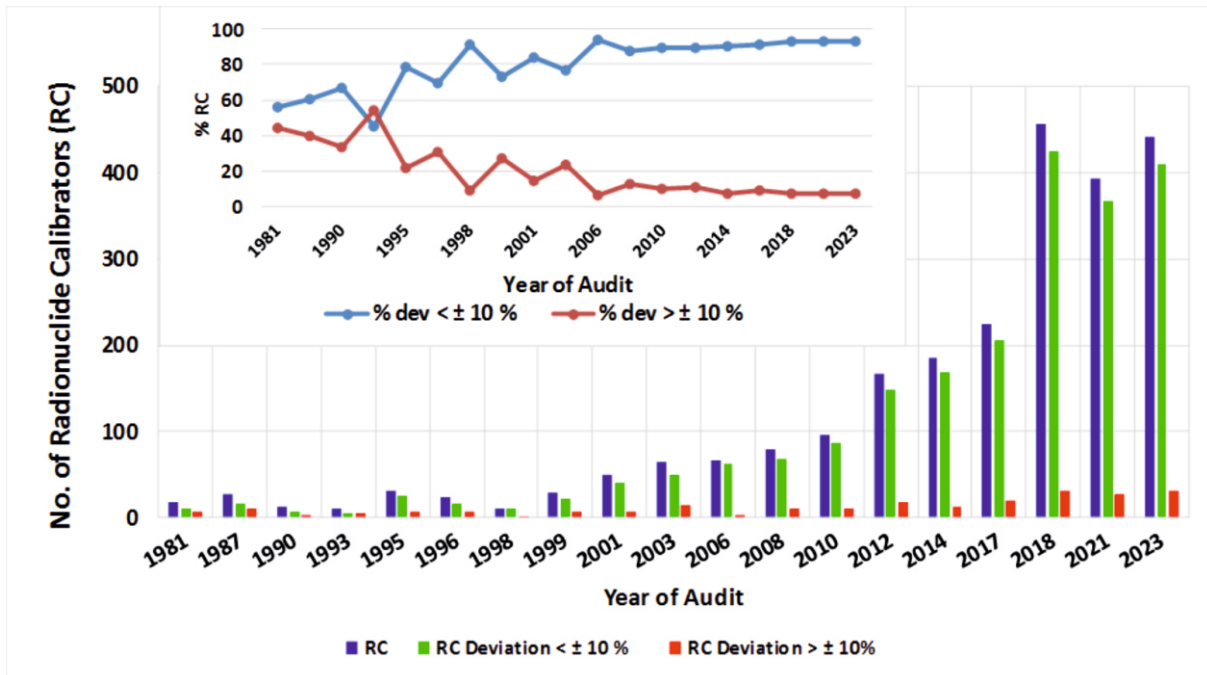


Fig.12: Summary of ¹³¹I National Audit results conducted from 1981 to 2023.

nuclear medicine. One such application is targeted therapy where the liquid form of radioisotope is administered orally or intravenously to the patients to specifically target the diseased tissue while sparing the surrounding healthy tissue. Therefore, it becomes very important to measure the activity of radioisotope, to be administered, accurately so that the patient receives optimum dose with minimal risk.

The safety and efficacy of the radiopharmaceutical (RP) depends on various factors and on the ability of the clinic to accurately determine the amount of radioactivity which determines the dose to the patient. Prior to administering the RP to the patient, the activity of the RP is measured at the

nuclear medicine centres using the radionuclide calibrators (RC). BARC has been conducting national audit programme biannually for activity measurements with RC over four decades (since 1979), Quality audit programmes (QAPs) help to ensure that the RCs are working satisfactorily so that the activity of the radiopharmaceutical measured before administering to patients is within the acceptable limits of 10% from the prescribed dose. The results of all the audits conducted over four decades, since 1979 to 2021 for Dose calibrators for ¹³¹I are shown in Fig.12 which shows an encouraging result, as the number of RCs whose deviation greater than ± 10% has declined tremendously over the years.



Fig.13: a) Manganese sulphate bath system, b) Thermal stag, c) Portable Thermal neutron water jig.

BARC ensures accurate activity measurements by means of various primary and secondary standards developed and maintained for radioactivity measurements.

The primary standards based on coincidence technique for activity measurements are a) Proportional counter based $4\pi\beta$ (PC)- γ coincidence counting system (Fig.8) and b) Liquid scintillation based $4\pi\beta$ (LS)- γ coincidence counting system (Fig.9) and c) Plastic scintillation based $4\pi\beta$ -(PS)- γ coincidence counting system (Fig.10).

The secondary standard for activity measurements for gamma emitting radionuclides is the re-entrant pressurized gamma ionization chamber (GIC) that has an excellent stability (Fig.11). The typical uncertainty of activity measurements with GIC is about $\pm 3\%$ at $k=2$. The GIC measurements are traceable to national and international standards.

Activities related to Neutron measurements (CCRI Section III)

Neutron measurements in the country are traceable to the national standards developed, established, and maintained at RSS, BARC. The primary standard for the neutron source yield measurement is the manganese sulphate bath system (Fig.13a) while that for thermal neutron fluence rate is the thermal stag (Fig.13b) whose fluence rate is traceable to international laboratories in terms of gold and manganese cross section. A water jig with a $5\text{Ci }^{241}\text{Am-Be}$ neutron source is regularly used for the onsite testing and calibration of start-up counters, DNM detectors and ion chambers used in power reactors to ensure the traceability to the national standards.

Quality management system

Currently, BARC is in the process of implementing Quality Management System as per ISO/IEC:17025 [7] and progressing for an international peer review, as required by CIPM-Mutual Recognition Arrangement (CIPM-MRA), for getting our Calibration Measurement Capabilities (CMC) published in the Key Comparison Database of BIPM (KCDB) so that calibration certificates issued by BARC would have global acceptability for international trade/commerce.

Conclusion

An overview of the metrological activities of ionizing radiation and the standards maintained per se at BARC are summarized briefly in the present paper. The international

equivalence of the radiological standards maintained at BARC has been well-established with the other national metrology institutes around the world as well as demonstrated traceability of measurements to international system (SI) through regular participation in the intercomparison programmes organized by BIPM, IAEA and APMP. In addition, metrological traceability of measurements in the country at the end user level too is very well established by providing calibration services and through conducting regular audit programmes for various radiation units. Summing up it can be ascertained that BARC is able to meet satisfactorily the demands in the field of nuclear measurements and corroborated measurement traceability in India. In the recent years as a DI, BARC is endeavouring and expanding the field of ionizing radiation metrology, to address the requirements of stakeholder such as radiotherapy centres, nuclear medicine centres, nuclear reactors and research, accelerators and radiation processing industries etc. The measurement traceability ascertains confidence in the crucial results needed for drug, device development and marketing, therapy planning and efficacy, disease screening, patient safety, and industry support for now and into the future.

References

- [1] IAEA TRS 398, Absorbed Dose Determination in External Beam Radiotherapy: An International Code of Practice for Dosimetry based on Standards of Absorbed Dose to Water, IAEA, 2006.
- [2] IAEA TECDOC 1274, Calibration of photon and beta ray sources used in brachytherapy Guidelines on standardized procedures at Secondary Standards Dosimetry Laboratories (SSDLs) and hospitals, IAEA, 2002.
- [3] IEC 61267, International Electrotechnical Commission, -Medical Diagnostic X-ray equipment, Radiation Conditions for use in the Determination of Characteristics, Geneva, 2005.
- [4] IAEA TRS 457, International Atomic Energy Agency, Dosimetry in Diagnostic Radiology: An international code of practice, 2007.
- [5] ISO/ASTM 51026, Practice for using the Fricke dosimetry system, 2015.
- [6] ISO/ASTM 52116, Practice for dosimetry for a self-contained dry storage gamma irradiator, 2013.
- [7] ISO/IEC:17025, General requirements for the competence of testing and calibration laboratories, 2017.

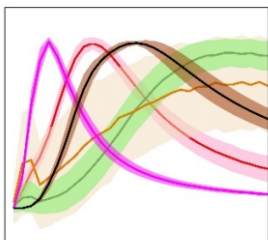
Artificial Intelligence

2

Improving TLD Personnel Dosimetry of Occupational Workers

Munir S. Pathan, S. M. Pradhan and T. Palani Selvam*

Radiological Physics and Advisory Division; Health, Safety & Environment Group, Bhabha Atomic Research Centre, Trombay – 400085, INDIA



Different Classes of Glow Curves of $\text{CaSO}_4:\text{Dy}$

ABSTRACT

Thermoluminescence dosimeter (TLD) based personnel monitoring is widely employed for recording occupational radiation doses. TLDs used in routine monitoring are subjected to diverse field conditions, including processing and handling that result in variability in the glow curve (GC) shape. The distortions in the shape of GC may lead to variations in the estimated dose. The present work is focused on: (a) investigation and classification of anomalies in GC using machine learning algorithms, (b) development of an artificial intelligence (AI) based decision support system for screening GCs, and (c) providing a predictive maintenance system for the TLD badge reader.

KEYWORDS: Personnel monitoring, Glow curves, Machine learning

Introduction

Luminescence-based dosimeters have been used in radiation dosimetry for decades. The property of emission of luminescence signal proportional to received radiation exposure makes the luminescence dosimeters suitable for radiation personnel monitoring as well as other radiation dosimetry-related applications. Hence, Thermoluminescence (TL)-based dosimeters are one of the most commonly used dosimeters in personnel monitoring of occupational workers. In India, about 0.25 million occupation workers are monitored for external exposure to ionizing radiation (beta, gamma and x-rays) using $\text{CaSO}_4:\text{Dy}$ -based TLD badges [1-3]. Presently, 16 TLD personnel monitoring laboratories provide TLD services across our country. The TLD badges are read using semiautomatic TLD badge readers that utilize hot N_2 -gas-based clamped heating for stimulation of TL dosimeters [4].

The Glow Curves (GCs) recorded in routine measurements may not always show the ideal characteristic shape. Various types of anomalies may appear from various sources like dosimeter, reader, zero dose signal, etc. At lower doses, the non-radiation-induced TL signal, originating due to the black body radiation from heated reader components and the dark current from the photomultiplier tube (PMT), causes the deviation in the shape of GC [5, 6].

The TLD reader-related factors such as variation in heating rate, cross-talk due to sequential heating [7], etc. may lead to deformities in the shape of GC. Other factors like dirt/dust/oil on the TL element, the coloration of the TL element, corrosion of the TLD card, aberration due to scratch/stress on the TL element, etc. also cause deformities in the shape of GC [8]. Hence, in routine personnel monitoring, screening of GCs is a mandatory procedure before dose computation.

Recent studies on the application of Machine Learning (ML) for anomalous GC identification, and estimation of

elapsed time after exposure for $\text{LiF}:\text{Mg}:\text{Ti}$ -based TL dosimeters have shown an impressive improvement in dosimetric outcomes [9-11]. In this work, we demonstrated the applicability of different ML algorithms for the identification of abnormal GCs as well as the classification of GCs based on associated abnormalities for the $\text{CaSO}_4:\text{Dy}$ -based personnel monitoring system. Further, an R-shiny based web-application is developed to deploy the ML models for routine TLD personnel monitoring. With implementation of ML algorithm about 99% classification accuracy with minimization of subjectivity and increase in the throughput of personnel monitoring laboratory can be achieved.

Materials and Methods

TLD personnel monitoring system

The TLD Badge comprises a TLD card and Cassette. The TLD card consists of three $\text{CaSO}_4:\text{Dy}$ -Teflon discs of thickness 0.8 mm and diameter 13.3 mm, and are mechanically clipped to a Nickel-plated Aluminium plate. The TLD cards are loaded in the cassette with filters to compensate for the energy dependence and to provide a gross estimation of energy/type of radiation [12]. To estimate the dose, the TLD badges are read using a semiautomatic TLD badge reader. Thermal stimulation is delivered using hot N_2 gas-based clamped heating to obtain the TL signal from the pre-irradiated dosimeter.

Dataset preparation

A dataset of ~3000 experimental GCs comprising the normal GCs, residual TL GCs, annealed background GCs, GCs with spikes, and delayed/early peak GC is prepared. The number of anomalous GC in the experimental dataset is limited due to the seldom occurrence of anomalies in routine monitoring, ~1500 GCs with anomalies are generated by simulation. For the simulation of GCs, the time-temperature profile of the TL element is simulated. The hot N_2 gas incident on the TL-element delivers heat to the TL element via forced convection. During the heating cycle, the TL element loses some heat to the surroundings due to the finite temperature

*Author for Correspondence: T. Palani Selvam
E-mail: pselvam@barc.gov.in

difference. The heat exchanges between hot gas, TL element, and surrounding is given in the following rate equation [13].

$$\frac{dT_d}{dt} = \frac{1}{C_d} \left(\frac{dH_d}{dt} - \frac{dH_s}{dt} \right) \quad (1)$$

Where dH_d/dt is the rate of heat transferred from hot gas to disc ($J s^{-1}$), dH_s/dt is the rate of heat transferred from heated disc to surrounding ($J s^{-1}$) and C_d is heat capacity of the disc ($J^\circ K^{-1}$).

$$\frac{dH_d}{dt} = P_d (T_g(t) - T_d(t)) \quad (2)$$

$$\frac{dH_s}{dt} = P_s (T_d(t) - T_{sr}) \quad (3)$$

Where $T_g(t)$ is the temperature of the gas, $T_d(t)$ is the temperature of the disc at time t ($^\circ K$), T_{sr} is temperature of surrounding ($^\circ K$), P_d is the thermal conductance of heated gas and disc interface ($J^\circ K^{-1} s^{-1}$), P_s is thermal conductance of disc and surrounding interface ($J^\circ K^{-1} s^{-1}$). Using the above equations (1 - 3), the time-temperature profile of the disc can be given by the following equation

$$\frac{dT_{disc}(t)}{dt} = \alpha(T_g(t) - T_d(t)) - \alpha'(T_d(t) - T_{sr}) \quad (4)$$

Where, $\alpha = P_d/C_d$ (s^{-1}), $\alpha' = P_s/C_d$ (s^{-1}), α' represents heat loss to surrounding.

Further, equation (4) is modified to account for radiative heat loss and gain via black body radiation from TL element to surrounding and surrounding to TL element respectively [14].

$$\frac{dT_{disc}(t)}{dt} = \alpha(T_g(t) - T_d(t)) - \alpha'(T_d(t) - T_{sr}) - \lambda_1 T_d(t)^4 + \lambda_2 T_{sr}^4 \quad (5)$$

Where T_{sr} is the temperature of the surrounding ($^\circ K$), λ_1 and λ_2 are constants having dimensions ($^\circ K^{-3} s^{-1}$). The rate equation given by equation (5) is solved numerically by the finite difference method to obtain the temperature profile of the TL element. The glow curve of $CaSO_4:Dy$ was simulated using the Randall-Wilkins model as given in equation (6) [15].

$$I(t) = -\frac{dn}{dt} = cn^b fe \left(-\frac{E}{kT_{disc}} \right) \quad (6)$$

Where $I(t)$ is TL intensity at time t , n is number density of trapped carriers (m^{-3}), b is order of kinetics, c is reader response factor (counts/TL intensity), E is activation energy (eV), f is frequency factor/pre-exponential factor (s^{-1}), k is Boltzmann constant ($J^\circ K^{-1}$). The ten-trap model is used for the simulation of the composite GC for clamped/exponential heating [16]. The simulated composite GC (blue line) and contributing peaks (dashed lines) along with experimental GC (pink line + markers) are shown in Fig.1.

The anomalous GC of early/delayed peak are simulated by altering the temperature profile by varying the value of the parameter “ α ”. Fig.2 shows the different types of GCs and variability in their shapes.

ML model tuning and evaluation

Supervised machine learning is the process of training a function/s to map an input to the output using the known output for a supplied set of inputs. It improves itself iteratively by comparing the estimated output to the desired ones and accordingly adjusting the parameters. In present work, we investigated three competing supervised learners for the

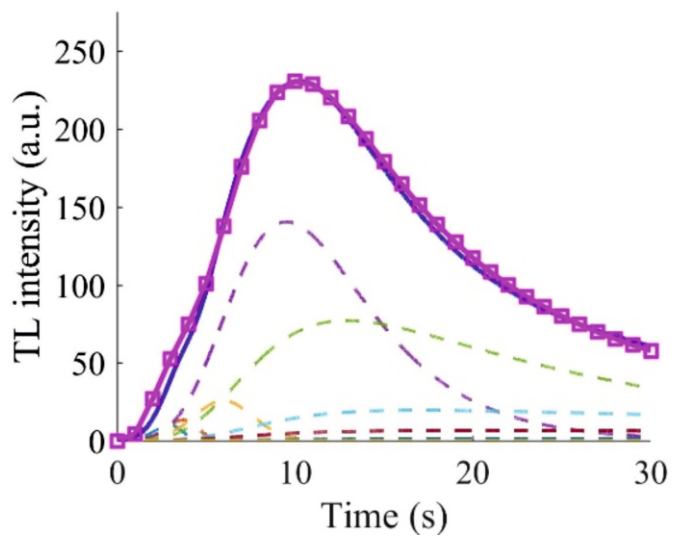


Fig.1: Simulated and experimental GC.

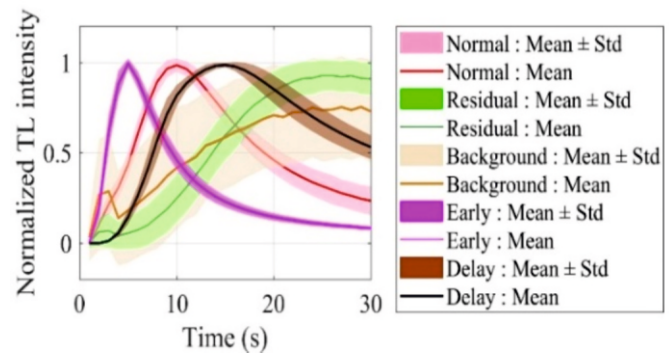


Fig.2: GCs of different class from dataset.

classification of abnormal GCs, Viz. Artificial Neural Network (ANN), Support Vector Machine (SVM), and Random Forest (RF). The Hyperparameters of ANN such as activation function, number of nodes/layers, learning rate, optimization method, etc. are tuned to obtain optimum classification accuracy. To obtain the accurate RF model, number of parameters (features) to be sampled randomly for each decision tree and the number of trees to be grown under a forest is tuned. Similarly, the SVM algorithm is optimized by tuning parameters like a penalty, margin, kernel, etc. The accuracy of classification of GCs is compared for all optimized ML models for selection of best of three algorithms.

Deployment of ML model

The selected ML model is deployed into routine personnel monitoring by integrating it with a graphical user interface (GUI) using R-shiny. The TLD badge reader software provides the GC files in *.txt or *.xlsx file format, these files consist of the cumulative TL counts at every second, N_2 -gas temperature, personnel number, TLD card ID, disc position and card position. These GC files are imported into the supplied as input after pre-processing to ML model. The models returns a data frame of class and probabilities of GCs. To diagnose the health of the TLD badge reader, the average probability of all normal GCs and a pie chart of the proportions of each class are generated. In addition to the GC screening, the software provides the dose calculation tool that searches and averages the control/background TL counts for a period of use of a particular institution, calculates net TL counts, and estimates dose as well as the type of radiation to which the TLD badge is exposed.

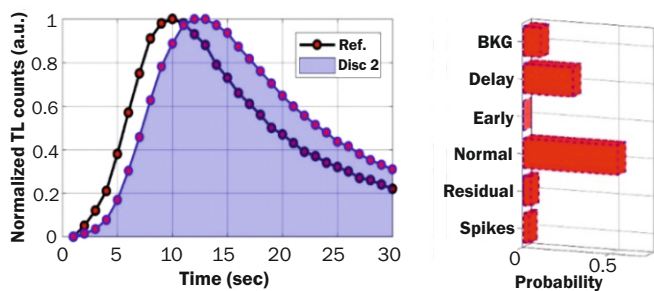


Fig.3: Delayed peak GC and its class probabilities.

Table 1: Comparison of the accuracy of algorithms.

Models	ANN	SVM	RF
Accuracy	0.9666	0.9611	0.9905

Results and Discussion

Identification of anomalous GC

The GCs are classified into six classes as per the type of GC and associated anomaly, viz. Normal GC, Annealed background, Residual GCs, Early peak GC, Delayed peak GC, and spikes in GC. The performance of each algorithm is analysed using a set of parameters as shown in Table 1.

The overall accuracy achievable for the test dataset from the RF algorithm is higher than that of ANN and SVM. Therefore, RF model is used for the development of application for screening of GCs. The RF model provides the probability of each class for a particular GC, the probability of a normal class between 0.8 and 1 is considered to be acceptable. If the probability of the normal class is less than 0.7, then significant deviation from the standard GC shape are observed. Fig.3 shows an example of normal GC with a slightly delayed peak indicating insufficient heating of the TL element, even though the GC is classified as normal GC, the probability of normal class is less than 0.75 and the probability of delayed peak is significant.

Further to validate the effectiveness of the use of probability as an indicator of TLD reader health, an experiment was conducted by decreasing the flow rate of N₂-gas by 20 %, and TLD cards exposed to various doses are read on such TLD readers. The average class probabilities of GCs of each disc from a normal TLD reader and faulty (simulated) TL are depicted in Fig.4. For normal TLD badge reader, the average probability of the normal class of GC is between 0.8 – 1 and for the rest of the classes it is negligible for all three discs. Similarly, for faulty TLD reader, the average probability of a normal class of GC is less than 0.7, indicating a major deviation in the shape of GCs. The average probability of delayed peak is significant, which indicates probable under-heating of TL elements.

AI-based GC screening tool

The screenshot of GUI is shown in Fig.5, the sidebar panel provides browsing, reader software selection, TL count threshold, probability threshold and combined ML + analytical decision [8] making options. The main window consists of several tabs, Viz. graphical, tables, analysis, summary, dose from GC and dose from dump. The graphical tab shows information related to TLD card like personnel number, card ID and readout date and three figures showing the plot of GC along with the class of GC, total TL counts and probability of normal class.

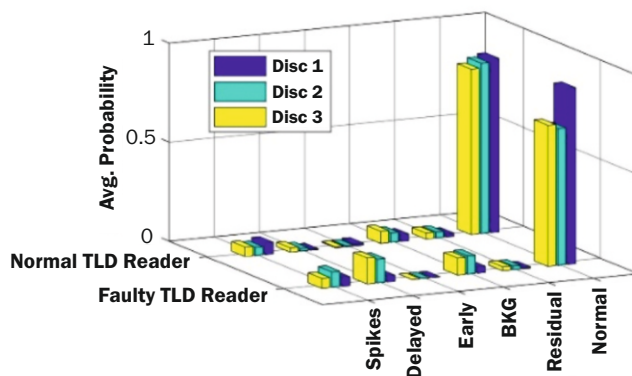


Fig.4: Mean class probability of normal GCs.

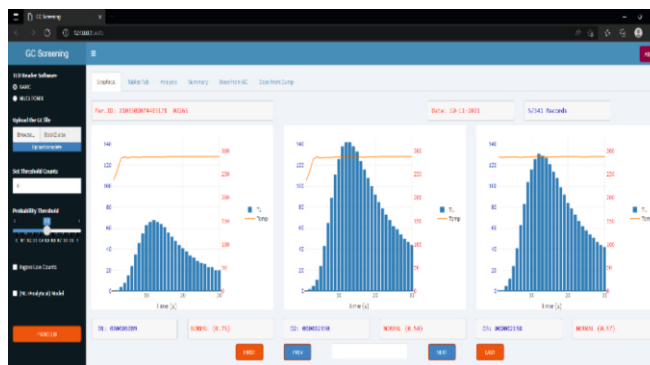


Fig.5: Screenshot of the graphical tab of GC screening software.

Conclusion

In routine personnel monitoring, thousands of cards are processed monthly and it needs to be ensured that the dosimetric accuracy is not compromised. The dosimetric accuracy mostly relies on the accuracy of the signal i.e. GC. With the continuous increase in the number of monitored occupational workers, there is a need for automation to increase the throughput of TLD personnel monitoring laboratories without compromising dosimetric accuracy. Therefore, the application of ML algorithms into the GC-screening process which is one of the mandatory steps in TLD processing will surely improve the throughput of the laboratory. Also, with human intervention, the variability in decisions about the correctness of GC results in subjectivity. The subjectivity can also be minimized with the use of AI-based algorithms. Further, the use of a probabilistic approach gives an insight into the anomaly as well as provides a health diagnosis of the TLD reader which serves as predictive maintenance system.

References

- [1] K .G. Vohra, et al., A personnel dosimeter TLD badge based on CaSO₄: Dy Teflon TLD discs. Health Physics, 1980, 38(2), 193-197.
- [2] A. S. Pradhan, and R. C. Bhatt, Metal filters for the compensation of photon energy dependence of the response of CaSO₄:Dy - Teflon TLD discs. Nuclear Instruments and Methods, 1979, 166(3), 497-501.
- [3] A. S. Pradhan, B. C. Bhatt and K. Ayyangar, Development of CaSO₄: Dyteflon discs thermoluminescence dosimetry. in Proceedings of the national symposium on thermoluminescence and its applications, Kalpakkam, February 12-15, 1975, 1976.
- [4] M. S. Kulkarni, P. Ratna and S. Kannan, A new PC based semi-automatic TLD badge reader system for personnel monitoring. in Proceedings of International Radiation Protection Association Conference, Hiroshima, Japan, 2000.

- [5] Van Dijk, J. W. E., Uncertainties in personal dosimetry for external radiation: a Monte Carlo approach. *Radiation Protection Dosimetry*, 2006, 121(1), 31-38.
- [6] Van Dijk, J. W. E. and Al Busscher, F, The zero signal and glow curves of bare LiF: Mg, Ti detectors in a hot gas TLD system. *Radiation Protection Dosimetry*, 2002, 101(1-4), 59-64.
- [7] M. S. Pathan, et al., Study of effect of consecutive heating on thermoluminescence glow curves of multi-element TL dosimeter in hot gas-based reader system. *Radiation Protection Dosimetry*, 2019, 187(4), 509-517.
- [8] S. M. Pradhan, C. Sneha, and M. M. Adtani, A method of identification of abnormal glow curves in individual monitoring using CaSO₄: Dy Teflon TLD and hot gas reader. *Radiation Protection Dosimetry*, 2011, 144(1-4), 195-198.
- [9] A. Gal and H. Datz, Automatic detection of anomalous thermoluminescent dosimeter glow curves using machine learning. *Radiation Measurements*, 2018, 117, 80-85.
- [10] A. Gal and H. Datz, Improvement of dose estimation process using artificial neural networks. *Radiation Protection Dosimetry*, 2019, 184(1), 36-43.
- [11] Kröniger, Kevin, et al., A machine learning approach to glow curve analysis. *Radiation Measurements*, 2019, 125, 34-39.
- [12] D. Datta, et al., HANDBOOK ON TLD-BASED PERSONNEL MONITORING (REV. 1-2018), in BARC Report. 2018, Bhabha Atomic Research Centre: BARC Press, Mumbai.
- [13] T. M. Piters and A. J. J. Bos, Effects of non-ideal heat transfer on the glow curve in thermoluminescence experiments. *Journal of Physics D: Applied Physics*, 1994, 27(8), 1747.
- [14] H. Stadtmann, A. Delgado and J. M. Gómez-Ros, Study of real heating profiles in routine TLD readout: Influences of temperature lags and non-linearities in the heating profiles on the glow curve shape. *Radiation Protection Dosimetry*, 2002, 101(1-4), 141-144.
- [15] G. Kitis, J. M. Gomez-Ros and Tuyn, W. N. Jan Thermoluminescence glow-curve deconvolution functions for first, second and general orders of kinetics. *Journal of Physics D: Applied Physics*, 1998, 31(19), 2636.
- [16] J. H. Souza, L. A. R. Da Rosa and C. L. P. Mauricio, On the thermoluminescence glow curve of CaSO₄: Dy. *Radiation Protection Dosimetry*, 1993, 47(1-4), 103-106.

Radiation Dosimetry

3

Self Reliance in Personnel Monitoring of Radiation Workers in India

Kshama Srivastava*, Rupali Pal and, A. K. Bakshi

Radiological Physics and Advisory Division; Health, Safety and Environment Group, Bhabha Atomic Research Centre, Trombay – 400085, INDIA



TLD badge

ABSTRACT

The Personnel Monitoring Service (PMS) equipped with in-house developed $\text{CaSO}_4:\text{Dy}$ based TLD badge has been provided to all radiation workers by BARC. Currently, more than 220,000 radiation workers are covered by the TLD Badge System for monitoring Gamma, X-ray and beta radiations. Neutron monitoring based on CR-39 detector is also provided to 3800 radiation workers. Complete self reliance has been achieved in the field of TLD based personnel monitoring.

KEYWORDS: Personnel monitoring, $\text{CaSO}_4:\text{Dy}$ Teflon disc, TLD badge, Neutron badge

Introduction

The Department of Atomic Energy (DAE) since its inception, has accorded high priority to safety in radiation activities (Atomic Energy Act, 1962 and Radiation Protection Rules 1977 and 2004). The measurement of occupational radiation doses of radiation workers started since the inception of the Department of Atomic Energy (DAE) as evident from the monitoring records of occupational doses available in the national dose registry since 1953 onwards [1]. Personnel Monitoring Service (PMS) has been provided to all radiation workers by Bhabha Atomic Research Centre (BARC) through the erstwhile Directorate of Radiation Protection (DRP) and Radiological Physics and Advisory Division (RPAD). Apart from the DAE, the monitoring service is extended to all the other Non-DAE institutions in the country and a few medical institutions from Nepal and Bhutan.

Film Badge System

Regular PMS based on photographic film dosimetry was started in 1957 for departmental radiation workers by the Radiological Monitoring Laboratory which was housed at the Tata Institute of Fundamental Research (TIFR), later known as Radiological Measurements Section [2]. The Film Badge consisted of two components: a film pack with double-layer emulsion coating on the plastic base and a metal holder to contain that film. The film pack had a 3cm x 4cm transparent polyester film with a cellulose acetate base of ~200 μm thick having more sensitive (fast) emulsion coating (grain size $\cong 2 \mu\text{m}$) on one side and less sensitive (slow) emulsion coating (grain size $\cong 1 \mu\text{m}$) the other side. This film, sandwiched between two black papers is enclosed in a lightproof plastic and has a flap to open in the darkroom for processing.

The film-pack was loaded into a metallic cassette having 5 metallic filters, namely plastic, cadmium, thin-copper, thick-copper, and lead (Fig.1). The thickness of all the filters is 1 mm except for the thin-copper filter (0.15 mm). These filters were incorporated to facilitate the identification of incident radiation, determination of energy and dose evaluation from

multiple radiation exposures of X-rays, beta, and gamma. The cadmium filter facilitated the dosimeter to record thermal neutron dose by $^{113}\text{Cd}(n, \gamma)^{114}\text{Cd}$ reaction as well. The radiation level was indicated by the optical density results under different filter regions due to the darkening of the film.

TLD Badge System

The TLD badge based on $\text{CaSO}_4:\text{Dy}$ Teflon was indigenously developed in 1975 at BARC [3,4]. It is currently used for countrywide Personnel Monitoring of more than 2,20,000 radiation workers in India through 17 monitoring laboratories. The TL phosphor has an optimum Dy concentration of 500 ppm (0.05 mol %) and exhibits a main TL glow peak at about 220 °C and two small satellite peaks on higher and lower temperature sides. The TL response is linear in the dose range of interest in radiation protection (0.1 mSv-1Sv). The $\text{CaSO}_4:\text{Dy}$ phosphor is embedded in Polytetrafluoroethylene (PTFE) (Teflon- 7A grade) in a weight ratio of 1:3. The TLD Badge comprises a TLD Card having three TLD Discs (13.3 mm dia and 0.8 mm thick), which are mechanically clipped on an aluminium plate (52.5 mm x 30.0 mm x 1.0 mm). The card is wrapped in thin paper (thickness ~10 mg/cm^2) containing printed information regarding the user and service period, and further sealed in plastic pouch (thickness ~ 3 - 4 mg/cm^2) before being loaded in the cassette (Fig.2).

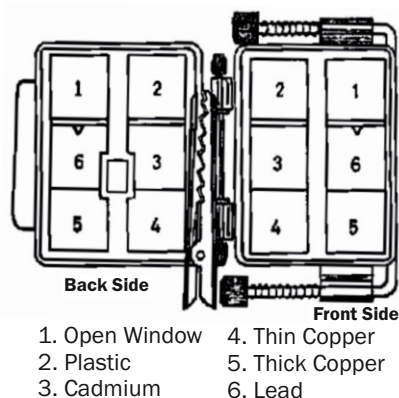


Fig.1: Film badge (chest holder).

*Author for Correspondence: Kshama Srivastava
E-mail: kshamas@barc.gov.in

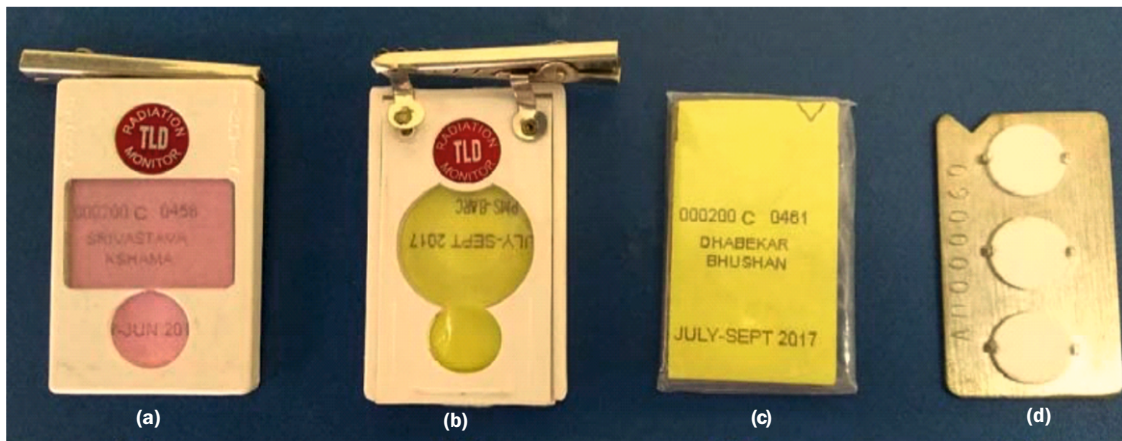


Fig.2: TLD Badge: (a) Front View, (b) Rear View, (c) TLD Card Loaded in Wrapper and Polythene Pouch, and (d) Bare TLD Card.

The plastic cassette has three filter regions: (i) metal filter combination of 1.0 mm Cu and 0.6 mm Al filter, (ii) 1.6 mm thick plastic filters, and (iii) open window. There are three types of TLD Badges in use: Chest Badge, Wrist Badge, and Head Badge for monitoring whole body dose, extremity dose and eye lens dose, respectively. TLD Badge is used for evaluating the dose received by radiation workers due to x-rays, gamma, and beta fields using a suitable dose evaluation algorithm [4]. TLD Badge exhibits an energy-dependent response for photons and beta radiation which is compensated by using multiple filters and the dose evaluation algorithm.

TLD Badge Reader Systems

The appropriate readout systems for the processing of the TLD Badges were also developed at BARC. Earlier, the manual TLD Badge Reader System (model TLDBR-3B) based on contact heating was used till 1999. Presently a PC-controlled semiautomatic TLD Badge Reader (model TLDBR-7B or equivalent) is being used for the readout of the TLD Card for Personnel Monitoring [5]. The Reader has provision for heating of TL discs by hot N₂ gas and automatic reading of 50 TLD Cards in ~100 minutes. This reader utilizes a reproducible, non-linear clamped heating profile for heating the dosimeter to get integral TL-signal measurement. The reader consists of microprocessor-based electronic control circuits, PMT housing, card transport system, N₂ gas heater and temperature control unit, cooling fans and solenoid to control the gas flow (Fig.3).

Neutron Personnel Monitoring Service

The CR-39 based neutron badges are being used for countrywide Fast Neutrons Monitoring (FNM) of 3800 workers

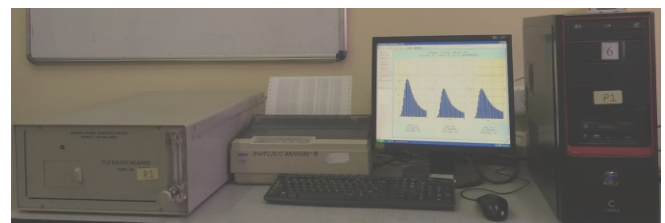


Fig.3: TLD Badge Reader (BR-7B).

from the field of nuclear reactors, accelerators, fuel processing plants, well-logging etc[7]. CR-39 (poly allyl diglycol carbonate-PADC) is a Solid State Nuclear Track Detector (SSNTD) and detects the fast neutrons (above 100 keV) by recoil proton mechanism. The FNM service is provided by a single centralized Laboratory of Radiological Physics & Advisory Division (RPAD), BARC on a quarterly basis. The neutron badge comprises a CR-39 detector (3 cm x 3cm x 0.075 cm) with a 1 mm thick polyethylene radiator in the front, sealed together in an air-tight triple laminated aluminized pouch which is further loaded in a plastic holder. Fig.4 shows all the components of the neutron badge along with the assembled Chest and Wrist Neutron Badge.

The CR-39 badges are processed by an Electro Chemical Etching (ECE) using a specially designed ECE cell wherein the electrode is dipped into the 7 N KOH solution in the cavity through which current is allowed to pass by applying high voltage [5]. The processed detectors are counted for tracks using an automated image analysis system developed by SESSD(erstwhile EISD), BARC.

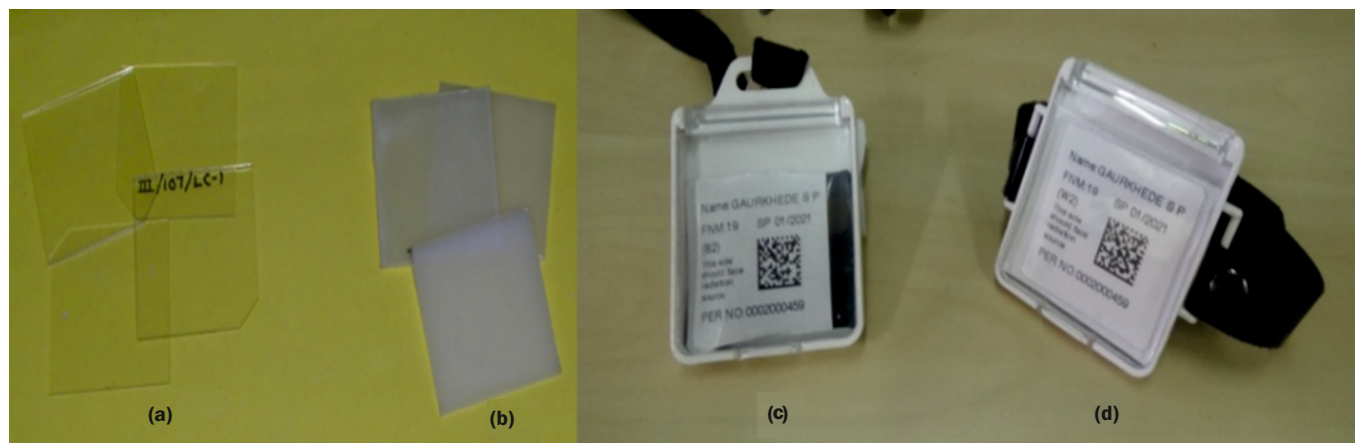


Fig.4: Neutron Badge components (a) CR-3 foils (b) Polyethylene radiator (c) Chest badge and (d)Wrist badge.

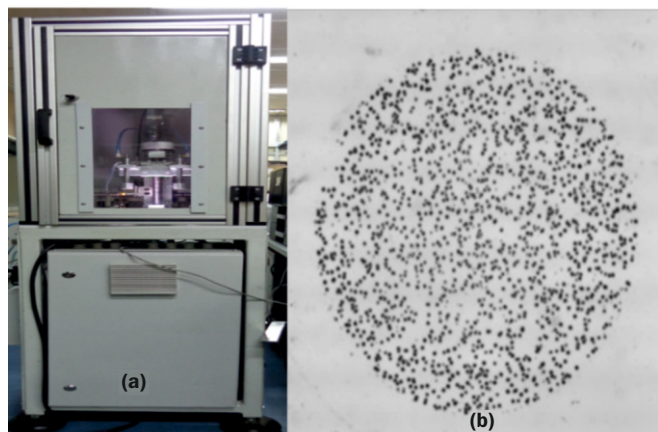


Fig.5: (a) Automated imaging system (b) Tracks in CR-39.

The automated imaging system with ‘vacuum pick-up and place’ feature has the capacity to process 100 CR-39 detectors at a time (Fig.5). Image capturing is done with 5MP camera and the software is capable of saving and importing track counting data against each bar-coded badge of radiation workers. The entire data is saved in an Excel sheet to communicate between the imaging system and ‘ANUKOSH’, a Neutron Dose Database Management Software which is also developed indigenously for dose report generation.

For higher neutron doses, Chemical Etching (CE) process is carried out at 7h in 7N KOH at 60°C and is calibrated for dose linearity up to 100mSv.

Technology Transfer of TLD Badge System

Technology transfer to several private companies to meet the industry requirements has made the TLD badge system commercially available and has helped in enhancing the infrastructure for further scaling of service as per demand. The standardization of production procedures of TLD badges, readers and dosimetric procedures, protocols has further paved the way for the decentralization of personnel monitoring services and economically viable for the private sector.

Expansion of Monitoring Service through Accredited Laboratories

To cater to this increased demand for personnel monitoring, BARC started an accreditation program in 1999 to share the workload with private sector for the multi-fold

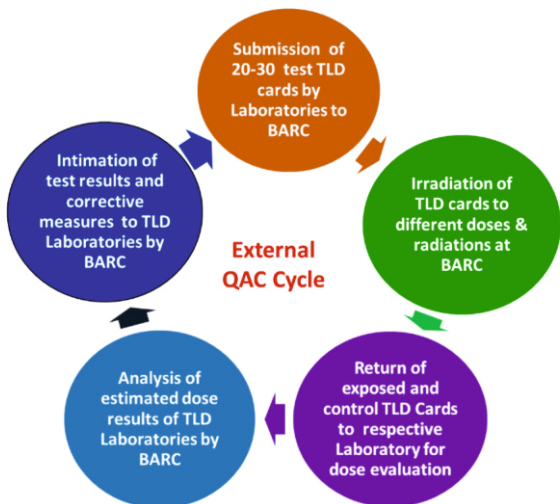


Fig.7: External Quality Assurance Check (QAC) conducted for TLD Laboratories in the country.

TLD Personnel Monitoring Laboratories

Accredited Labs – 12

BARC Labs - 5

Govt. Labs for DAE workers	Private Labs for Non-DAE workers	RPAD Labs for DAE Workers
1. TLD Lab, TAPS, Tarapur	1. Renentech Lab, Mumbai 2. Avanttec Lab, Chennai 3. Ultra-Tech Lab, Bhilai	1. TLD Lab, BARC-DAE, Mumbai 2. TLD Lab, BARC - Tarapur 3. TLD Lab, VECC, Kolkata, 4. TLD Lab, NFC, Hyderabad 5. TLD Lab, KARP, Kalpakkam
2. TLD Lab, MAPS, Kalpakkam		
3. TLD Lab, RAPS, Rawatbhata		
4. TLD Lab, NAPS, Narora		
5. TLD Lab, KAPS, Kakrapar		
6. TLD Lab, KGS, Kaiga		1. TLD Lab, BARC-DAE, Mumbai 2. TLD Lab, BARC - Tarapur 3. TLD Lab, VECC, Kolkata, 4. TLD Lab, NFC, Hyderabad 5. TLD Lab, KARP, Kalpakkam
7. TLD Lab, KKNPP, Kudankulam		
8. TLD Lab, IGCAR, Kalpakkam		
9. TLD Lab, BHAVINI, Kalpakkam		

Fig.6: 17 TLD Personnel Monitoring Laboratories in the country.

expansion of this service. The methodologies were developed, and required documentation was made available for the accreditation of TLD laboratories. At present, out of total 17 laboratories in the country, 12 laboratories are accredited by BARC, including 3 from the private sector, 7 from NPCIL and one each at IGCAR and BHAVINI (Fig.6). The remaining five TLD monitoring laboratories of RPAD, BARC provide service, mainly to radiation workers of BARC and other DAE facilities. The entire Non-DAE workload of approx. 2,00,000 radiation workers from medicine, industry, agriculture and research applications are covered by the three private TLD laboratories. These accredited laboratories are provided with technical and scientific support by BARC. The expansion of services through Accredited Laboratories has helped to meet the service demand and disseminate the technical know-how developed at this centre over the years.

Quality Assurance in TLD Personnel Monitoring

Quality Assurance (QA) plays an important role in such a widespread monitoring program to ensure the accuracy and reliability of service as per the international performance standards. QA program includes internal QA check by the processing laboratory and adequate check on their performance by an external/neutral entity. In India, a program of External Quality Assurance Check (QAC), was devised for periodic performance evaluation of various monitoring laboratories through a postal exercise [2,8]. This external QAC was initiated in 1985 and total 47 QAC cycles have been completed so far. Under this program, the performance of each TLD laboratory is assessed in radiation categories of the photon, beta and mixed photon-beta field as per the acceptance criterion of the American National Standards Institute (ANSI) and Trumpet Curve method ISO 14146.

In neutron personnel monitoring, internal QA is maintained by the processing laboratory by calibrating and standardizing all the procedures and equipment. The neutron dosimetry group, RP&AD has participated in EURADOS intercomparison exercise-2017. Response of BARC neutron badge was within the acceptable limits(0.5–2.0) as per ISO-14146 [9].

Conclusion

In routine personnel monitoring, thousands of cards are processed monthly and it needs to be ensured that the dosimetric accuracy is not compromised. The dosimetric accuracy mostly relies on the accuracy of the signal i.e. GC. With the continuous increase in the number of monitored occupational workers, there is a need for automation to increase the throughput of TLD personnel monitoring

laboratories without compromising dosimetric accuracy. Therefore, the application of ML algorithms into the GC-screening process which is one of the mandatory steps in TLD processing will surely improve the throughput of the laboratory. Also, with human intervention, the variability in decisions about the correctness of GC results in subjectivity. The subjectivity can also be minimized with the use of AI-based algorithms. Further, the use of a probabilistic approach gives an insight into the anomaly as well as provides a health diagnosis of the TLD reader which serves as predictive maintenance system.

References

- [1] Vohra, K., et al., A personnel dosimeter TLD badge based on CaSO₄:Dy Teflon TLD discs. *Health Physics*, 1980. 38(2): 193-197.
- [2] Pradhan, A. and R. Bhatt, Metal filters for the compensation of photon energy dependence of the response of CaSO₄: Dy-teflon TLD discs. *Nuclear Instruments and Methods*, 1979. 166(3): 497-501.
- [3] Pradhan, A., C. Bhuwan, and K. Ayyangar. Development of CaSO₄: Dyteflon discs thermoluminescence dosimetry. in *Proceedings of The National Symposium on Thermoluminescence and Its Applications*, Kalpakkam, February 12-15, 1975. 1976.
- [4] Kulkarni, M., P. Ratna, and S. Kannan. A new PC based semi-automatic TLD badge reader system for personnel monitoring. in *Proceedings of International Radiation Protection Association Conference*, Hiroshima, Japan. 2000.
- [5] Van Dijk, J., Uncertainties in personal dosimetry for external radiation: a Monte Carlo approach. *Radiation Protection Dosimetry*, 2006. 121(1): 31-38.
- [6] WE van Dijk, J. and F. Al Busscher, The zero signal and glow curves of bare LiF: Mg, Ti detectors in a hot gas TLD system. *Radiation Protection Dosimetry*, 2002. 101(1-4): 59-64.
- [7] Pathan, M.S., et al., Study of effect of consecutive heating on thermoluminescence glow curves of multi-element TL dosimeter in hot gas-based reader system. *Radiation Protection Dosimetry*, 2019. 187(4): 509-517.
- [8] Pradhan, S., C. Sneha, and M. Adtani, A method of identification of abnormal glow curves in individual monitoring using CaSO₄: Dy Teflon TLD and hot gas reader. *Radiation Protection Dosimetry*, 2011. 144 (1-4): 195-198.
- [9] Amit, G. and H. Datz, Automatic detection of anomalous thermoluminescent dosimeter glow curves using machine learning. *Radiation Measurements*, 2018. 117: 80-85.
- [10] Amit, G. and H. Datz, Improvement of dose estimation process using artificial neural networks. *Radiation Protection Dosimetry*, 2019. 184(1): 36-43.
- [11] Kröniger, K., et al., A machine learning approach to glow curve analysis. *Radiation Measurements*, 2019. 125: 34-39.
- [12] Datta, D., et al., HANDBOOK ON TLD-BASED PERSONNEL MONITORING (REV. 1-2018), in BARC Report. 2018.
- [13] Piters, T. and A. Bos, Effects of non-ideal heat transfer on the glow curve in thermoluminescence experiments. *Journal of Physics D: Applied Physics*, 1994. 27(8): 1747.
- [14] Stadtmann, H., A. Delgado, and J. M. Gómez-Ros, Study of real heating profiles in routine TLD readout: Influences of temperature lags and non-linearities in the heating profiles on the glow curve shape. *Radiation Protection Dosimetry*, 2002. 101(1-4): 141-144.
- [15] Kitis, G., J. Gomez-Ros, and J.W. Tuyn, Thermoluminescence glow-curve deconvolution functions for first, second and general orders of kinetics. *Journal of Physics D: Applied Physics*, 1998. 31(19): 2636.
- [16] Souza, J., L. Da Rosa, and C. Mauricio, On the thermoluminescence glow curve of CaSO₄: Dy. *Radiation Protection Dosimetry*, 1993. 47(1-4): 103-106.

Systems for Radiological Surveillance & Monitoring

4

Integrated Environmental Radiation Monitor with Autonomous Profiler for Underwater Radiation Monitoring

Pratip Mitra*, S. S. Salunkhe, T. Mukundan, Anisha Kumari, S. G. Gavvas, P. R. Ninawe, Saurabh Srivastava, G. Priyanka Reddy, S. Garg, and A. Vinod Kumar

Environmental Monitoring and Assessment Division; Health, Safety and Environment Group, Bhabha Atomic Research Centre, Trombay – 400085, INDIA



Autonomous vertical profiler

ABSTRACT

Environmental Monitoring and Assessment Division (EMAD) is involved in the design and development of Geiger-Mueller (GM) Tube based standalone Environmental Radiation Monitors (ERMs) with online data communication. National Institute of Oceanography (NIO) has developed Autonomous Vertical Profiler (AVP) for controlled underwater movement for measuring below-surface parameters along with Radiofrequency (RF) based data communication. BARC and NIO have collaboratively designed an integrated Environmental Radiation Monitor with Autonomous Vertical Profiler (ERM-AVP) in order to develop a single system capable of underwater radiation monitoring.

KEYWORDS: Environmental monitoring, Underwater radiation monitoring

Introduction

Autonomous underwater gamma radiation monitoring is important for monitoring of liquid radioactive waste discharge points of nuclear facilities, radiological surveillance of coastal areas and detection of release of radiation or radiological substances from waterborne vehicles. This type of monitoring and/or surveillance can provide valuable input for national level emergency preparedness program of the Department of Atomic Energy (DAE). EMAD, BARC, under the Indian Environmental Radiation Monitoring Network (IERMON) project, has established a countrywide network of standalone solar powered ERMs, for monitoring of gamma dose rate in air, with Global System for Mobile communications (GSM) based real-time data communication [1, 2]. NIO has developed a battery-powered motor-driven in-situ robot profiler [3], called AVP, for controlled underwater movement and measurement of vertical structure of water column at high resolution along with RF based data communication. In this work, an integrated ERM-AVP system has been designed and developed jointly by BARC and NIO for underwater monitoring of gamma dose rate.

The ERM-AVP System

The ERM-AVP is a DC thruster driven robot profiler [3] that can be programmed by the user to descend through the water column down to a certain pre-set maximum depth while stopping for specified periods of time at different depths en route to sense and store the gamma radiation levels at those depths. After completing its downward mission, it ascends slowly to the surface of the water without propulsion, due to its in-built positive buoyancy.

On breaking the water surface, it transmits its coordinates recorded using Global Positioning System (GPS),

the measured gamma dose rate data and the vehicle parameters via RF communication to a remote PC. The system has an installed echo sounder enabling bottom detection and a pressure sensor providing depth data, both of which can facilitate in stopping the thruster in case of an emergency in terms of seabed proximity or pressure overshoot.

Description of AVP

The AVP (Fig.1), developed by NIO [4], consists of three main sections:(i) the nose cone (bottom) (ii) the hull (middle) and (iii) the tail cone (top). The nose cone is free-flooding, i.e. it permits water to enter as the sensors housed in this section are water-tight and pressure-proofed. The nose cone is machined from an Acetal SA 550-grade cylinder. The hull is made from an open cylindrical aluminium alloy tube section and contains the electronics including the ERM PCBs and the batteries. The hull is sealed at both ends with removable aluminium alloy end-plates. The hull assembly has been pressure-tested in a pressure chamber up to 300 m. The tail cone is also free-flooding and is fixed on the rear end-plate of the hull. It serves the purpose of gripping the thruster body, of accommodating pressure-proof foam for extra buoyancy and also provides a means of locating the GPS and satellite antennas tubs through it. The system has been designed to have a large separation between the centre of buoyancy (C_b) and the centre of gravity (C_g), which helps to keep the AVP stable and vertical in orientation before a dive [4]. Technical specifications of the AVP are summarized in Table 1.

The electronic architecture of AVP is based on ARM based microcontrollers. A user-friendly Graphical User Interface (GUI) using LABVIEW enables mission programming, vehicle data monitoring, data acquisition and downloading, plotting etc. The GUI is loaded on a remote PC and interacts with the AVP through a radio modem connected to a serial port.

*Author for Correspondence: Pratip Mitra
E-mail: pratipm@barc.gov.in



Fig.1: Autonomous Vertical Profiler (front side view).

Table 1: Technical Specifications of AVP.

Parameter	Value
Length	1.17 m
Diameter	0.18 m
Weight	13 - 16 kg; varies on installed sensors
Material	Hull: Aluminium alloy; End cones: Acetal
Propulsion	Single DC thruster
Electronics	ARM based
GUI	LABVIEW based
Speed	0.1 -1.0 m/s
Depth	200 m (max)
Batteries	Lithium ion polymer (324 W- h)
Communication	RF (2.4 GHz)
Vehicle sensors	Pressure, Echo sounder, GPS
Scientific sensors	Depth, ERM

Description of ERM

The ERM, developed by BARC [1], measures gamma dose rate. It consists of two PCBs, each (Fig.2) containing one big (high sensitivity, low dose rate) and one small (low sensitivity, high dose rate) energy compensated GM tubes, accommodated inside the hull of the AVP.

The PCBs (Fig.3) accept 5 V input from the battery of AVP and produce 500 V bias voltages for the GM tubes. The shaped output pulses from the GM tubes are fed to the microcontroller of the AVP, which counts the pulses and stores the count rates when it is underwater. Upon reaching the water surface, the count rates are transmitted via RF to a remote PC where the calibration factors are applied to convert the measured count rates to the required dose rates. The ERM PCB consumes 50 mA (max) current. Two such PCBs are used for simultaneous measurement of gamma dose rate. Table 2 summarizes the technical specifications of the ERM.

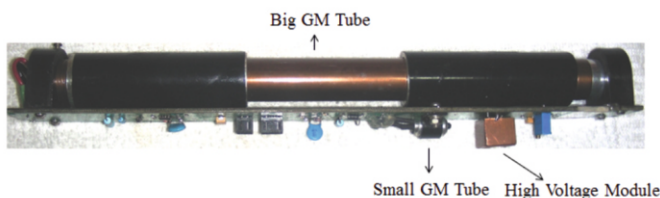


Fig.2: The ERM PCB (Top view).

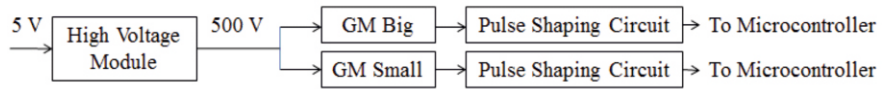


Fig.3: Block diagram of an ERM PCB.

Table 2: Technical Specifications of ERM.

Parameter	Value
Detected Radiation	Gamma
Detectors	Energy Compensated Geiger- Mueller Tubes
Energy Response	35 keV – 2MeV (in air)
Measurement Range (Combined)	50 nGy/h – 20 Gy/h (in air)
Operating Temperature	-20 ⁰ C – 60 ⁰ C(in air)
Relative Humidity	Up to 100%
Power Requirement	5 V, 50 mA for each of the two PCBs

Results and Discussion

Two units of the ERM-AVP were fabricated by M/s. Control Technologies, Bengaluru, an industrial partner of NIO, Goa, under license from BARC. These units were field-tested in Mumbai Harbour Bay (Arabian Sea). Both units satisfactorily operated in their underwater missions.

Conclusion

The indigenously developed state-of-the-art integrated ERM-AVP is a useful addition to the family of radiation monitoring systems for DAE's emergency response program when it comes to surveillance/security of coastal and/or port areas. These cost-effective indigenously developed systems can be effectively used in large numbers by DAE's Emergency Response Centres (ERCs).

Acknowledgements

ERM-AVP has been designed and developed under an MoU between BARC and NIO. The AVP is a proprietary item of NIO and the ERM is a proprietary item of BARC. The integrated system has been produced by Control Technologies, Bangalore (industrial partner of NIO), under a license from BARC.

References

- [1] Patel M. D., Ratheesh M. P., Prakasha M. S., Salunkhe S. S., Nair C. K. G., Vinod Kumar A. and Puranik V. D., Multi-Detector Environmental Radiation Monitor with Multichannel Data Communication for Indian Environmental Radiation Monitoring Network (IERMON), BARC Newsletter, 320, (2011): 31-34.
- [2] Garg S., Ratheesh M. P., Mukundan T., Patel M. D., Vinod Kumar A., Puranik V. D. and Nair C. K. G., The Architecture and Functions of Central Monitoring Station of Indian Environmental Radiation Monitoring Network (IERMON), BARC Newsletter, Founder's Day-Special Issue, October (2011): 419-422.
- [3] Desa E., Pascoal A., Desa E., Mehra P., Madhan R. and Naik G. P., Controlled Thruster Driven Profiler for Coastal Waters, US Patent No. 6786087, 7 September 2004.
- [4] Madhan R., Dabholkar N, Navelkar G, Desa E, Afzulpurkar S, Mascarenhas A., and Prabhudesai S., Autonomous profiling device to monitor remote water bodies, Current Science, 102(2), (2012): 169-176.

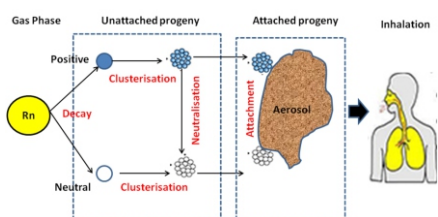
Inhalation Dose Assessment

5

Programs Deploying Indigenous DTPS and DRPS

Rosaline Mishra*, R. Prajith, R. P. Rout, Jalaluddin S., A. T. Khan and B. K. Sapra

Radiological Physics and Advisory Division; Health, Safety & Environment Group, Bhabha Atomic Research Centre, Trombay – 400085, INDIA



Inhalation dose due to Radon Progeny

ABSTRACT

Inhalation dose assessment has been improved by the development of Direct Radon and Thoron progeny sensors (DRPS and DTPS). These are indigenously developed in RP&AD, BARC. DRPS and DTPS are deposition based, passive, time integrated alpha particle detectors for direct measurement of progeny concentrations. Programs deploying DTPS and DRPS, both in national level surveys and international scientific research collaborations has been undertaken.

KEYWORDS: Direct Radon Progeny Sensors (DRPS), Direct Thoron Progeny Sensors (DTPS), Inhalation dose

Introduction

Inhalation of ^{222}Rn , ^{220}Rn and their progeny contribute to more than 50% i.e. 1.29 mSv, out of 2.5 mSv of total annual effective dose to humans from all natural sources of radiation (Fig.1). The primary exposure pathway for ^{222}Rn and its progeny from their exhalation to the absorbed organ dose is shown as a block diagram in Fig.2(a). Specifically, the progeny of ^{222}Rn , ^{220}Rn , that are generated by radioactive decay from the parent gas, exhibit a dynamic behavior by attachment to aerosols followed by segregation into unattached (0.5-5 nm diameter) and attached progeny (100-500 nm). Thus they become a part of indoor aerosol, available for inhalation Fig.2(b). Upon inhalation, the unattached and attached progeny deposit in the different regions of the respiratory tract (Fig.3) and undergo subsequent radioactive decay, contributing to inhalation dose. More precisely, progeny alone contribute to >95% of the total inhalation dose. Inhalation dose is given by:

$$D = (C_g \cdot DCF_g + C_p \cdot DCF_p) \cdot T \cdot OF$$

where, C_g : Gas (^{222}Rn , ^{220}Rn) activity concentration,

DCF_p : Dose Conversion Factor (g- gas, p- progeny)

T : Exposure time

OF : Occupancy factor

C_p : Progeny (^{222}Rn , ^{220}Rn) activity concentration

The major domain for the measurement of ^{222}Rn , ^{220}Rn and their Progeny are a) Public domain (dwellings, schools, offices) and b) Occupational domains (Uranium mines, Thorium plants). It had been a general practice to measure the gas concentration and estimate the progeny concentration using an assumed equilibrium factor and calculate the inhalation dose. But after the indigenous development of Direct Radon and Thoron progeny sensors (DRPS and DTPS) in RP&AD, BARC, progeny are directly measured for inhalation dose assessment. DRPS and DTPS are absorber mounted SSNTDs (LR115) [1-4] where detection takes place by selective registration of alpha-particle energies emitted from the

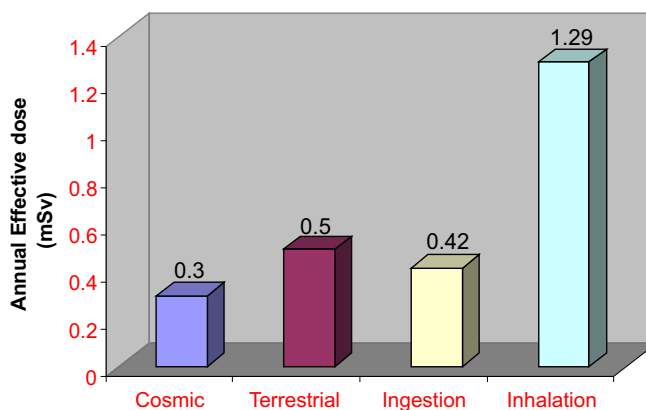


Fig.1: Annual effective dose due to natural sources of radiation.

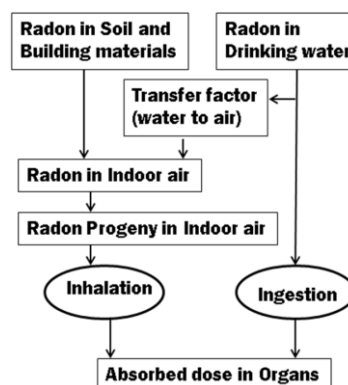


Fig.2(a): Primary Exposure Pathways of Radon towards dose contribution.

deposited progeny activity. They can be used in different modes (Fig.4) to extract various progeny parameters. These were calibrated in 8m^3 Radon calibration chamber (Fig.5) installed in RP&AD, BARC (temperature range 20-60°C and humidity range 40-95%) and in real indoor environments.

*Author for Correspondence: Rosaline Mishra
E-mail: rosaline@barc.gov.in

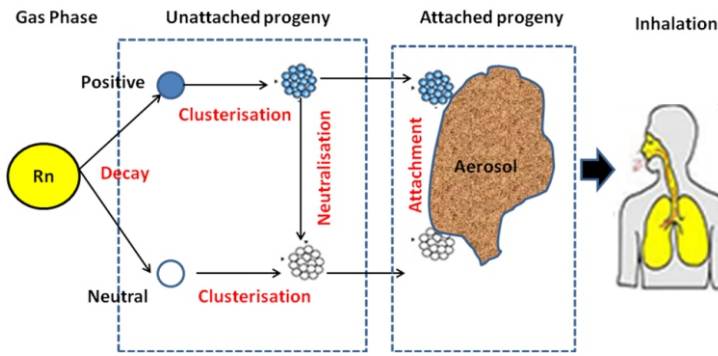


Fig.2(b): Indoor Radioactivity.

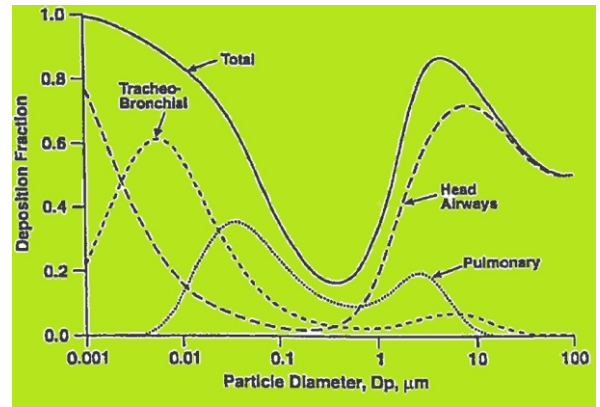


Fig.3: Fractional deposition of inhaled progeny in human respiratory tract.

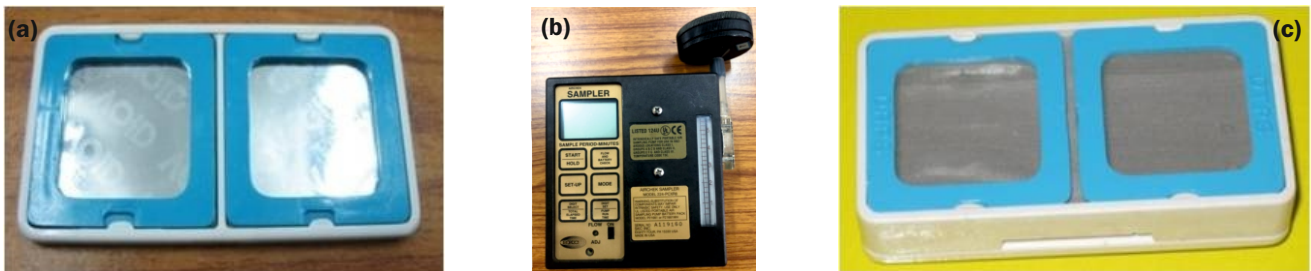


Fig.4: Direct Progeny Sensor a) Bare-mode, b) flow-mode, c) capped-mode.



Fig.5: Outside and inside view of the calibration chamber.

National Programs using DRPS and DTPS

DRPS and DTPS were used in National surveys for inhalation dose assessment in indoor environments. Under the scheme of BRNS (Board of Research in Nuclear Sciences: Nationwide project), ~ 4500 houses in 58 districts of 15 states in India were surveyed for direct measurement of progeny concentrations using DRPS and DTPS, over a period of 2-3 years. The program comprised of: a) the study of seasonal variation of progeny activity concentration b) Dependence on indoor conditions like building materials and ventilation rates (Fig.6). Higher radon progeny concentration (EECR) and thoron progeny concentration (EECT) was observed in winter season in the houses of Shivalik hills of Jammu and Kashmir (Fig.7) [5]. Similar trend of higher progeny concentration and inhalation doses were observed for all the dwellings. Fig.8 shows the maximum progeny concentration obtained in the mud-floor houses in Garhwal region [6]. In other parts of India also, we higher progeny concentration were obtained in mud houses. Fig.9 shows the higher progeny concentrations in the poorly ventilated houses of Tehri-Garhwal [7]. In addition, the ventilation rate and air turbulence in the indoor environments play an important role in controlling the inhalation dose. Effect of good ventilation conditions are observed in the High background radiation areas of Kerala and Odisha, wherein good ventilation conditions contributed to inhalation doses similar to that measured in normal background radiation areas even though the gamma dose rates are ten times higher in HBRAs. Higher progeny concentrations were generally measured in Garhwal Himalayan region of Uttarakhand, which calls for more detailed study in the region. All the relevant data in the projects were compiled for “UNSCEAR global survey for Public exposure 2007-2020”.



Fig.6: DTPS and DRPS in inside of different types of houses.

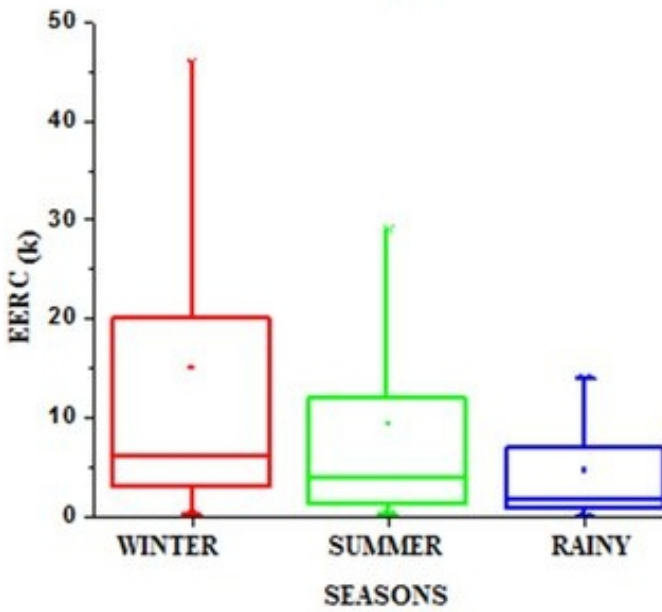


Fig. 7: Progeny concentration in different seasons in indoors of Shivalik hills (Jammu Kashmir) [5].

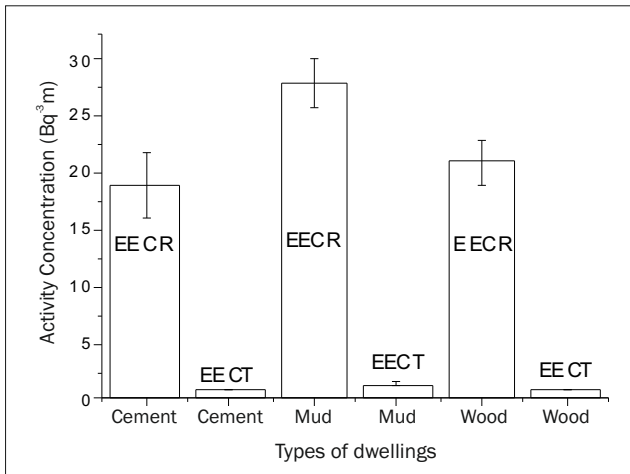
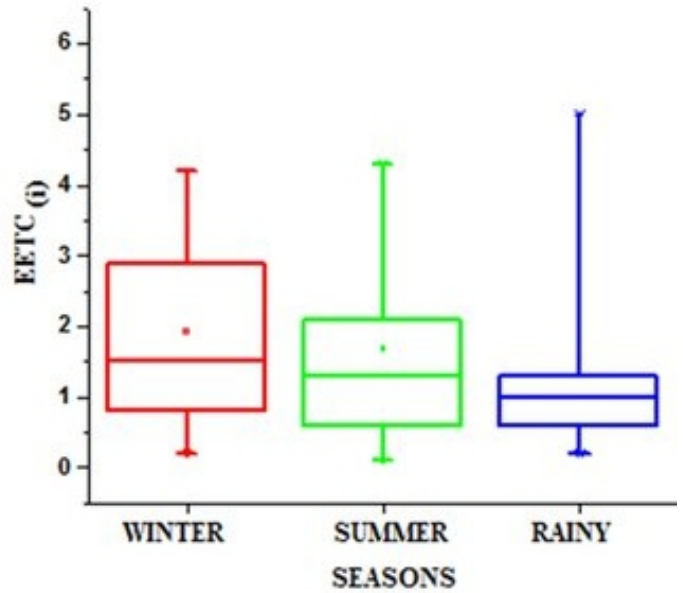


Fig. 8: Progeny concentration in different types of houses in Garhwal region [6].

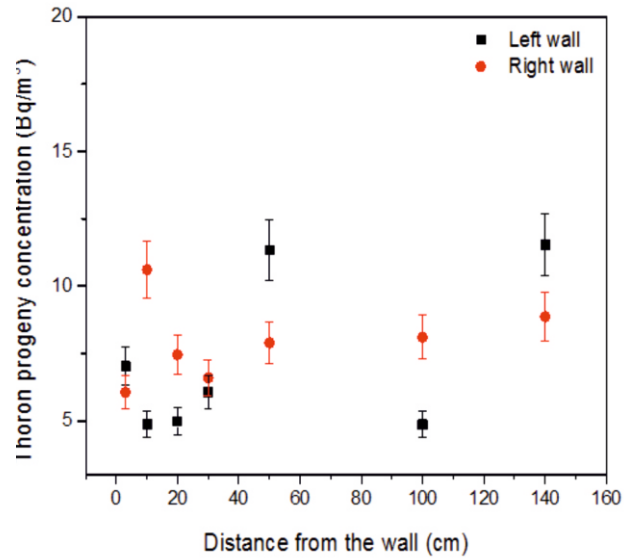


Fig. 10(a): Results in HMGU Thoron experimental house by DTPS

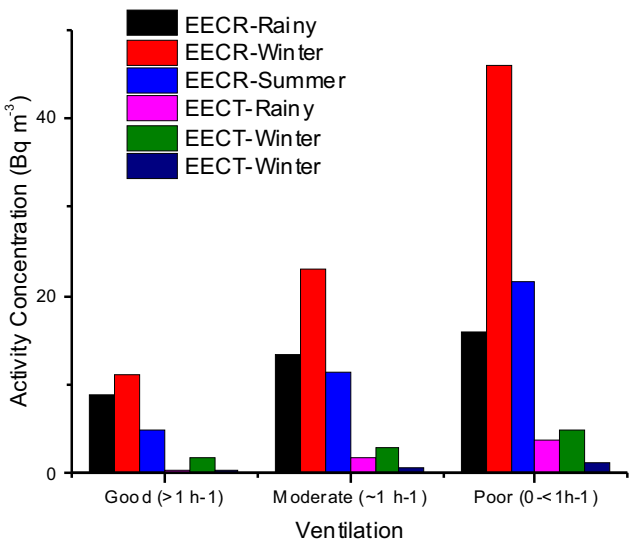


Fig. 9: Progeny concentration as a function of ventilation conditions indoors in different seasons in Tehri-Garhwal region [7].

International Collaborations

DRPS and DTPS were the first complete system in the world, developed for direct measurement of progeny concentration, which generated a lot of interest in the scientific community. This resulted in research collaborations with institutions from ~10 countries in which DRPS and DTPS were deployed in schools, dwellings, underground laboratories and caves. Under Indo-German collaboration project with Helmholtz Zentrum, Munich, the thoron progeny distribution was studied using DTPS (Fig.10(a)) in their Thoron experimental test-house (Fig.10(b)) [8]. In 25 primary schools of Banja Luka (Republic of Srpska), DTPS and DRPS were used to measure progeny concentration along with RADUET for radon gas measurements (Fig.11(a,b)) and hence long term equilibrium factor was measured [9]. Fig.12 shows the Radon concentration distribution using DRPS along with NRPB (UK), NRPB-SSI detector and Raduet system in ~100 dwellings in Hungary [10]. 'RaThoGamma' kit (Fig.13) comprising of TLDs, Radtrak-Radosys (Hungary), RSKS-Radonova (Sweden) and DRPS/DTPS (India), was used for a case-control study in



Fig.10(b): Thoron Experimental House in Helmholtz Zentrum, Munich [8].

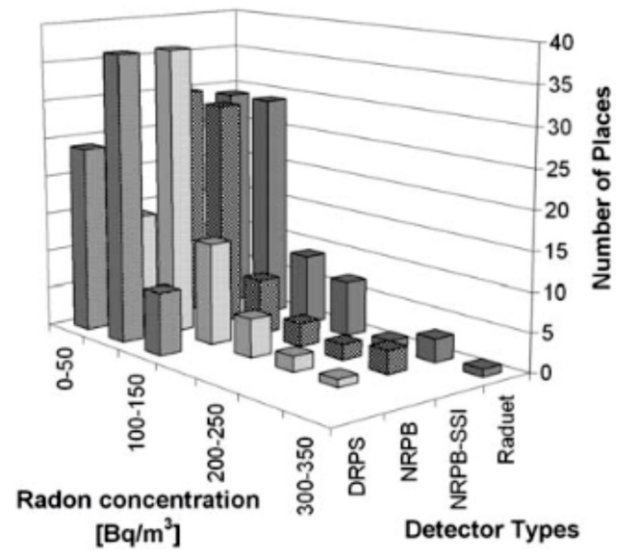


Fig.12: Radon concentration distribution using DRPS (India), NRPB (UK, NRPB-SSI and Raduet detectors. [10].

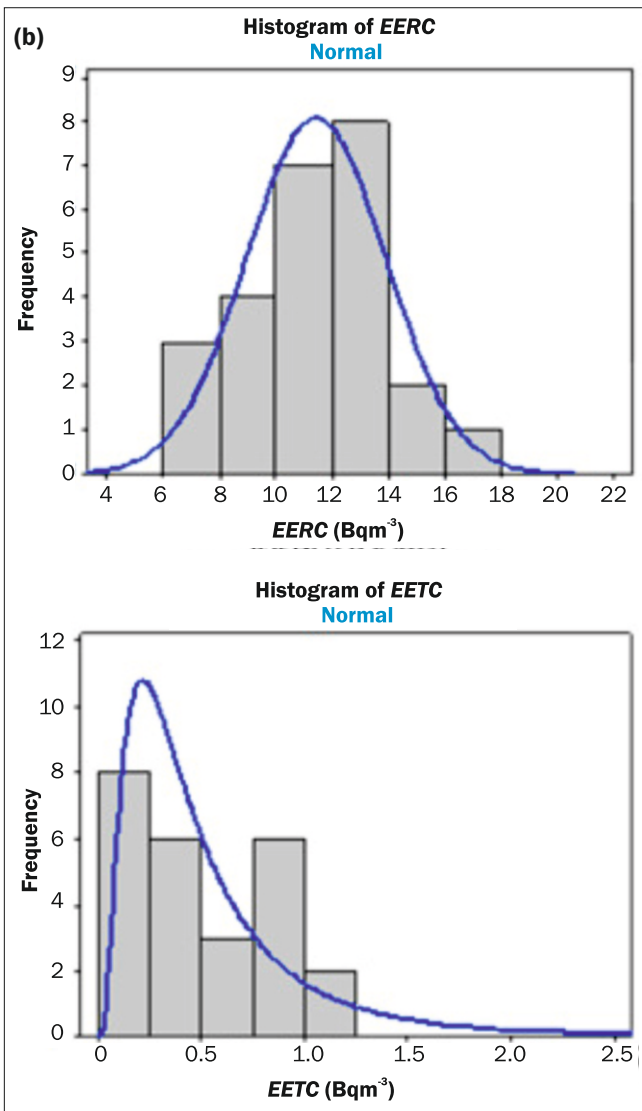


Fig.11: (a) DRPS and DTPS set deployed in schools, b) Histograms of EERC and EETC in 25 primary schools of Republic of Srpska [9].



Fig.13: DRPS/DTPS in RaThoGamma kit of environmental radioactivity measurement in Romania [11].

Uranium mine area of Bihor county, Romania, in which annual effective doses were measured to be 3 times higher in the case-sample compared to control-sample and ~4 times higher than the world average [11].

Conclusion

The development of DTPS and DRPS has led to an improvement in inhalation dose assessment by directly measuring the progeny concentration. Multiple programs using DRPS and DTPS both in national level and through International collaborations has resulted in country-wide mapping, large number of publications and Ph.D programs.

Acknowledgements

The authors acknowledge all the research groups from various institutes both under BRNS projects as well as under International collaboration for their involvement in application of DRPS and DTPS.

References

- [1] Rosaline Mishra, Y. S. Mayya, Study of a deposition based Direct Thoron Progeny Sensor (DTPS) technique for estimating Equilibrium Equivalent Thoron Concentration (EETC) in indoor environment, *Radiation Measurements*, 2008, 43, 1408-1416.
- [2] Rosaline Mishra, Y. S. Mayya, H. S. Kushwaha, Measurement of $^{220}\text{Rn}/^{222}\text{Rn}$ progeny deposition velocities on surfaces and their comparison with theoretical models, *J. Aer. Sci.*, 2009, 40, 1-15.
- [3] Rosaline Mishra, B. K. Sapra, Y. S. Mayya, Development of an integrated sampler based on direct $^{222}\text{Rn}/^{220}\text{Rn}$ progeny sensors in flow-mode for estimating unattached/attached progeny concentration, *Nucl. Instrum. and Meth. in Phys. Res. B.*, 2009, 267, 3574-3579.
- [4] Y. S. Mayya, R. Mishra, R. Prajith, B. K. Sapra, H. S. Kushwaha, Wire-mesh capped deposition sensors: novel passive tool for coarse fraction flux estimation of radon thoron progeny in indoor environments, *Science of the total environment*, 2010, 409(2), 378-383.
- [5] M. Kaur, Ajay Kumar, Rohit Mehra, Rosaline Mishra. Assessment of radon, thoron, and their progeny concentrations in the dwellings of Shivalik hills of Jammu and Kashmir, India. *Environmental Geochemistry and Health* (2020), <https://doi.org/10.1007/s10653-020-00767-0>.
- [6] R. C. Ramola, Mukesh Prasad, Tushar Kandari, Preeti Pant, Peter Bossew, Rosaline Mishra & S. Tokonami. Dose estimation derived from the exposure to radon, thoron and their progeny in the indoor environment *SCIENTIFIC Reports* (2015) 6:31061
- [7] Pooja Panwar, Abhishek Joshi, Mukesh Prasad, R. C. Ramola. Radiological dose estimation due to exposure to attached and unattached fractions of radon and thoron progeny concentrations. *Journal of Radioanalytical and Nuclear Chemistry*, 2022, 331, 1967-1974
- [8] Rosaline Mishra, M. Joshi, O. Meisenberg, S. Gierl, R. Prajith, S. D. Kanse, R. Rout, B. K. Sapra, Y. S. Mayya, J. Tschiersch, Deposition and spatial variation of thoron decay products in a thoron experimental house using the Direct Thoron Progeny Sensors *Journal of Radiological Protection*, 2017, 37, 2, 379-389.
- [9] Z. Curguz, Z. Stojanovska, Z. S. Zunic, P. Kolarz, T. Ischikawa, Y. Omori, R. Mishra, B. K. Sapra, J. Vaupotic, P. Ujic, P. Bossew. Long-term measurements of radon, thoron and their airborne progeny in 25 schools in Republic of Srpska. *Journal of Environmental Radioactivity*, 2015, 148, 163-169.
- [10] G. Szeiler, J. Somlai, T. Ishikawa, Y. Omori, R. Mishra, B. K. Sapra, Y. S. Mayya, S. Tokonami, A. Csordás, T. Kovács. Preliminary results from an indoor radon thoron survey in Hungary. *Radiation Protection Dosimetry*, 2012, 152, 1-3, 243-246.
- [11] T. Dicu, B. D. Burghel, A. Cucos, Rosaline Mishra, B. K. Sapra, Assessment of annual effective dose from exposure to natural radioactivity sources in a case-control study in Bihor county, Romania, *Radiation Protection Dosimetry*, 2019, 185, 10, 15-24.

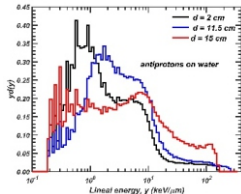
Medical Applications

6

Antiproton Radiotherapy: A Monte Carlo-based Microdosimetric Approach

Arghya Chattaraj and T. Palani Selvam*

Radiological Physics and Advisory Division; Health, Safety & Environment Group, Bhabha Atomic Research Centre, Trombay – 400085, INDIA



Microdosimetric distributions of 126 MeV antiproton at different depths in water

ABSTRACT

Antiprotons are advantageous in radiotherapy as their annihilation physics results in an enhanced energy deposition at tumor location. Further, knowledge on Relative Biological Effectiveness (RBE) and Quality Factor (Q) is important to make a complete assessment on their usefulness in radiotherapy. Microdosimetric techniques serve as a powerful tool to calculate RBE and Q. These parameters are calculated for 126 MeV antiprotons at 1 μm site size in water using the FLUKA-based Monte Carlo code.

KEYWORDS: Microdosimetry, Monte Carlo, Antiproton

Introduction

The goal of the radiotherapy is to deliver high dose to the tumour and spare the surrounding normal tissues. Radiotherapy uses low LET (Linear Energy Transfer) radiations such as ^{60}Co , Mega-voltage X-rays (4–15 MV), Electrons (4–18 MeV) and high LET radiations such as protons and carbon ions. Note that high LET particles have enhanced Relative Biological Effectiveness (RBE) as compared to low LET radiation. The possibility of using antiprotons in radiotherapy is reported in the literature [1-5]. This study focuses on microdosimetry-based investigation of 126 MeV antiprotons for radiotherapy using the Monte Carlo techniques.

What is Antiproton?

Antiproton (\bar{p}) is the antiparticle of proton (p). It is a negative heavy ion without any electronic structure. It is discovered by Emilio Segre and Owen Chamberlain in 1955. Antiproton is a spin $\frac{1}{2}$ particle having mass of $938.3 \text{ MeV}/c^2$. The antiprotons are stable, but they are typically short-lived as any collision with proton or neutron will cause annihilation. Antiproton consists of two up antiquarks and one down antiquark ($\bar{p} \equiv \bar{u}\bar{u}\bar{d}$). Proton is made of two up quarks and one down quark ($p \equiv uud$). Charge of each quark is $1/3$ whereas each antiquark has $-1/3$. Hence, the electric charge of proton is 1 whereas it is -1 for antiproton. Similarly, magnetic moment of antiproton is negative which is positive for proton.

Production of Antiprotons

Currently few laboratories in the world such as CERN and Fermi National Accelerator Laboratory produce antiprotons [4-7]. CERN produces antiprotons at clinically relevant energies (47 and 126 MeV). The Antiproton Decelerator (AD) at CERN produces low-energy antiprotons for studies of antimatter, and creates antiatoms. The low energy antiproton beam lines at CERN is shown in Fig.1. A 26 GeV/c proton beam from Proton Synchrotron is fired into a block of metal. (typical target is a thin, highly dense rod of iridium metal of 3-mm diameter and 55 cm in length embedded on graphite

enclosed by a sealed water-cooled titanium case). These collisions create a multitude of secondary particles, including antiprotons having different energies. The peak production occurs at antiproton energy of 3.6 GeV. These antiprotons are (a) collected at this production energy in the AD ring, (b) decelerated to lower energies, and (c) cooled using stochastic cooling as well as electron cooling to decrease beam emittance. These antiprotons exit from the accelerator vacuum through a 15 μm titanium window and pass several non-destructive beam monitors before entering the biological target. The total charge extracted from the accelerator can be measured using fast current transformer. Depending on the experimental requirements, the antiproton beam focus can be changed between $r = 4 - 15 \text{ mm}$.

Interaction of Antiprotons with Matter

At high velocities, antiprotons and protons behave in a similar manner in terms of energy deposition in the medium. However, after slowing down in the medium, antiprotons are captured by a nucleus and annihilate on its surface [2, 8-10]. The basic idea of antiproton radiotherapy is to use the excess



Fig.1: Panoramic view of the low energy antiproton beam lines at CERN (Ref: <https://home.cern/news/news/physics/making-antimatter-transportable>).

*Author for Correspondence: T. Palani Selvam
E-mail: pselvam@barc.gov.in

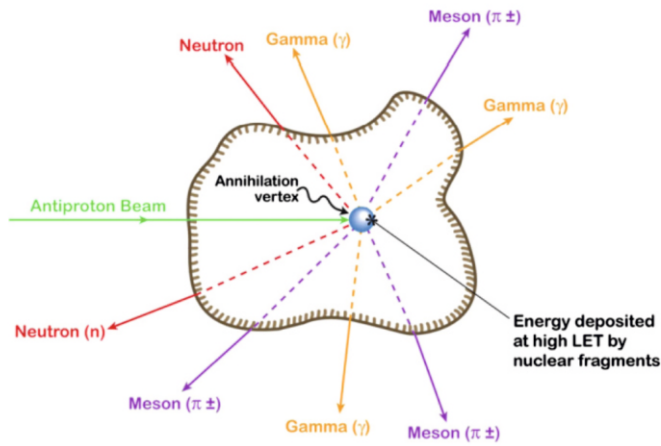


Fig.2: Annihilation event produced by an antiproton stopping in matter [10].

energy deposited from the antiproton–nucleus annihilation near the Bragg peak. Fig.2 represents annihilation event experienced by an antiproton while stopping in matter. As depicted in Fig.2, during annihilation several secondary particles are produced. In the annihilation process 1.88 GeV (twice proton rest-mass) is released and converted, on average, into 4-5 pions (π^+ , π^- and π^0).

The average kinetic energy of each Pion is about 300 MeV. The 300 MeV charged Pion has a range of many tens of centimeters in water. π^0 meson is highly unstable and decays instantaneously into high energy gamma-rays with roughly 70–300 MeV. The antiproton can also annihilate by combining with a neutron in nucleus in which the decay products are mostly high energy Pions. Most of the energy produced from the annihilation of antiproton is deposited over a very wide region. Antiproton rarely produces K-meson in antiproton-nucleon annihilation. Mostly 1 or 2 charged Pions penetrate the nucleus and induce an intra-nuclear cascade which results in production of high-LET charged fragments. These fragments have a very short range in the target and will deposit their kinetic energy in the immediate vicinity of the annihilation vertex.

Microdosimetric Quantities

Microdosimetry is evaluation of statistical distribution of energy deposition events at cellular and sub-cellular levels [11]. The microdosimetric quantity, lineal energy, y is defined as $y = \epsilon / \bar{l}$ where ϵ is energy imparted to the volume of interest by a single energy deposition event and \bar{l} is the mean chord length [12]. $\bar{l} = 2d/3$, where d is site diameter. $f(y)$ is number of events with event size between y and $y + dy$ and $d(y) = yf(y) / \bar{y}_F$ is dose probability density of y .

Methods and Materials

The present study utilized FLUKA code (version 2011 – 3.0) and considered 126 MeV antiproton beam of $5 \times 5 \text{ cm}^2$ field size at the surface of the $20 \times 20 \times 20 \text{ cm}^3$ water phantom. Absorbed dose in water is scored at various depths along the central axis. Similarly, depth-dose profile of 126 MeV protons is also calculated for a comparison. To calculate on-axis microdosimetric distributions at $1 \mu\text{m}$ site size, Tissue-Equivalent Proportional Counter (TEPC) is filled with TE-propane gas of density $7.784 \times 10^{-5} \text{ g/cm}^3$ and is centered at depths $d = 2, 8, 9.5, 11.5$ and 15 cm in the water phantom. 10^{10} primary particles are simulated. Using the calculated microdosimetric distributions, RBE and Q are calculated. The Microdosimetric Kinetic Model (MKM)-based RBE at 10% survival level can be calculated using the equation [12]:

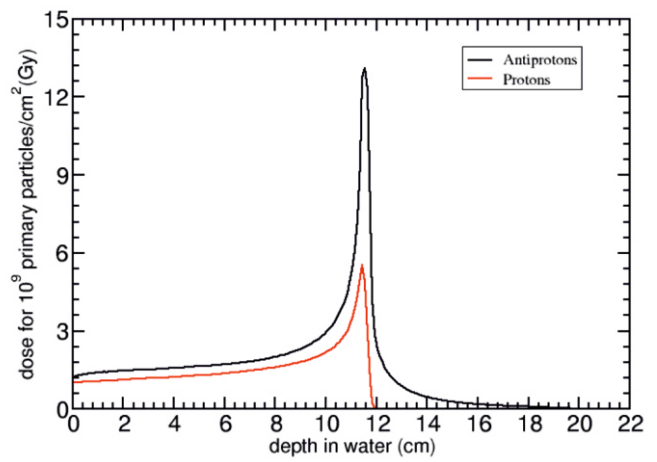


Fig.3: FLUKA-calculated depth–dose profiles in water for 126 MeV antiprotons and protons [6]. The Bragg peak is at 11.5 cm depth.

$$RBE = \frac{\sqrt{\alpha_x^2 - 4\beta_x \ln(0.1)} - \alpha_x}{\sqrt{\alpha_t^2 - 4\beta_t \ln(0.1)} - \alpha_t} \times \frac{\beta_t}{\beta_x}$$

Where $\alpha_x = \alpha_0 + \beta_x z^{*}_{10}$ and z^{*}_{10} is dose-mean specific energy corrected for saturation effect.

The MKM parameters are taken from Kase et al [13] for HSG tumour cell: $\beta_t = \beta_x = 0.05 \text{ Gy}^2$, α_x (200 kV_p X-rays) = 0.19 Gy^{-1} , $r_c = 0.42 \pm 0.04 \mu\text{m}$, $\alpha_0 = 0.13 \pm 0.03 \text{ Gy}^{-1}$, $\rho = 1 \text{ g/cm}^3$ and $y_0 = 150 \text{ keV}/\mu\text{m}$. Q is calculated using the recommendations of ICRU Report 40 [14].

Depth Dose Profile

Fig.3 presents the on-axis depth-dose profiles of 126 MeV antiprotons and protons in water. The Bragg peak appears at about 11.5 cm for both antiprotons and protons. Note that tumor location coincides with the location of Bragg peak. As compared to protons, dose from antiprotons is higher by a factor of 2.6 and 1.3 at the Bragg peak and in the entrance region, respectively.

Microdosimetric Distribution

The microdosimetric distribution is plot of $yd(y)$ on a linear scale versus y on a log-scale. Fig.4 presents on-axis microdosimetric distributions of 126 MeV antiproton at $d = 2, 11.5$ and 15 cm in water. As the depth increases from 2 to 11.5 cm, the kinetic energy of antiproton decreases and hence the peak position of the distributions is shifted toward higher

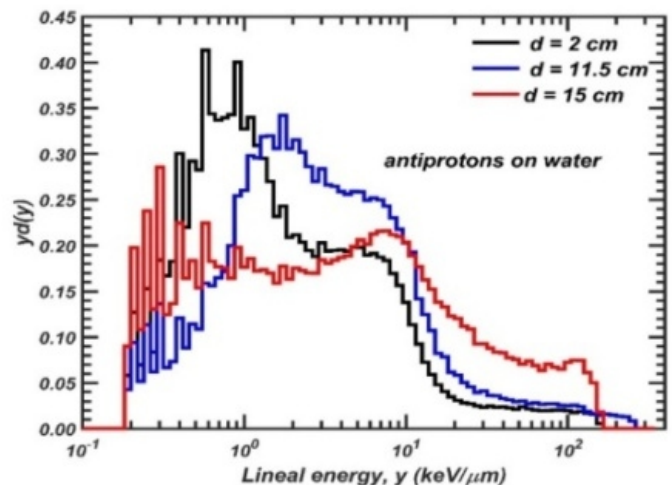


Fig.4: FLUKA-calculated on-axis microdosimetric distributions of 126 MeV antiprotons in water at different depths.

Table 1: Comparison of FLUKA-calculated, values of RBE and \bar{Q} for 126 MeV proton and antiproton.

D (cm)	Proton		Antiproton	
	RBE	\bar{Q}	RBE	\bar{Q}
2	0.98±0.03	0.95±0.004	1.02±0.03	1.66±0.004
8	0.98±0.03	1.01±0.004	1.02±0.03	1.63±0.004
9.5	0.99±0.03	1.14±0.003	1.07±0.03	2.27±0.003
11.5	1.02±0.03	1.51±0.009	1.27±0.03	5.11±0.009
15	1.40±0.02	6.78±0.007	1.11±0.03	4.09±0.007

y-values. The peak height of the distribution at d = 11.5 cm is smaller than that at d = 2 cm. The long tail part in the distribution at d = 11.5 cm is due to the high-LET radiations generated from the annihilation of antiprotons. The distribution at d = 15 cm is spread over a wide range of y-values and there is no prominent peak.

Table 1 presents the FLUKA-calculated on-axis RBE and \bar{Q} values for 126 MeV antiprotons and protons at different depths in water. \bar{Q} and RBE of antiprotons and protons are insensitive to depth in the plateau region. At the Bragg peak, values of RBE and \bar{Q} of antiprotons are higher by a factor of 1.25 and 3.4, respectively, as compared to protons. The enhancement in RBE and \bar{Q} is significant in terms of radiobiological effects.

Conclusion

The study shows that antiproton radiotherapy is advantageous as compared to protons considering enhancements in the absorbed dose, RBE and \bar{Q} at the Bragg peak. However, the annihilation products of antiprotons such as high energy gamma, pions and neutrons are of great concern in terms of shielding and the associated radiation protection issues. Hence, the technical and economic viability of the application of antiprotons for radiotherapy treatment need to be investigated thoroughly.

References

- [1] Gray, L and Kalogeropoulos, T. E. "Possible biomedical applications of antiproton beams: focused radiation transfer" Radiation Research, 1984, 97,246.
- [2] Bassler, N., Holzscheiter, M. H. and Jakel, O. et al. "The antiproton depth-dose curve in water". Physics in Medicine & Biology, 2008, 53, 793–805.
- [3] Bassler, N., Hansen, J. W. and Palmans, H. et al. "The antiproton depth-dose curve measured with alanine detectors". Nuclear Instruments and Methods in Physics Research Section B, 2008, 266, 929-36.
- [4] Bassler, N., Alsner, J., Beyer, G. et al. "Antiproton radiotherapy". Radiotherapy and Oncology, 2008, 86, 14-9.
- [5] Holzscheiter, M. H., Agazaryan, N. and Bassler, N. et al. "Biological effectiveness of antiproton annihilation". Nuclear Instruments and Methods in Physics Research Section B, 2004, 221, 210-4.
- [6] Chattaraj, A. and Selvam, T. P. "Comparison of 126 MeV antiproton and proton – a FLUKA-based microdosimetric approach". Physics in Medicine & Biology, 2022, 67, 185014
- [7] Jackson, G. P. "Practical Uses of Antiprotons". Hyperfine Interactions, 2003, 146/147, 319-23.
- [8] Inokuti, M. "Interactions of antiprotons with atoms and molecules". Nuclear Tracks in Radiation Measurements, 1989, 16, 115-23.
- [9] Lewis, R. A., Smith, G. A. and Howe, S. D. "Antiproton portable traps and medical applications". Hyperfine Interactions, 1997, 107, 155-64.
- [10] Hall, E. J. "Antiprotons for radiotherapy?". Radiotherapy and Oncology, 2006, 81, 231-2.
- [11] ICRU. "Microdosimetry". ICRU report 36 (Bethesda, MD: ICRU), 1983.
- [12] Newpower, M., Patel, D. and Bronk. L. et al. "Using the Proton Energy Spectrum and Microdosimetry to Model Proton Relative Biological Effectiveness". International Radiation Oncology Biology Physics, 2019, 104(2), 316-24.
- [13] Kase, Y., Kanai, T., Matsumoto, Y. et al. "Microdosimetric Measurements and Estimation of Human Cell Survival for Heavy-Ion Beams". Radiation Research, 2006, 166, 629-38.
- [14] ICRU. "The quality factor in radiation protection" ICRU Report 40 (Bethesda, MD: ICRU), 1986.

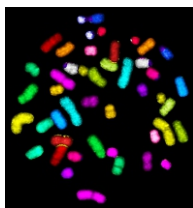
Medical Applications

7

Classical & Molecular Cytogenetics as a Tool for Clinical Investigation of Genetic/Acquired Abnormalities

Rajesh K. Chaurasia, Nagesh N. Bhat and B. K. Sapra*

Radiological Physics and Advisory Division; Health, Safety & Environment Group, Bhabha Atomic Research Centre, Trombay- 400085, INDIA



Metaphase spread probed with 24 color multiplex-FISH

ABSTRACT

In this study, a comparative evaluation of classical and molecular cytogenetics is made with special emphasis on advancement of Fluorescence in-situ hybridization (FISH) based techniques. Cytogenetic investigation of a rare genetic abnormality, wiskott aldrich syndrome (WAS), was carried out in a male child. Results indicated that the subject was prone to genetic instability when challenged with radiation stress. Another case of male-sterility was cytogenetically analyzed, wherein the abnormality detected was the presence of two spots corresponding to sequences of Y-chromosome and this may contribute to the onset of infertility in the individual.

KEYWORDS: Molecular cytogenetics, Fluorescence in-situ hybridization (FISH), Multiplex-FISH, Clinical cytogenetic-investigations, Wiskott aldrich syndrome, Male-sterility

Introduction

Cytogenetics deals with the chromosomal studies, where in fine structure, number and behavior of chromosomes are analysed and related with the respective functions. It defines how structural and numerical chromosomal-abnormalities/changes, lead to development of genetic diseases/abnormalities (inherited and acquired) [1]. Cytogenetics is not a new branch of science, it is deeply rooted in genetics and cytology [2]. With the advancement of precise controlling methods on cell cycle-regulation, preparation of chromosomes, removal of non-target interfering molecules from the cell, development of highly precised DNA/RNA binding fluorescence probes and refined fluorescence techniques for fine capturing and analysis of structural details, cytogenetics has gained a significant advancement in current status of science [3]. Cytogenetics has gained substantial attention in recent years in the field of clinical investigations, for example, understanding the molecular basis of inherited and/or acquired genetic abnormalities, emergence and development of malignancies and cell transformations induced by any physical, chemical or biological agents [4].

Classical Cytogenetics

Conventional cytogenetics had its own glorious era, it was extensively-explored for diagnosis and prognosis of wide spectrum of inherited and acquired genetic abnormalities for several decades [5]. It has also been extensively used for characterization of specific chromosomal aberrations and their correlation on development of clinical syndromes for instance mental retardation, developmental delay, congenital and other anomalies [7]. Conventional karyotyping methods, considered as gold standard, depends on; 1) Giemsa staining of whole chromosome (continuous staining, Fig.1A) and 2) Banding of chromosomes (G and C banding using Giemsa,

Fig.1B). These methods have potential to quantify loss or gain of comparatively bigger (in mega-base pair range) portion of genome, their rearrangements within and between the chromosomes [6]. Metaphase cytogenetics is a major contributor to understand the genetic basis of cancer, its monitoring and tumor staging [8]. In addition, classical cytogenetics has significantly contributed in the field of biodosimetry of planned and unplanned radiation exposures such as medical and accidental exposures [9].

However, conventional cytogenetics is a time consuming and labor-intensive process. It majorly relies on Giemsa staining, which is limited by poor resolution (Fig.1). Clinically relevant submicroscopic chromosomal abnormalities (in kilobase pair range) such as, minor loss (deletion) or gain (insertion) or rearrangements (within or between the chromosomes) remains undetectable [10]. Primarily, a trained or expert cytogeneticist is required to analyze and karyotype G-banded chromosomes [11].

Molecular Cytogenetics

Molecular cytogenetic techniques have evolved as an indispensable addition or even improved alternative to conventional cytogenetics; it enhances interpretation of numerical and complex structural chromosomal aberrations by bridging the gap between conventional and molecular cytogenetics [12].

FISH based molecular cytogenetic techniques can precisely detect, qualitatively and quantitatively, microscopic and submicroscopic genomic changes (in kilobase range, i.e., ~50-100-fold higher than conventional Giemsa staining). With the advanced FISH based techniques, such as development of locus specific and whole chromosome painting probes, spectral karyotyping (multiplex-FISH and multi-BAND-FISH) and Comparative Genome Hybridization (CGH), molecular cytogenetics have emerged as highly-effective diagnostic and research tool [13].

*Author for Correspondence: B. K. Sapra
E-mail: bsapra@barc.gov.in

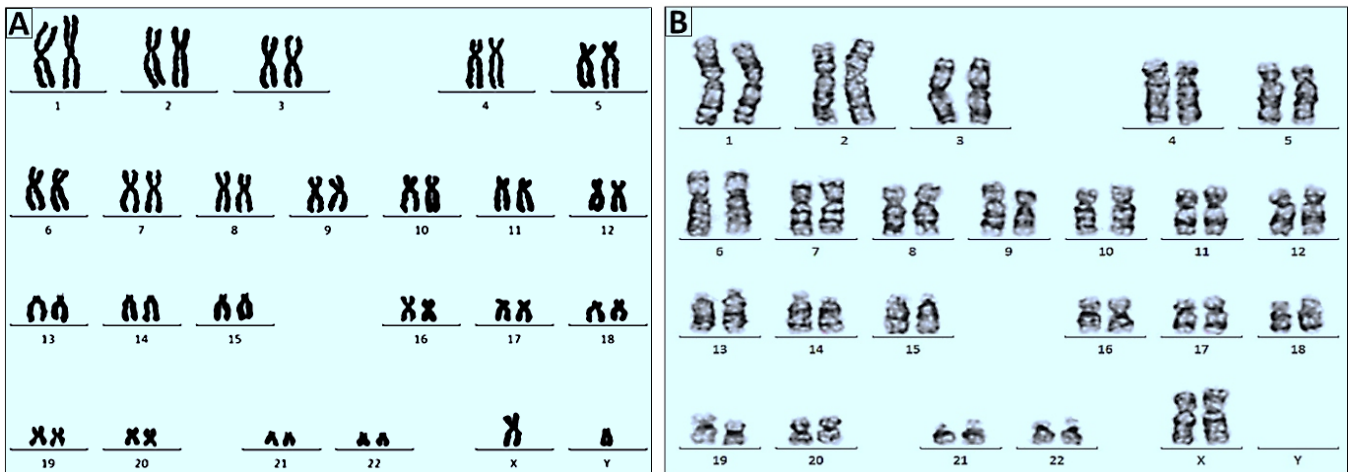


Fig.1: Representative illustrations of (A) A control karyotyped metaphase, having no aberration, stained with Giemsa and (B) A control karyotyped G-banded metaphase, having no aberration, stained with Giemsa.

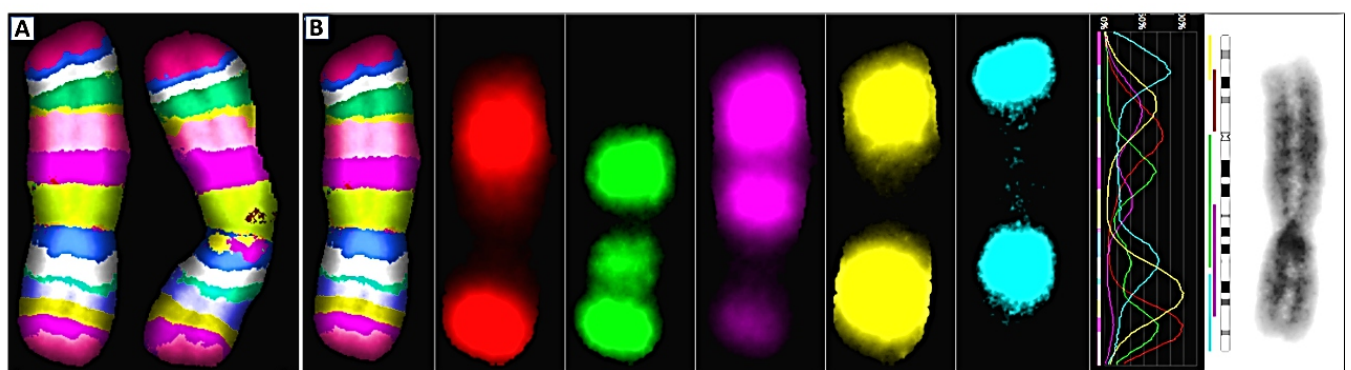


Fig.2: Representative illustrations of (A) A metaphase chromosome pair (second pair), probed with multi-BAND-FISH probes, different regions of the same chromosomes are painted with probes of different colors and (B) Mono-color karyo-gram of chromosome (second pair), observed under different set of filters (total five set of filters were used).

Until recently, detection, identification and quantification of intra-chromosomal changes was limited by poor resolution, as it was based on classical G or R-banding technique. G and R banding is limited to just two alternate light and dark banding patterns. It is tedious and perplexing to identify and quantify, intra-chromosomal and/or complex changes/rearrangements, involving different regions of the same chromosome or different regions of the different chromosomes. An advanced FISH based technique; mBAND-FISH has made this job easy by creating a series of colored bands along the axis of the subject chromosome, which is easy to identify and quantify (Fig.2). It is based on applying region specific partial paint probes, linked with quantitative color ratio analysis (carried out by automated software, ISIS) [14, 15]. Another advance tool, multiplex FISH, covers whole genome, paints all 24 types of human chromosomes with different colors and facilitates detection and quantification of microscopic changes that are genome-wide (Fig.3). FISH based techniques has widened its horizon to multiple directions aiming at different applications by targeting sequences of DNA and RNA [16].

Clinical investigations of human genetic abnormalities

Cytogenetic techniques have been established at the Biodosimetry Laboratory of RPAD, BARC, primarily for biodosimetry of excess exposures of radiation workers to low and high LET radiation. Nonetheless, these techniques are equally useful in evaluation of various clinical parameters. To

demonstrate the potential applications of these techniques in clinical investigations, the established cytogenetic techniques and their dose response curves (generated for various biological indicators) were employed for two cases of inherited genetic abnormalities/instabilities namely, (1) An immunodeficient, wiskott aldrich syndrome (WAS) patient, and (2) A genetically sterile male.

Case study-I: Cytogenetic analysis of wiskott aldrich syndrome:

Wiskott Aldrich Syndrome (WAS) is an X-linked primary immunodeficiency disorder. The gene responsible for WAS is located on the short arm of the X chromosome at Xp11.22-p11.23 [17]. Abnormalities in cell-mediated, humoral, and innate immunity have been observed in WAS patients. This abnormality in immune system majorly involves T lymphocytes. WAS patients are associated with both quantitative and qualitative defects in T and B cells [18,19]. Serum levels of immunoglobulin IgG, IgM, and IgA are often low and IgE levels are often high in patients with WAS [20]. Mutation in WAS gene affects the synthesis and/or activity of WAS protein, this may lead to immunodeficiency, X-linked-neutropenia, autoimmunity, X-linked thrombocytopenia, genomic instability and sometimes hematologic malignancy too [21]. In this study, genetic instability in the blood sample of a immune-deficient male patient suffering from WA-syndrome was carried out by cytogenetic end points, employing reciprocal and nonreciprocal translocations, dicentrics and chromosomal fragments.

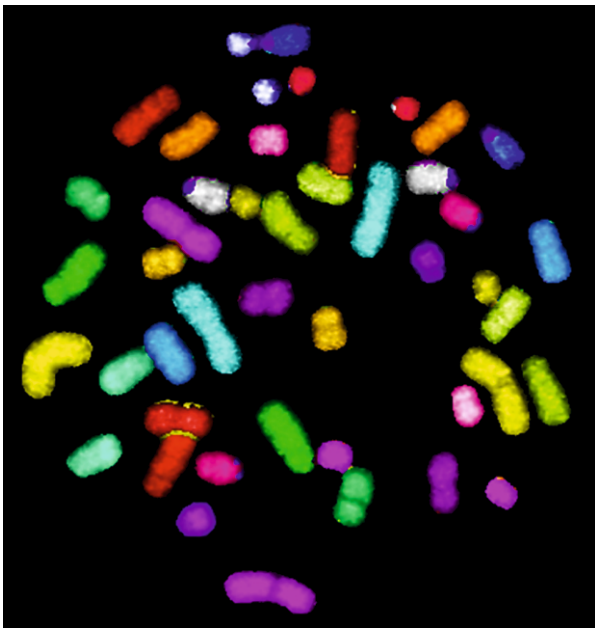


Fig.3: Representative illustration of a metaphase spread probed with 24 color multiplex-FISH; all pairs of the chromosomes are painted with probes of different colors.

Observations

Spontaneous and radiation induced chromosomal aberrations were analyzed in the lymphocytes of the WAS patient and a comparison was made with the lymphocytes of a healthy volunteer (control). No difference in the background frequency of dicentric and chromosomal fragments was observed. Instead, the unirradiated WAS cells possess considerably high yield of chromatid breaks, (~ 5%) in comparison to control sample (none in 500 metaphases analyzed). The reason for presence of excess chromatid break is not very clear, inherent genomic instability in WAS (22), could be the probable reason. Irradiated (2 Gy) WAS sample showed 51% excess yield of dicentrics (Fig.3A and B), 59.1% excess yield of reciprocal translocation (Fig.3C and D) and 80% excess yield of non-reciprocal translocation, in comparison to blood-sample obtained from healthy individual irradiated with the same dose. Dicentrics and translocations are formed as a result of mis-repair of DNA double strand breaks. Overall, 51 to 80% excess mis-repair events were observed in WAS lymphocytes over control lymphocytes. These results indicate that lymphocytes of WAS patients are more sensitive towards radiation in comparison to control lymphocytes and are less efficient in maintaining their chromosomal integrity. These findings are in agreement with recent reports, deciphering R-loop mediated genomic instability in WAS patients [23]. In addition, γ H2AX foci decay kinetics has also shown that, foci persistence is significantly higher in number up to 48 h, after irradiation (data not shown here). In the view of above outcomes, it can be concluded that high radio-sensitivity/genetic instability can lead to higher level of cellular transformation or lethal aberrations and/or other genetic complications in WAS patients.

Case study-II: Cytogenetic investigation of a genetically sterile male:

Sterility in males is not a very rare phenomenon, 7% of the male population suffers with this problem [24]. The aetiology of infertility is majorly known in two-third of the affected population while, in one-third population it still remains unidentified. The usual reason for sterility in males is, chromosomal aberrations (numerical or structural), infection

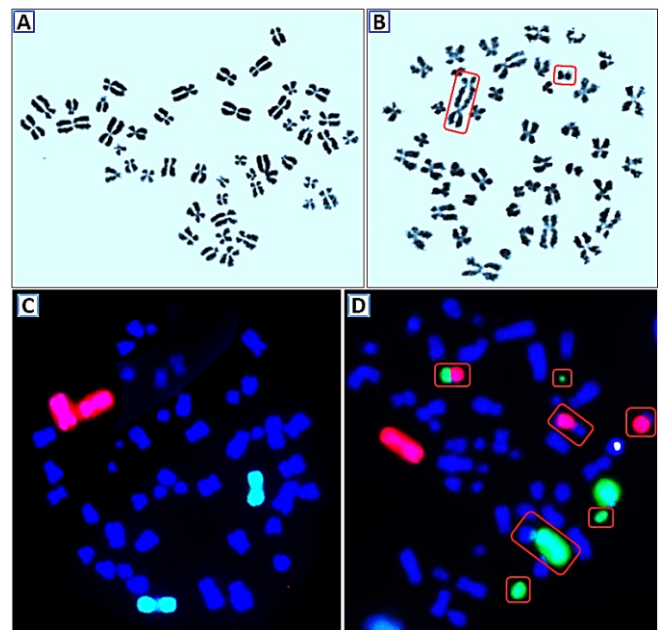


Fig.4: Representative images of lymphocyte-metaphase spread obtained from wiskott aldrich syndrome patient (A) Giemsa stained, control metaphase with no radiation exposure, (B) Giemsa stained metaphase (exposed with 2 Gy) with a dicentric and a fragment. Metaphase spread processed with two color FISH for chromosome pair one and two (first pair hybridized with green probes and second pair hybridized with red probes) (C) Control metaphase with no radiation exposure and (D) Metaphase (exposed with 2 Gy) with multiple aberrations, viz., reciprocal and non-reciprocal translocations, chromosomal fragments involving painted chromosomes.

and/or abnormal gland functioning and over exposure of some environmental stresses [25]. 2 - 14% sterile male population possess chromosomal abnormalities (structural and/or numerical) [26] indicating that chromosomal abnormalities may have profound role in progression of sterility in males.

In this study, cytogenetic analysis, to check the integrity of the chromosomes, was carried out in the blood sample of a subject suffering from infertility (unable to reproduce). Subject was in his fertile age. Intactness/integrity of chromosomes were analyzed by GO-FISH and two color-FISH.

Observations

Cytogenetic analysis, to evaluate the integrity of the chromosomes was carried out in the blood sample of a male subject, using FISH and a comparison was made with the blood sample of a healthy male volunteer. GO-FISH for chromosome-Y was carried out in isolated and unstimulated lymphocytes. Results have shown that subject lymphocytes were possessing two red spots corresponding to Y-chromosome (one large and one small, red spot), per cell (Fig.5B), though control lymphocytes possess only one large red spot per cell (Fig.5A). These findings indicate the presence of two Y-chromosomes of different sizes in each lymphocyte of the subject, which is not normal.

Further analysis was carried out with the metaphase FISH, using whole chromosome paint probe for chromosome-Y in the blood sample of the subject and the healthy control volunteer. Again, two red spots (one large and one small) corresponding to Y-chromosome was observed in metaphases too. Upon analysis of Y-chromosome in metaphases, it was observed that morphology and integrity of Y-chromosome was slightly altered, p arm appeared to be a little shorter than the usual size, as indicated by large red spot observed in GO-FISH. It was also observed that a small region

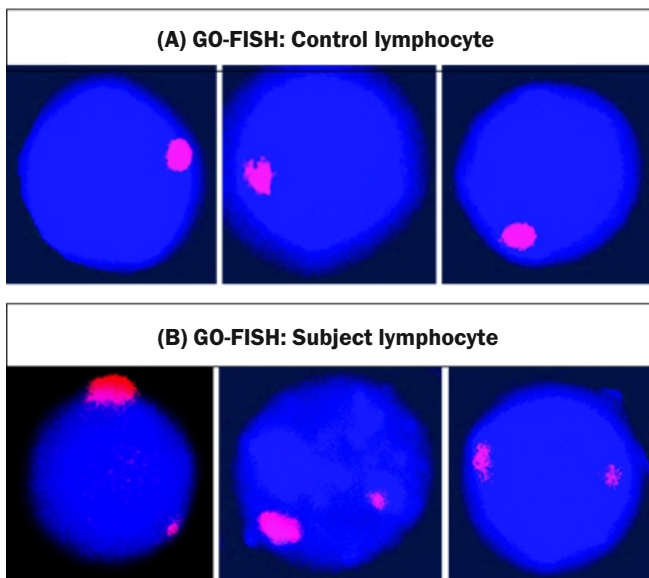


Fig.5: Interphase lymphocytes with GO-FISH, painted with whole chromosome paint probe for Y-chromosome. (A) Lymphocytes from a healthy volunteer (control) with one spot per cell for Y-chromosome. (B) Subject lymphocytes (sample) with two spots of Y-chromosome (one large and one small, red spot) per cell.

of Y-chromosome was translocated to C-group chromosome. This observation, supports the small red spot observed in GO-FISH. As observed, Y-chromosome is morphologically altered and the additional small spot observed may be attributed to translocation of a small region of Y-chromosome with C-group chromosome. In case of control sample (healthy volunteer), only one large red spot, with intact morphology of Y-chromosome, was observed, as in GO-FISH, which is normal. No translocations or morphological changes are observed in metaphase of normal individual.

Terminal region of p-arm of Y-chromosome, possess crucial sex determining genes (SRY genes) and hence is pronounced as sex-determining region of Y (27). In this case study, sex-determining region of Y is translocated to C-group chromosome, this change in the location of these crucial genes, may be affecting the functioning of these sex determining genes and may be contributing to genetic basis of sterility in the subject. Further investigations may be warranted to make final conclusion of this case study.

Conclusion

In former decades, innovative technical advancements in cytogenetics, have substantially enhanced the detection and quantification of chromosomal aberrations/changes and potentially-facilitated in clinical and non-clinical investigations. FISH based techniques, in combination with karyotyping, have played central role in these technical advancements. Molecular cytogenetics have expanded beyond FISH, such as, comparative genomic hybridization (CGH), which offers genome wide screening with better resolution and high precision.

In this study, cytogenetic investigation clearly demonstrated genetic instability in a pediatric case of WA-syndrome and chromosomal basis of sterility in a male patient. Similarly, other human genetic abnormalities like, Severe Combined Immunodeficiency (SCID), Fanconi anaemia and different forms of malignancies can be investigated employing these advanced cytogenetic techniques to understand the genetic/chromosomal basis and possible consequences of these severe diseases/syndromes.

Acknowledgement

The authors of the article would like to thank and express their sincere gratitude for constant encouragement and technical supports received from all the members of Environment and Biodosimetry Section of RP&AD.

References

- [1] Fechheimer, N. S., 1968. Consequences of chromosomal aberrations in mammals. *Journal of Animal Science*, 27(suppl_1), 27-50.
- [2] Kannan, T. P. and Alwi, Z. B., 2009. Cytogenetics: past, present and future. *Malaysian Journal of Medical Sciences*, 16(2).
- [3] ISO 20046:2019(Main) Radiological protection – Performance criteria for laboratories using Fluorescence In Situ Hybridization (FISH) translocation assay for assessment of exposure to ionizing radiation.
- [4] Wan, T. S., 2017. Cancer cytogenetics: An introduction. *Cancer Cytogenetics*, 1-10.
- [5] Ozkan, E. and Lacerda, M. P., 2020. Genetics, Cytogenetic Testing And Conventional Karyotype.
- [6] Kang, J. U. and Koo, S. H., 2012. Evolving applications of microarray technology in postnatal diagnosis. *International journal of molecular medicine*, 30(2), pp.223-228.
- [7] Nowakowska, B. and Bocian, E., 2004. Molecular cytogenetic techniques and their application in clinical diagnosis. *Medycynawiekurozwojowego*, 8(1), 7-24.
- [8] Malla, T. M., Najar, A. H., Masoodi, S. R. and Shah, Z. A., 2022. Cytogenetics: a reliable tool for the diagnosis and prognosis of hematological malignancies. *JMS SKIMS*, 25(2).
- [9] Ainsbury, E., Barquinero, J. F., Beinke, C., Blakely, W. F., Braselmann, H., Carr, Z., Di Giorgio, M., Fenech, M., Garcia, L. O., Kodama, Y. and Lindholm, C., 2011. Cytogenetic dosimetry: applications in preparedness for and response to radiation emergencies.
- [10] Martin, C. L. and Warburton, D., 2015. Detection of chromosomal aberrations in clinical practice: from karyotype to genome sequence. *Annual Review of Genomics and Human Genetics*, 16, 309-326.
- [11] Yang, X., Wen, D., Wu, X., Zhao, Z., Lacny, J. and Tseng, C., 2010. A comprehensive cytogenetics tutorial program, encompassing changeable G-band resolutions. *Computer methods and programs in biomedicine*, 99(1), 66-74.
- [12] Liehr, T., 2021. Molecular cytogenetics in the era of chromosomics and cytogenomic approaches. *Frontiers in Genetics*, 1944.
- [13] Balajee, A. S. and Hande, M. P., 2018. History and evolution of cytogenetic techniques: Current and future applications in basic and clinical research. *Mutation Research/Genetic Toxicology and Environmental Mutagenesis*, 836, 3-12.
- [14] Chudoba, I., Plesch, A., Lörch, T., Lemke, J., Claussen, U. and Senger, G., 1999. High resolution multicolor-banding: a new technique for refined FISH analysis of human chromosomes. *Cytogenetic and Genome Research*, 84(3-4), 156-160.
- [15] Johannes, C., Chudoba, I. and Obe, G., 1999. Analysis of X-ray-induced aberrations in human chromosome 5 using high-resolution multicolour banding FISH (mBAND). *Chromosome Research*, 7(8), 625-633.
- [16] Shakoori, A.R., 2017. Fluorescence in situ hybridization (FISH) and its applications. In *Chromosome Structure and Aberrations* (343-367). Springer, New Delhi.

- [17] Buchbinder, D., Nugent, D. J. and Fillipovich, A. H., 2014. Wiskott-Aldrich syndrome: diagnosis, current management, and emerging treatments. *The application of clinical genetics*, 7, 55.
- [18] Humblet-Baron, S., Sather, B., Anover, S., Becker-Herman, S., Kasprowicz, D. J., Khim, S., Nguyen, T., Hudkins-Loya, K., Alpers, C. E., Ziegler, S. F. and Ochs, H., 2007. Wiskott-Aldrich syndrome protein is required for regulatory T cell homeostasis. *The Journal of clinical investigation*, 117(2), 407-418.
- [19] Prete, F., Catucci, M., Labrada, M., Gobessi, S., Castiello, M. C., Bonomi, E., Aiuti, A., Vermi, W., Cancrini, C., Metin, A. and Hambleton, S., 2013. Wiskott-Aldrich syndrome protein-mediated actin dynamics control type-I interferon production in plasmacytoid dendritic cells. *Journal of Experimental Medicine*, 210(2), 355-374.
- [20] Blaese, R. M., Strober, W., Levy, A. L. and Waldmann, T. A., 1971. Hypercatabolism of IgG, IgA, IgM, and albumin in the Wiskott-Aldrich syndrome: a unique disorder of serum protein metabolism. *The Journal of Clinical Investigation*, 50(11), 2331-2338.
- [21] Bosticardo, M., Marangoni, F., Aiuti, A., Villa, A. and Grazia Roncarolo, M., 2009. Recent advances in understanding the pathophysiology of Wiskott-Aldrich syndrome. *Blood, The Journal of the American Society of Hematology*, 113(25), 6288-6295.
- [22] Notarangelo, L. D., Miao, C. H. and Ochs, H. D., 2008. Wiskott-aldrich syndrome. *Current opinion in hematology*, 15(1), 30-36.
- [23] Sarkar, K., Han, S. S., Wen, K. K., Ochs, H. D., Dupré, L., Seidman, M. M. and Vyas, Y. M., 2018. R-loops cause genomic instability in T helper lymphocytes from patients with Wiskott-Aldrich syndrome. *Journal of Allergy and Clinical Immunology*, 142(1), 219-234.
- [24] Claman, P., 2004. Men at risk: occupation and male infertility. *Fertility and sterility*, 81, 19-26.
- [25] Dohle, G. R., Colpi, G. M., Hargreave, T. B., Papp, G. K., Jungwirth, A., Weidner, W.E.A.U. and EAU Working Group on Male Infertility, 2005. EAU guidelines on male infertility. *European urology*, 48(5), 703-711.
- [26] Ravel, C., Berthaut, I., Bresson, J. L. and Siffroi, J. P., 2006. Prevalence of chromosomal abnormalities in phenotypically normal and fertile adult males: large-scale survey of over 10 000 sperm donor karyotypes. *Human Reproduction*, 21(6), 1484-1489.
- [27] Capel, B., Rasberry, C., Dyson, J., Bishop, C. E., Simpson, E., Vivian, N., Lovell-Badge, R., Rastan, S. and Cattanach, B. M., 1993. Deletion of Y chromosome sequences located outside the testis determining region can cause XY female sex reversal. *Nature genetics*, 5(3), 301-307.

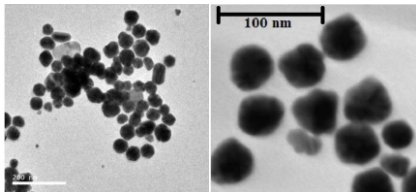
Medical Applications

8

Dosimetry in Nanoparticles-aided Radiotherapy

Nitin Kakade, Rajesh Kumar, S. D. Sharma*, Rajesh K. Chaurasia, N. N. Bhat and B. K. Sapra

Radiological Physics and Advisory Division; Health, Safety & Environment Group, Bhabha Atomic Research Centre, Trombay – 400085, INDIA



TEM images of gold and silver NPs

ABSTRACT

In nanoparticles-(NPs) aided radiotherapy, cancer cells selectively receive higher radiation dose due to high-Z NPs (gold and silver). Analytical and MC computation shows similar dose enhancement for gold and silver for photon energy ranging from 50-70 keV. Hence, silver can be a cost-effective alternative to gold for NPs-aided brachytherapy using ^{170}Tm source. For dosimetric verification, a method using in-house synthesised NPs-loaded alginate film and unlaminated radiochromic film is explored. Further, radiation sensitivity of in-house synthesized Tryptophan-coated gold NPs and Gallic-acid coated silver NPs are investigated using in-vitro measurement.

KEYWORDS: Dose enhancement, NPs-aided radiotherapy, unlaminated film dosimetry

Introduction

Radiotherapy (RT) is one of the important modality for cancer treatment. However, the lack of selectivity between the tumor and the normal cells is one of the main limitation of RT [1]. In the treatment of radioresistant tumour, relatively higher radiation dose is required. The delivery of higher tumor dose is limited due to the lower tolerance dose of the normal cells present in the vicinity of the tumor [2]. This problem can be solved by making tumour more radiosensitive compare to the healthy tissues. The radiosensitisation of the tumour can be achieved by infusing nanoparticles (NPs) in the tumour. Due to the hypoxic nature of tumour, the tumor vascularization structure has high porosity (pore size ~ 400 nm). The size of NPs (10-100 nm) being smaller than this pore size can passage from blood to the tumor cells and accumulate there. The preferential accumulation of NPs inside the tumor cells can be achieved via active and passive targeting methods [3]. The NPs of high atomic number with superior biocompatibility are preferred radio-sensitizing agents [4].

The therapeutic technique of increasing radio-sensitivity of cancer cells due to the infusion of NPs is known as NPs-aided RT [5]. The dose enhancement factor (DEF), ratio of dose to the tumor infused with and without NPs, is used to measure the radio-sensitivity. The dose enhancement in the tumour can be attributed to higher photoelectric cross section of high-Z NPs present in the tumour. As the photoelectric cross section is higher at lower energies, the low energy photon emitting brachytherapy sources or similar modalities producing photon/X-rays of lower energy are useful for NPs-aided RT.

Dose enhancement studies for clinical brachytherapy sources: Monte Carlo study

Gold NPs (AuNPs) are being used as radio-sensitizer due to their high-Z and bio-compatibility. However, they are relatively expensive and there is a need of cost effective alternatives to AuNPs. In recent years, the bio-compatible silver NPs (AgNPs) have been developed. To study the equivalence between AuNPs and AgNPs in terms of dose enhancement, the

DEFs were estimated for photons ranging from 20 to 1250 keV using EGSnc based Monte Carlo code. Almost same dose enhancements were observed for AuNPs and AgNPs at photon energies ranging from 50-70 keV (Fig.1) [6]. ^{170}Tm source (E_{avg} : 66.7 keV) lies in this optimal energy range. Hence, the dose enhancements in the prostate tumour for ^{170}Tm and other low energy brachytherapy sources were estimated (Table 1).

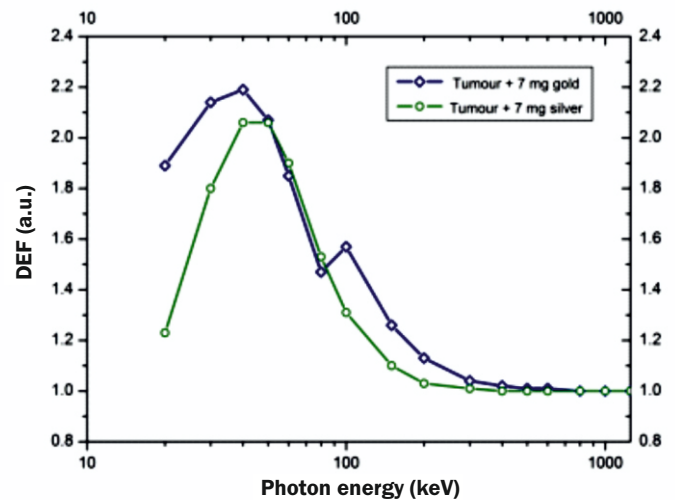


Fig.1: Comparison of DEFs for tumour infused with gold and silver.

Table 1: Monte Carlo estimated dose enhancement factor for brachytherapy sources.

Brachytherapy Source	Average DEF (Gold)	Average DEF (Silver)
^{170}Tm (E_{avg} : 66.7 keV)	1.94 ± 0.01	1.92 ± 0.01
^{125}I (E_{avg} : 28 keV)	1.98 ± 0.01	1.56 ± 0.01
50 kVp (E_{avg} : 66.7 keV)	2.06 ± 0.01	1.61 ± 0.01
^{103}Pd (E_{avg} : 21 keV)	1.60 ± 0.01	1.17 ± 0.01
^{169}Yb (E_{avg} : 93 keV)	1.65 ± 0.01	1.57 ± 0.01

*Author for Correspondence: S. D. Sharma
E-mail: sdsharma@barc.gov.in

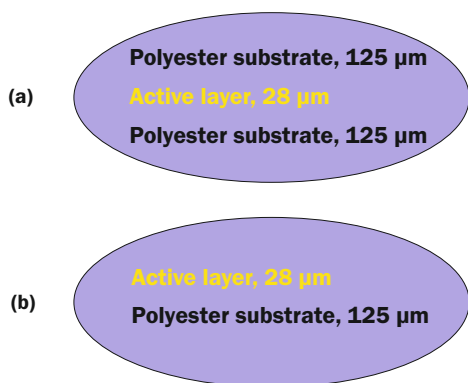


Fig.2: Schematic diagram of (a) laminated and (b) un laminated Gafchromic EBT3 film.

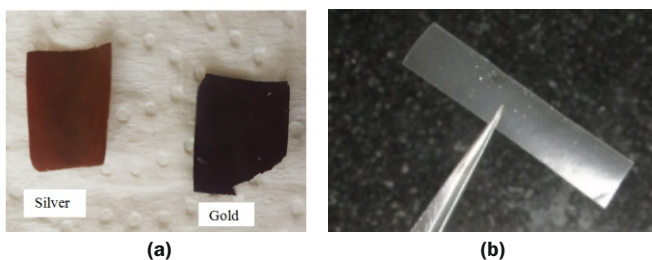


Fig.3: (a) Photograph showing pieces of silver nanoparticles embedded alginate film (left) and gold nanoparticles embedded alginate film (right) and (b) Alginate film.

In the case of ^{170}Tm source, DEFs of 1.94 ± 0.01 and 1.92 ± 0.01 were recorded for AuNPs and AgNPs, respectively [7]. Hence, the AgNPs can be cost effective alternatives to AuNPs when the treatment is delivered using ^{170}Tm brachytherapy source.

Experimental Measurement of DEFs

The routinely used radiochromic film dosimeters (e.g. Gafchromic EBT3 film) find limited applications as the dose enhancement is mainly driven by low range photoelectrons and Auger electrons produced in the immediate micro-environment of NPs. The polyester layer (125 μm) present in Gafchromic EBT3 film makes dose enhancement difficult to measure. Hence, Gafchromic EBT3 film was customized (i.e. un laminated film) by ISP technologies, USA, on our request (Fig.2). This customized film, *un laminated EBT3 film*, was explored for the quantification of dose enhancement.

For the dosimetric measurement, AuNPs-embedded alginate film (AuNPs-Alg film) and AgNPs-embedded alginate film (AgNPs-Alg film) were synthesised (Fig.3). These films were characterised using standard technique. The surface plasmon resonance (SPR) at 400 nm and 550 nm was recorded for AgNPs and AuNPs, respectively during UV-Vis absorption spectroscopy. The Atomic Force Microscopy measured average particle size of AgNPs and AuNPs were found to be 13 ± 2 nm and 15 ± 2 nm, respectively.

The combination of NPs-embedded films and un laminated EBT3 film was explored for the measurement of DEFs for ISO wide spectrum X-rays (E_{avg} ranging from 57 to 137 keV), high energy X-rays (6 and 10 MV) and 50 kVp X-rays generated by electronic brachytherapy device. The un laminated EBT3 film can able to measure the dose enhancement (Max DEF of 29%) [8, 9]. However, the laminated film could not measure any kind of dose enhancement.

Dose Enhancement Using In-vitro Measurement

Tryptophan-coated AuNPs (Trp-AuNPs) and Gallic-acid coated AgNPs (Gal-AgNPs) were synthesised in-house (Fig.4).

The SPR of AuNPs and AgNPs was recorded at 550 nm and 420 nm, respectively. TEM measured average particle size of AuNPs and AgNPs was 49.5 ± 5.1 nm and 40.5 ± 3.1 nm, respectively. The cytotoxicity and time dependent absorption of NPs in breast carcinoma cells (MCF-7 cells) was studied to optimise the parameter required for higher radiosensitization at lower cytotoxicity. Depending on the % cell viability (Trp-AuNPs: 93.85 to 89% and Gal-AgNPs: 85.98 to 82.10 %) at different concentrations, NPs concentration of 0.5 mM was optimised to attain % cell viability $\geq 85\%$. The time dependant absorption of NPs shows that the internalisation of NPs increased rapidly up to 24 hr (Fig.5). Hence, 24 hr time interval between NPs infusion and radiation delivery was optimised.

Fig.6 shows the % cell survival of breast carcinoma cells due to radiation dose from low energy X-rays (30, 57 and 104 keV) and high energy gamma rays from telecobalt unit.

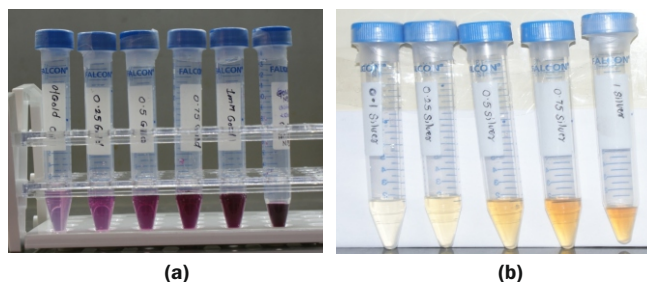


Fig.4: Photographs showing different concentrations of (a) gold NPs and (b) silver NPs.

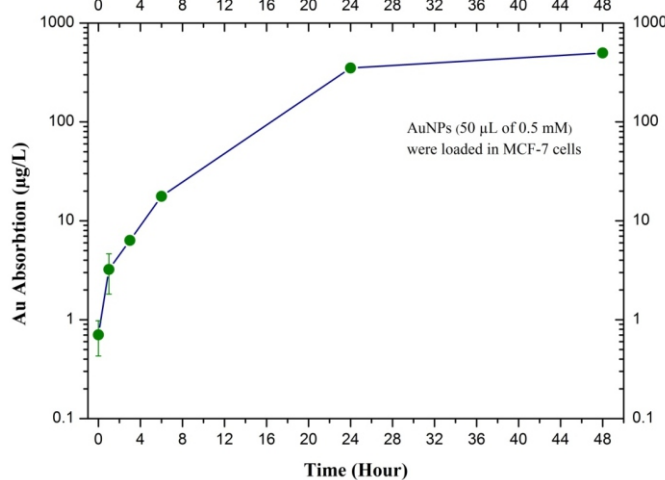


Fig.5: Time dependant absorption of Trp-AuNPs.

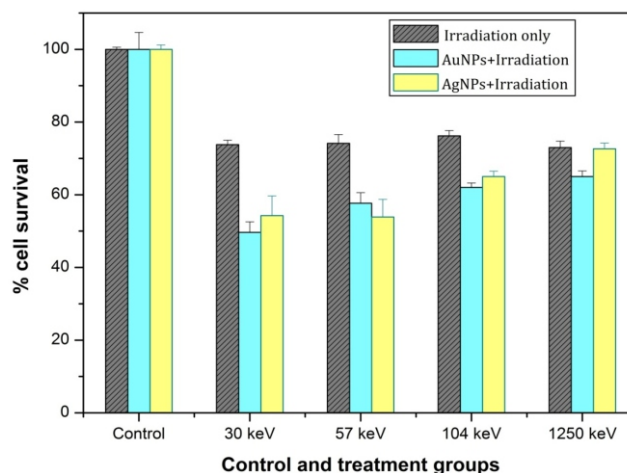


Fig.6: Cell survival of control group and treatment groups.

The radiation sensitivity of 1.50 to 1.23 (Trp-AuNPs) and 1.35 to 1.17 (Gal-AgNPs) was observed for X-rays ranging from 30-104 keV. However, high energy gamma rays could not show radio-sensitisation effect.

Conclusion

The significant dose enhancement is observed for low energy photons. Hence, ^{170}Tm based brachytherapy, 50 kVp X-rays from electronic brachytherapy and/or similar modalities producing X-ray or gamma radiations of optimal energy can be used for NPs-aided RT. A proposed dosimetry method of using unlaminated radiochromic film can be used to measure DEFs. Further, Trp-AuNPs and Gal-AgNPs can be used as a radio sensitizer for NPs-aided RT. However, our results are based on an *in-vitro* measurement. The detailed investigations using *in-vivo* techniques and detailed clinical trials are necessary before its clinical use.

References

- [1] Pottier, A., E. Borghi, and L. Levy, The future of nanosized radiation enhancers. *The British journal of radiology*, 2015, 88 (1054), 20150171-20150171.
- [2] Prasanna, P.G.S., et al., Normal tissue protection for improving radiotherapy: Where are the Gaps? *Translational cancer research*, 2012, 1(1),35-48.
- [3] Qian, X., et al., In vivo tumor targeting and spectroscopic detection with surface-enhanced Raman nanoparticle tags. *Nat Biotechnol*, 2008, 26(1), 83-90.
- [4] Zein, R., W. Sharrouf, and K. Selting, Physical Properties of Nanoparticles That Result in Improved Cancer Targeting. *Journal of Oncology*, 2020, 2020, 5194780.
- [5] Porcel, E., et al., Platinum nanoparticles: a promising material for future cancer therapy? *Nanotechnology*, 2010, 21(8), 085103.
- [6] Kakade, N. R., et al., Cost effectiveness of silver nanoparticle over gold nanoparticle in nano-particle aided radiotherapy. *Journal of Medical Physics*, 2018, 43(suppl1),72.
- [7] Kakade, N. R., et al., Equivalence of silver and gold nanoparticles for dose enhancement in nanoparticle-aided brachytherapy. *Biomed. Phys. Eng. Express*, 2019. 5(5): p. 055015.
- [8] Kakade, N. R., et al., Application of unlaminated EBT3 film dosimeter for quantification of dose enhancement using silver nanoparticle-embedded alginate film, *Biomed. Phys. Eng. Express*, 2022, 8, 035014.
- [9] Kakade, N. R., et al., Measurement of dose enhancement factor for Xoft electronic brachytherapy device using nanoparticle embedded alginate film and radiochromic film, *J Can Res Ther*, 2021, (doi: 10.4103/jcrt.jcrt_207_21).

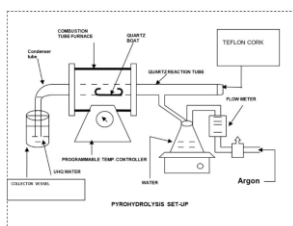
Emergency Preparedness

9

Nuclear Forensics Approach to Address Nuclear Emergencies & Radiological Preparedness

S. Mishra^{*1}, R. S. Sathyapriya¹, Amar Pant¹, Sukanta Maity¹, Sandeep Police¹, Amit Kumar Verma¹, R. K. Prabhath², Jis Romal Jose², Anilkumar S. Pillai¹ and A. Vinod Kumar¹

¹Environmental Monitoring and Assessment Division, ²Radiation Safety Systems Division; Health, Safety and Environment Group, Bhabha Atomic Research Centre, Trombay – 400085, INDIA



Pyro-hydrolysis setup

ABSTRACT

HSEG, BARC has taken the initiative to develop reference library of forensic signatures in front end nuclear materials. Analytical methods have been developed for elemental, isotopic, anionic, radiological and chronological characterization of uranium rich materials. Uranium mine and mill samples have been collected from different locations in India and analyzed for different Nuclear Forensic (NF) signatures to generate India-specific NF library. Artificial intelligence and machine learning based NF analysis tool has been developed in-house for signature pattern tracking and possible origin assessment.

KEYWORDS: Nuclear and Radiological Threats, Nuclear forensics, Nuclear material

Introduction

Nuclear Forensic Analysis (NFA) is an interdisciplinary science requiring collection of information from various stages of nuclear fuel cycle, production of radioactive sources, expertise in various domains of physico-chemical analysis and interpretation. NFA involves comprehensive characterization of the Nuclear Material (NM) or radioactive material found out of regulatory control and comparison with reference information. It provides clues for tracing the history, origin and intended use of the material, which ultimately supports the investigating agency in the prosecution of those responsible. Provenance determination of an interdicted material is a vital step in Nuclear Forensic investigation. Therefore, it is required to have a National Nuclear Forensic Library (NNFL) of the NF signatures (elemental, anionic, isotopic composition, morphology etc.) of the nuclear material encountered in nuclear fuel cycle starting from uranium ore.

Important NF signatures, techniques used for their measurement, derived information and the references used for interpretation are given in the illustration in the following page. For generation of NNFL and to identify the characteristic signatures in front end nuclear fuel cycle materials, representative U-mine and mill samples from operational plants have been collected including U-ore and Uranium Ore Concentrate (UOC) samples. UOC commonly known as yellow cake, comprises sodium di uranate (SDU), magnesium di uranate (MDU), ammonium di uranate (ADU), uranyl oxides, uranyl peroxides etc. and are the starting material for nuclear fuel production. These materials are of high interest from forensic point of view and are the most intercepted material [1]. These compounds are produced by mining and milling of uranium ore or from secondary sources like phosphorites and other sources.

A large number of samples from these sources were collected and characterized for different NF signatures.

Radio-analytical Techniques in NF Analysis

In direct Radiometric techniques, alpha or gamma spectrometry are used directly to measure the characteristic radiation in the samples, whereas in indirect methods nuclei of the element of interest is either excited or activated to emit radiation which is then used to quantify the elemental concentration in the sample. Particle Induced Gamma Emission (PIGE) and Neutron Activation Analysis (NAA) are two such techniques used for quantifying elemental composition in the bulk matrix.

Gamma Spectrometry

P-type High Purity Germanium (HPGe) detector with carbon window having a relative efficiency of 60% and 50% HPGe with Al window are used. Digital spectrometric device with Multi-Channel Analyser (MCA) and spectral analysis InterWinner 8.0 and Gamma Vison software are used for the characterisation.

In secular equilibrium matrix (^{238}U – $^{234\text{m}}\text{Pa}$), the gamma energies 63.3 keV (3.7%) of ^{234}Th , 766 keV (0.317%) and 1001 keV (0.842%) of daughter $^{234\text{m}}\text{Pa}$, are considered for analytical purposes [2]. The prominent gamma energies emitted by ^{235}U are 143.7 keV (10.96%), 163.3 keV (5.08%), 185.7 keV (57.2%) and 205.3 keV (5.01%). The 185 keV gamma-line of ^{235}U and 1001 keV gamma-line $^{234\text{m}}\text{Pa}$ are used for the estimation of ^{235}U and ^{238}U concentration, respectively. Fig. 1 shows the gamma spectrum of U metal samples.

Presence of fission products or activation products, ^{236}U and ^{232}U in the investigated samples gives the clue to the production history and initial feed of the sample [3].

Alpha Spectrometry

Alpha spectrometry (AS) is used for quantifying both short lived ^{210}Po , ^{232}U , ^{228}Th and ^{238}Pu and long-lived ^{238}U and ^{230}Th radionuclides, for uranium isotopic composition analysis and radiochronometry.

*Author for Correspondence: S. Mishra
E-mail: suchim@barc.gov.in

Parameter	Measurement Method	Information	Interpretation by comparison
Uranium isotopes and ratio	AS, TIMS, MC-ICP-MS, SIMS, AMS, RIMS	Intended use, origin	NFL
Plutonium isotopes and ratio	AS, HRGS, TIMS, MC-ICP-MS, SIMS, RIMS	Type of reactor	Model Calculations, NFL
Radionuclide impurities	HRGS	Process history, Irradiation status	NFL
Metallic impurities (Concentration, patterns)	ICP-MS, ICP-OES, GD-MS, GF-AAS, NAA, EDXRF, PIGE	Process history, Origin	Process Knowledge, NFL, known samples
Anionic Impurities	Ion Chromatograph	Process history, Origin	Process Knowledge, NFL, known samples
Stable isotope ratios (Nd, Sr, Pb, O, S)	TIMS, MC-ICPMS, HR-ICP-MS, IRMS	Origin, Process history	NFL, known samples
Macroscopic appearance	Optical Microscopy	Process history	Process knowledge
Microscopic appearance	SEM, TEM	Process history	Process Knowledge, NFL, known samples
Radio isotopes	HRGS, LSC, AS, ICP-MS	Intended use, Age	Model Calculations
Non-metallic impurities	GC-MS	Process history	Process Knowledge, NFL, known samples
Particle analysis	SIMS, FT-TIMS	Origin, Process history	Process Knowledge, NFL, known samples

NFL: Nuclear Forensic Library, AS: Alpha Spectrometer, TIMS: Thermal Ionisation Mass Spectrometer, MC-ICP-MS: Multi Collector-Inductively Coupled Plasma Mass Spectrometer, SIMS: Secondary Ionisation Mass Spectrometer, AMS: Accelerator Mass Spectrometer, RIMS: Resonance Ionisation Mass Spectrometer, HRGS: High Resolution Gamma Spectrometry, ICP-OES: Inductively Coupled Plasma Optical Emission Spectrometry, GD-MS: Glow Discharge Mass Spectrometer, NAA: Neutron Activation Analysis, EDXRF: Energy Dispersive X Ray Fluorescence, PIGE: Particle Induced Gamma Emission, HR-ICP-MS: High Resolution- Inductively Coupled Plasma Mass Spectrometer, IRMS: Isotope Resolution Mass Spectrometer, SEM: Scanning Electron Microscope, TEM: Transmission Electron Microscope, LSC: Liquid Scintillation Counter, GC-MS: Gas Chromatograph-Mass Spectrometer, FT-TIMS: Fourier Transform-Thermal Ionisation Mass Spectrometer.

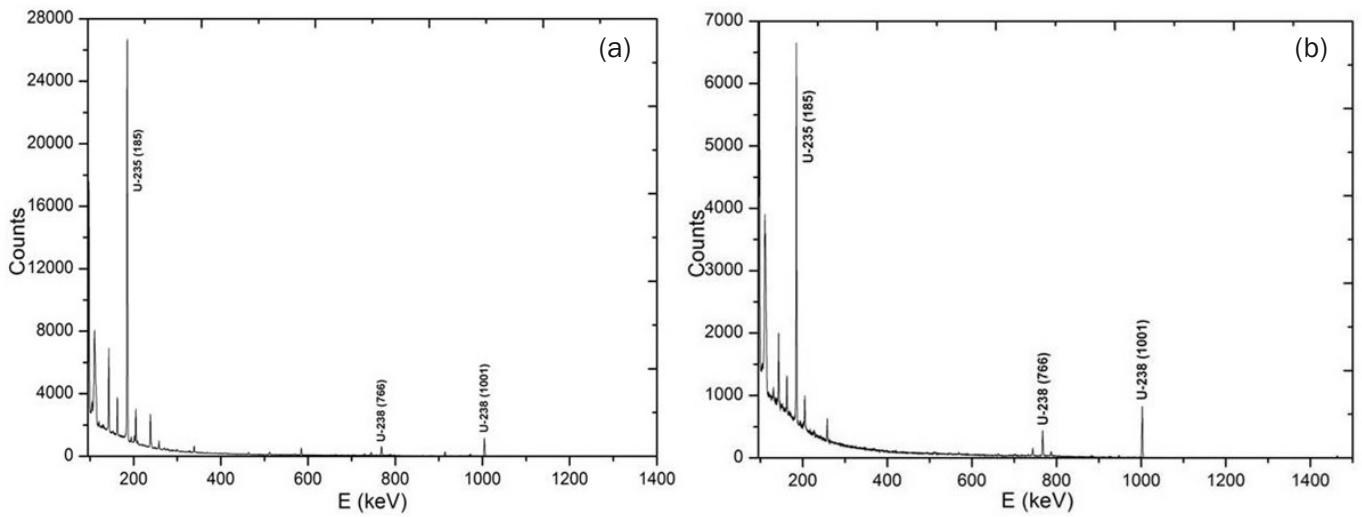


Fig.1: Gamma spectrum of investigated Natural Uranium (left) and Depleted Uranium (right) samples.

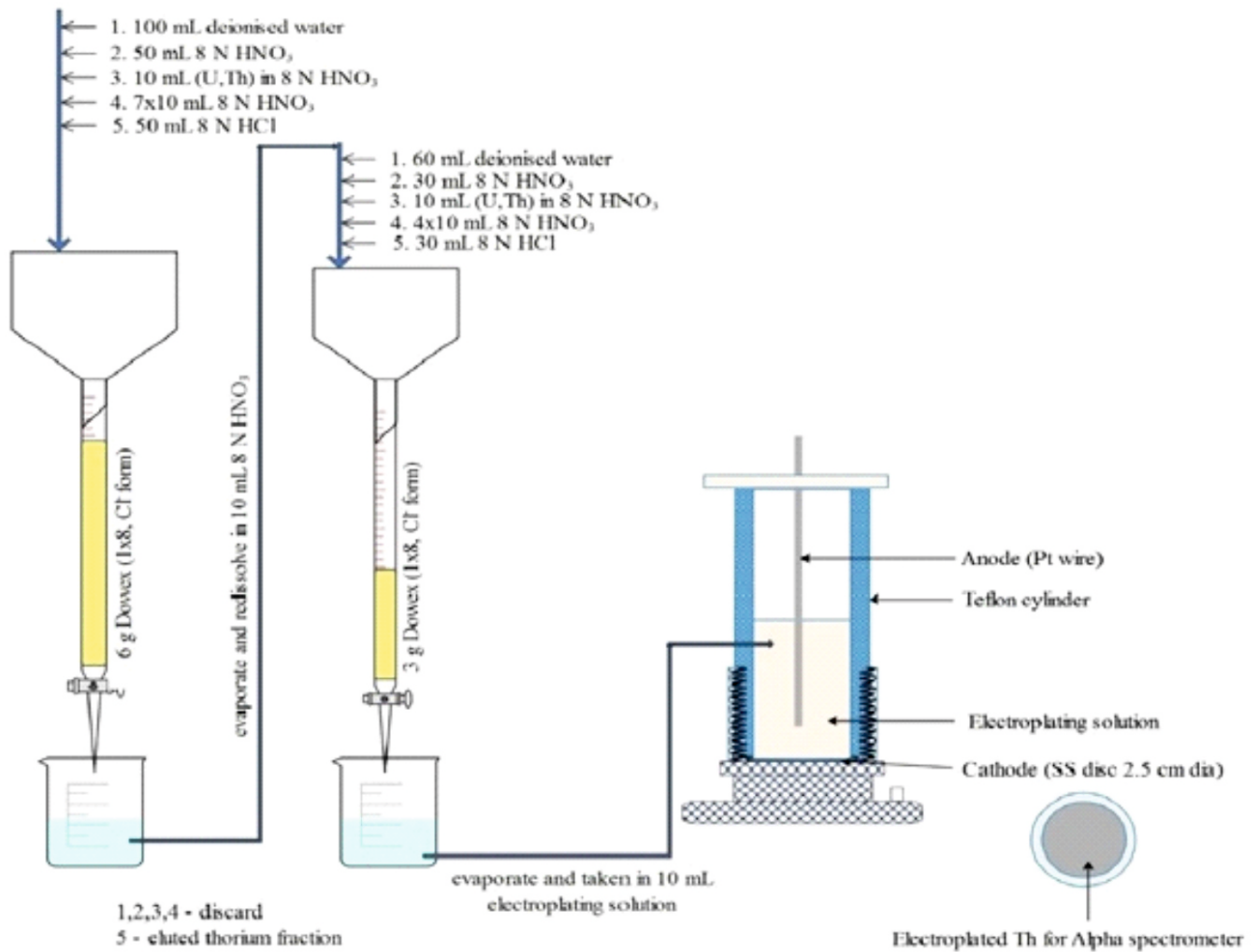


Fig.2: Schematics of anion exchange purification method for thorium and electrodeposition.

A radiochemical method with double column separation was developed using Isotope Dilution-AS for age determination of natural U metal samples using ^{234}U and ^{230}Th parent daughter ratio, with age history from 11 to 50 years. Schematics of thorium purification from bulk uranium metal is depicted in Fig.2. The age of U-metal confiscated from public domain was thus estimated to be 39 ± 4 years [4]. The typical alpha spectrum for nat U and Depleted U samples are shown in Fig.3. Flow-chart of the method to quantify ^{210}Po in various biological samples like hair, blood and teeth for preparedness for polonium poisoning incidents is shown in Fig.4 [5].

Particle Induced Gamma Emission(PIGE)

The external (in air) PIGE setup installed at FOlded Tandem Ion Accelerator (FOTIA), BARC was used for the determination of low Z elements like Al, Si, Na and F in Uranium ore powder samples for NFL.

Cellulose based hydraulic pelletization was replaced by Mylar packed samples for current normalization of low energy proton beam was done using 25 μm tantalum window of the FOTIA setup shown in Fig.5 [6].

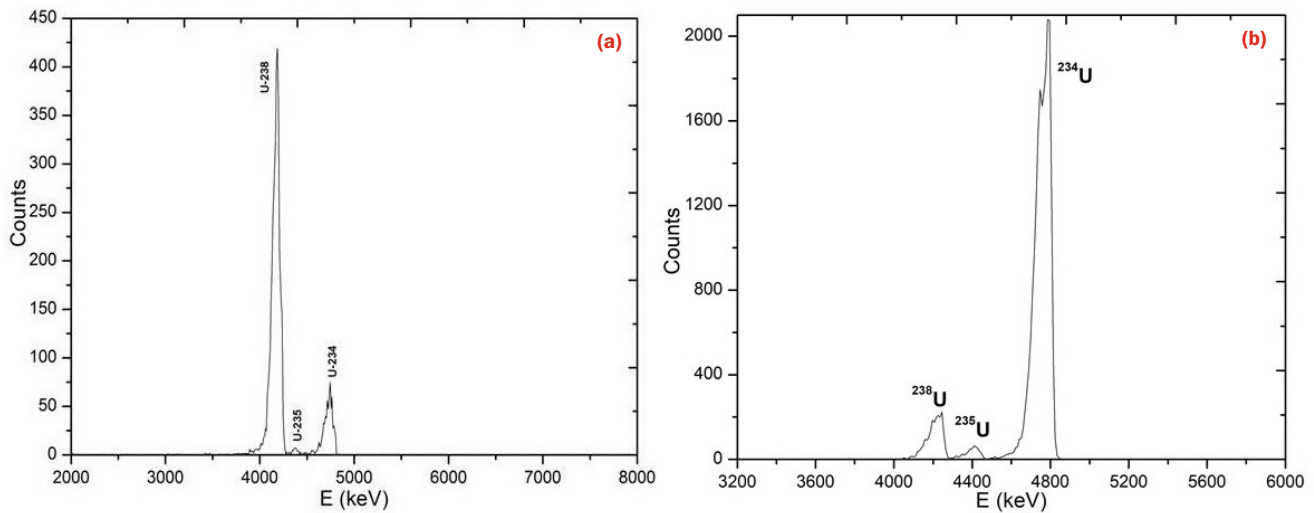


Fig.3: Alpha spectrum of (a) Depleted Uranium; (b) Enriched Uranium.

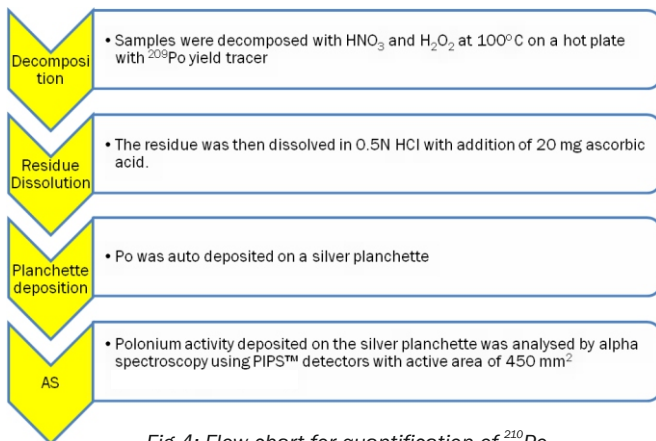


Fig.4: Flow-chart for quantification of ²¹⁰Po.

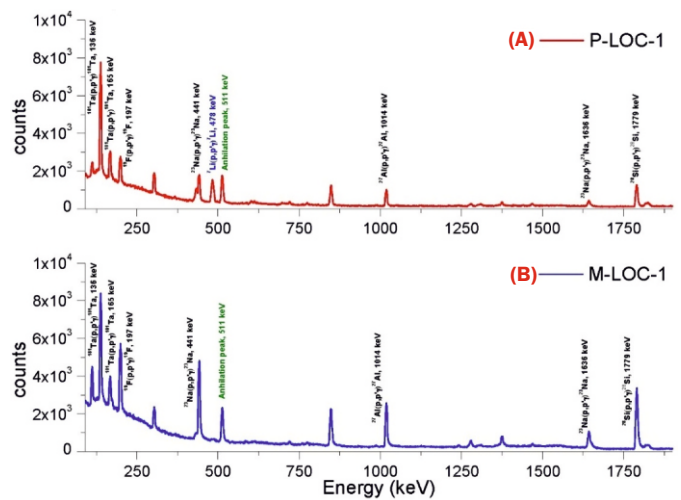


Fig.5: PIGE spectrum of ore sample (A) in-situ pelletised sample; (B) Mylar packed sample.

PIGE technique using high energy proton can be used to identify the type of uranium fuel (like uranium carbide, uranium oxide, uranium nitride or uranium silicide) without destroying the sample.

Neutron Activation Analysis

NAA is used for analysis of trace element and many REEs in Uranium ore samples. By varying the irradiation and cooling time, a range of elements like Na, Sc, Cr, Mn, Zn, Fe, Co, Sb, Cs, La, Ce, Nd, Sm, Eu, Tb, Yb, Lu, Hf, Ta and Th can be analyzed using instrumental NAA whereas Pr and Er requires RNAA [7]. Irradiation facilities at Dhruva and APSARA-U research reactors are being used for analysis of mine samples using NAA in HS&EG, BARC.

Mass Spectrometry in NF Analysis

Considering the complexity and specificity of NF samples, various analytical procedures have been developed for various signatures using MS. Trace elemental impurities, rare earth element (REE) pattern and uranium isotopic ratio has been identified as important NF signatures in front end materials. Dissolution techniques for U-ore samples have been developed using both Microwave digestion (ETHOS UP, Milestone) and electrically alkali fusion fluxer (K1 Prime Fluxer, Katanax). For analysis of trace metals, GF-AAS (ContraA 800:

Analyticjena) and ICP-AES (Ultima 2: Horiba JobinYvon) from our laboratory and TQ-ICPMS(iCAPTQ, Thermo Scientific) at IIT-B Monash Research Academy, Mumbai are used. The mine and mill samples are analysed for different trace elements like (Sc, V, Cr, Mn, Co, Ni, Cu, As, Se, Rb, Sr, Y, Mo, Ag, Cd, Sb, Ba, La, Ce, Pr, Nd, Sm, Eu, Gd, Dy, Ho, Er, Tm, Yb, Lu, Tl, Pb, Th, U) and these data can serve as reference trace elements for NF investigation. Chondrite-normalized REE pattern (CN-REE) for U-ore samples from different mines has been generated and shown in Fig.6. Uranium separation methodology has been developed for these samples using ion exchange and extraction chromatography. CN-REE pattern has been generated for UOC samples and is found to be unaltered when compared with the parent ore sample from which it is produced [8].

Small variation in ²³⁴U/²³⁸U and ²³⁵U/²³⁸U isotopic ratio can distinguish geographic origin of NU material. For precise Uranium isotopic ratio measurement, separation methodology in uranium ore and UOC samples has been developed using ion exchange and extraction chromatography. The extraction scheme for U separation in U ore samples using UTEVA spec resin (Fig.7) and a typical alpha spectrum of U isotopes in a uranium separated ore sample (Fig.8) are given. The isotope ratio in ore samples was analyzed using TIMS [9].

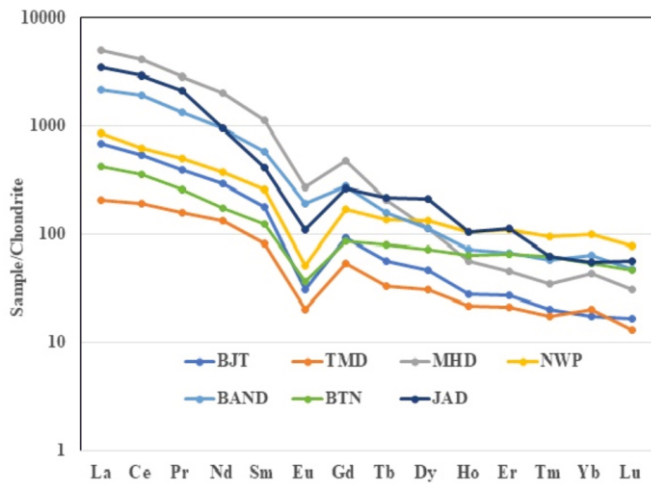


Fig.6: Typical Chondrite Normalised REE pattern for U-ore samples from different mines at Shinghbhum Shear Zone, Jharkhand.

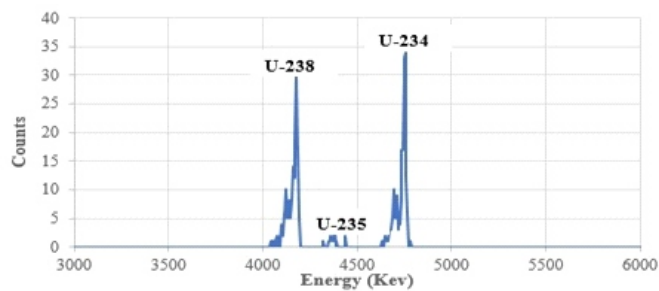


Fig.8: Typical alpha spectrum of U isotopes in separated ore sample.

Characterization of Anionic Impurities in Ore and UOC Samples as NF Signature

In the case of UOC, the anionic composition will provide the evidence for the type of processing (acid or alkali leaching). Ion chromatography (Eco IC: Metrohm) was used for anion analysis using EPA Method 300. A typical ion chromatogram for ore sample is shown in Fig.9. For the extraction of anions from the U ore samples both water leaching and pyrohydrolysis (Fig.10) methods were used.

Morphological Characterization of UOC Samples for NF Investigation

The image texture analysis (a new method) can be applied for NF investigation, wherein different colours or surface topography can also be obtained. Angle measure technique (AMT) incorporated with multivariate data analysis, may be applied for interpretation of image texture [10]. UOC samples of different process history are being analysed for generation of scanning electron microscopic images.

Development of a Nuclear Forensic Analysis Tool

A server based web application in MEGH BARC cloud portal, has been developed for the management of nuclear forensic data and analysis. The developed nuclear forensic analysis tool is named as NFAT, which consists of two parts, PostgreSQL based database module to store and manage the forensic signature data of known samples and an analysis module to provide a forensic assessment of the questioned sample. Machine learning based algorithms have been used for developing the forensic analysis tool. Classification algorithms are appropriate for the multivariate analysis in the nuclear forensics to identify the origin of the intercepted

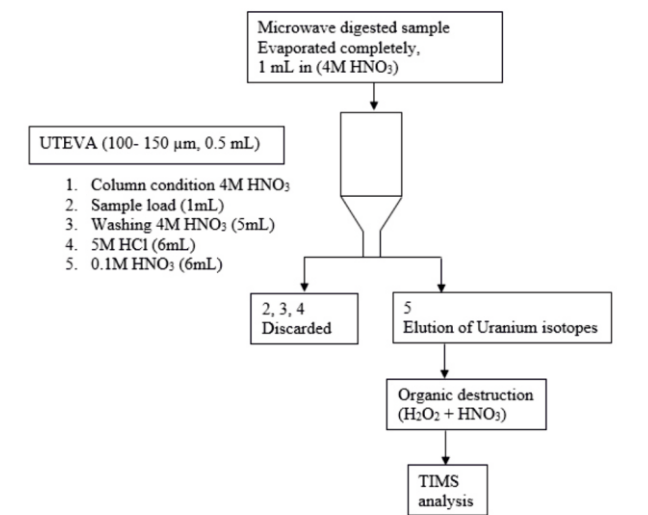


Fig.7: Extraction scheme for uranium separation in uranium ore by extraction chromatography.

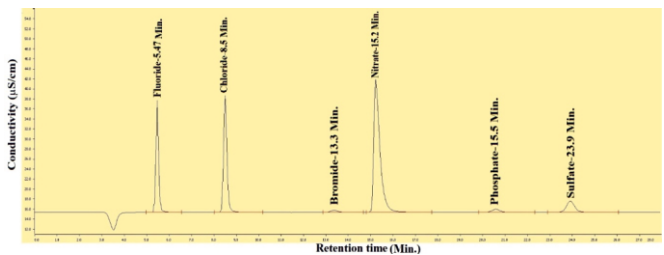


Fig.9: Typical Ion chromatograph for water extracted uranium ore sample.

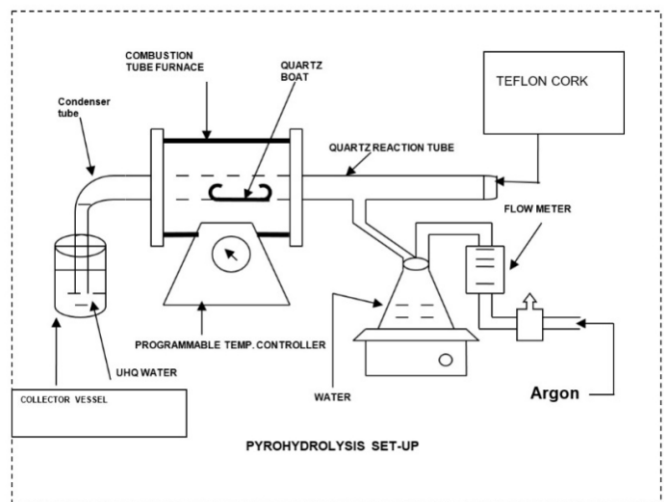


Fig.10: Pyro-hydrolysis set-up facility at EMAD laboratory.

material on the basis of training data in the nuclear forensic library (reference data). The output of the algorithms provides the prediction probability associated with each label for a given input data. The final qualitative prediction result is obtained by finding the label with highest probability. Various classification algorithms were attempted with different sets of nuclear forensic data available in the open literature. Four classification algorithms such as Artificial Neural Network (ANN), Decision tree classification (DT), Random Forest Classification (RF), and Gaussian Naïve Bayes Classifier (GNB) were found to give decent prediction accuracy. The

classification algorithms were built, trained and tested in Python using an open source library called 'Sklearn'. ANN was built with ReLU activation function, Stochastic Gradient Descent Optimiser, and four hidden layers. DT and RF were built with Gini impurity criterion. The algorithms were trained with 70% of the training data and remaining 30% of the data was used for validating it. Developed tool has been tested successfully for the three sets of reference data i.e. Indian Ore Major Elements, Indian Ore Trace Elements and Indian Ore Radioactive Isotopes.

Conclusion

Nuclear Forensics is an efficient tool in support of the prevention, preparedness and response to nuclear or radiological threat, and can also act as a deterrent towards the nuclear smuggling/terrorism with convincing attribution capability. However, many challenges like material type and related handling problems, instrumentation, availability of standard reference material for quality assurance, availability of national and international database, complexity in the data interpretation and the required expertise etc. associated with nuclear forensics practices limits its application only to a few laboratories. Initiatives have been taken for the establishment of nuclear forensic capability at HSEG, BARC and successfully developing the analytical procedures for characterization of nuclear materials and nuclear forensic signature library for front end materials and machine learning based analytical tool for NF interpretation.

Acknowledgements

Authors sincerely acknowledge authorities of Uranium Corporation of India Limited as well as Nuclear Fuel Complex for providing samples for different stages of front end materials.

References

- [1] IAEA, 2021. IAEA Incident and Trafficking database (ITDB). Incidents of nuclear and other radioactive material out of regulatory control 2021 Fact Sheet. <http://www-ns.iaea.org/security/itdb.asp>.
- [2] S. Anilkumar, A. K. Deepa, K. Narayani, A. K. Rekha, P. V. Achuthan, G. Krishnamachari, D. N. Sharma, "Estimation of ^{235}U concentration in some depleted uranium samples by high resolution gamma-ray spectrometry using 185 keV and 1001 keV gamma-energies of ^{235}U and $^{234\text{m}}\text{Pa}$," J. Radio. Nuc. Chem., 2007, 274, 161-166.
- [3] K. Siemon, A. Esterlund, J. Van Aarle, M. Knaack, W. Westmeier, P. Patzelt, "A new measurement of the gamma-ray intensities of $^{234\text{m}}\text{Pa}$ accompanying the decay of ^{238}U ," Appl. Radiat. Isot., 1992, 43, 873-880.
- [4] R. K. Prabhath, R. S. Sathyapriya, S. Mishra, S. K. Suman, S. Anilkumar, S. Murali, "Application of radio-analytical technique for determination of "Age" of nuclear materials for nuclear forensics," J. Radiat. Res. Appl. Sci. 2022 a, 15(1), 213-218.
- [5] R. S. Sathyapriya, R. K. Prabhath, S. Mishra, " ^{210}Po quantification in biological samples for application in Nuclear forensics", Proceedings of 9th DAE - BRNS Biennial Symposium (Webinar) on Emerging Trends in Sep. Sci. Technol. (e-SESTEC-2020); 197.
- [6] R. K. Prabhath, R. S. Sathyapriya, S. Mishra, V. Sharma, S. Murali, R. Acharya. "Development of a simple non-destructive method to quantify low Z elements in ore samples using tantalum as an external current normalizer in external (in-air) PIGE method for Nuclear Forensic applications." J. Radio. Nuc. Chem., 2022b, Oct 14, 1-8.
- [7] H. G. Stosch, "Neutron Activation Analysis of the Rare Earth Elements (REE) - With Emphasis on Geological Materials," Phy. Sci. Rev., 2016, 1(8), 20160062. doi:org/10.1515/psr-2016-0062.
- [8] S. Mishra, R. K. Prabhath, R. S. Sathyapriya, S. Murali, A. V. Kumar, "Application of Inductively Coupled Plasma Mass Spectrometry (ICPMS) for determination of Rare Earth Element pattern in Uranium ore and Uranium ore concentrate (UOC) samples for origin assessment," Proceedings of 32nd ISMAS symposium on Mass Spectrom., 2019, 222-225.
- [9] S. Mishra, S. K. Sahoo, P. Chaudhury, K. S. Pradeepkumar, "Measurement and validation of uranium isotope ratio in uranium ore for isotopic fingerprinting," Radiat. Protect. Environ., 2017, 40, 3-8.
- [10] S. V. Kucheryavski, K. Kvaal, M. Halstensen, P. P. Mortensen, C. K. Dahl, P. Minkinen, K. H. Esbensen, "Optimal corrections for digitization and quantification effects in angle measure technique (AMT) texture analysis," J. Chemometrics., 2012, 22, 722-737.

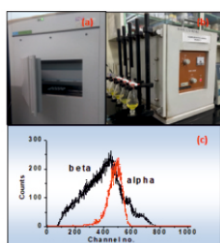
Emergency Preparedness

10

Emergency Radio-bioassay Methodologies for First Responders & Public Approach

Supreetha P. Prabhu¹, Priyanka J. Reddy¹, Sonal M. Wankhede¹, Soumitra Panda¹, Nanda Raveendran¹, Pramilla D. Sawant^{*1}, Probal Chaudhury¹ and M. S. Kulkarni²

¹Radiation Safety Systems Division, ²Health Physics Division; Bhabha Atomic Research Centre, Trombay – 400085, INDIA



(a) Ultra low background LSC (b) Automated solvent extraction equipment (c) Typical gross α/β spectrum obtained using PSA technique

ABSTRACT

Following radiation emergency, first responders and the affected public are required to be assessed for internal contamination due to α/β emitting radionuclides. Timely assessment of internal contamination is necessary for triaging people for medical intervention. As a part of preparedness and response to any radiation emergency, rapid radio-bioassay methodologies are required. The present article highlights application of Liquid Scintillation Counter for screening of gross α/β activities and Solid Extraction Chromatography based radiochemical separation methods for sequential separation and estimation of radionuclides in bioassay samples at BARC.

KEYWORDS: Radiation emergency, Internal contamination, Rapid techniques, Bioassay samples, First responders

Introduction

Major nuclear accidents like Chernobyl and Fukushima, necessitated efforts in developing better capabilities for emergency preparedness and response. This includes assessment of external and internal radionuclide exposures to first responders (e.g. radiation-safety, emergency medical, fire-protection, police personnel's etc.) and the affected population. In-vivo and in-vitro monitoring techniques are usually employed to estimate internal contamination due to radionuclides. Assessment of internal contamination by radionuclides emitting non-penetrating radiations like α and β is quite challenging. It requires collection of samples, like Nasal Swab (NS), excreta etc., as early as possible, in a controlled manner to avoid inadvertent contamination from external sources [1].

Urine is one of the most universally used matrices for internal contamination assessment due to its non-invasive sample collection, easy availability and adequate sensitivity to meet the requirements. In case of radiation emergency, large numbers of individuals need to be monitored in a short duration to expedite the decision for prompt medical intervention, if required. Hence, it is necessary to develop rapid and reliable bioassay methods.

Clinical Decision Guide (CDG)

National Council on Radiation Protection and Measurements [1] has defined operational quantity, CDG i.e., intake corresponding to internal dose of 250 mSv, to assist physicians in making treatment decisions to reduce any long-term health consequences due to internal contamination.

Methodologies developed need to be sensitive enough to detect activity in biological samples corresponding to derived CDG values (Table 1). Derived CDG are values of activity levels in bioassay samples corresponding to 1 CDG intake.

Gross α/β measurements using Liquid Scintillation Counter

Ultra-Low Level Liquid Scintillation Counter (LSC, Model: Quantulus 1220) equipped with Pulse Shape Analysis (PSA) circuit was used for gross α/β measurements due to its high sensitivity, low detection limits and 100% counting efficiency for α emitting radionuclides [RNs]. Spectral Quench Parameter of External Standard [SQP(E)] is used to determine the counting efficiency for each sample through calibration curves. Optimization of α/β separation was carried out using ²⁴¹Am and ⁹⁰Sr/⁹⁰Y as α and β standards respectively. The optimum PSA setting was determined where there was equal and minimum spillover of α pulses into the β Multichannel Analyzer (MCA) and vice a versa (Fig.1a). Optimized PSA settings were plotted against corresponding SQP(E) values as shown in Fig.1b.

All subsequent measurements were performed using the defined optimum PSA settings. The sample to scintillator ratio was maintained at 1:10 for NS/tissue samples and 5:10 for urine samples. Optiphase HiSafe III scintillator and 20 mL

Table 1: Derived CDG values in urine for a few selected radio RNs [1-2].

RN and absorption type	Derived CDG values in urine (Bq/100 mL) for time T (days)				
	1 d	7 d	10 d	15 d	30 d
²³⁹ Pu (M)	1.1E-01	1.2E-02	7.3E-03	5.4E-03	4.6E-03
U(nat.) (M)	1.9E+02	5.4E+00	4.5E+00	3.6E+00	2.2E+00
²⁴¹ Am (M)	1.0E+00	3.4E-02	2.8E-02	2.3E-02	1.5E-02
²¹⁰ Po (M)	1.1E+00	2.0E+00	2.0E+00	1.8E+00	1.5E+00
⁹⁰ Sr (F)	3.5E+04	3.3E+03	2.1E+03	1.4E+03	5.0E+02

*Author for Correspondence: Pramilla D. Sawant
E-mail: pramillas@barc.gov.in

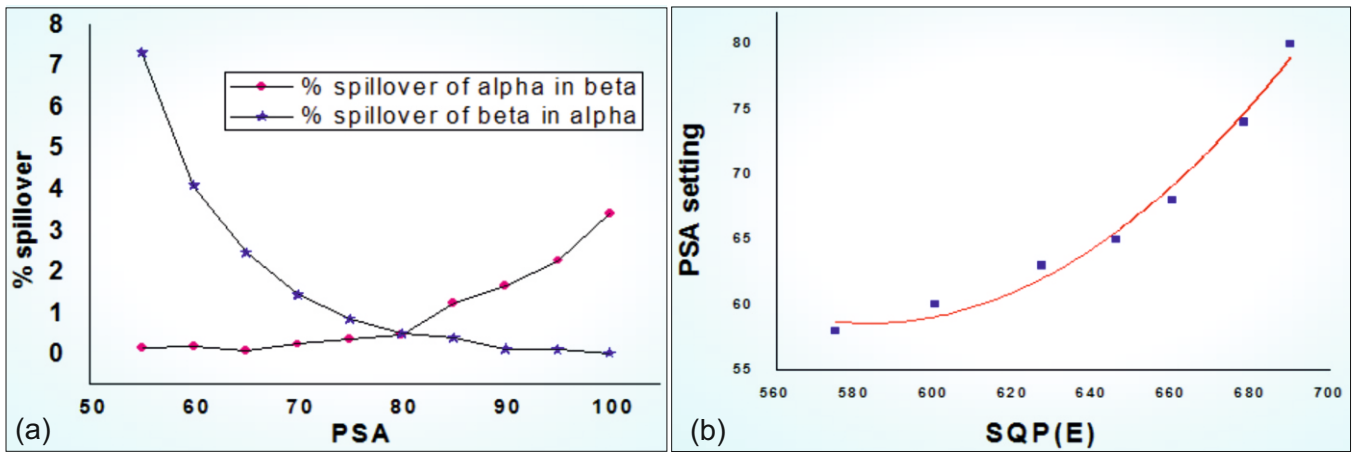


Fig.1: (a) Spill over for determination of optimum PSA setting using ²⁴¹Am, ⁹⁰Sr/⁹⁰Y standards, (b) Variation of SQP(E) against optimized PSA setting.

capacity polyethylene vials were used for standardization purpose. The gross count rate for α and β were determined and the corresponding activities were calculated using the following equations:

$$A_{\alpha} = \frac{Z_{\alpha} E_{\beta} - Z_{\beta} E_{\beta f}}{E_{\alpha} E_{\beta} - E_{\alpha f} E_{\beta f}} \quad (1)$$

$$A_{\beta} = \frac{Z_{\beta} E_{\alpha} - Z_{\alpha} E_{\alpha f}}{E_{\alpha} E_{\beta} - E_{\alpha f} E_{\beta f}} \quad (2)$$

Where, E_{β} , E_{α} and $E_{\beta f}$, $E_{\alpha f}$ are the counting and spillover efficiencies for β and α respectively, Z_{α} is the α count rate in α MCA and β spillover ($A_{\beta} E_{\beta f}$) in the same MCA. Similarly, Z_{β} is β count rate that is a combination of both β disintegrations ($A_{\beta} E_{\beta}$) and α spillover ($A_{\alpha} E_{\alpha f}$) in β MCA.

In case of any radiation emergency, it may not be feasible to determine the SQP(E) for each and every sample and its corresponding optimal PSA value. To overcome this concern,

an average SQP(E) corresponding to ‘typical’ urine was estimated by measuring SQP(E) in 100 individual urine samples and the quench distribution curve obtained is shown in Fig.2. The average SQP(E) was found to be 700 (SD = ± 27) with optimal PSA value of 82.

Background measurements were performed by collecting bioassay samples from the unexposed individuals to determine Minimum Detectable Activity (MDA) [3] based on optimized PSA. These are given in Table 2 for various counting times (CT).

The optimized CT using Quantulus 1220 LSC for screening gross α/β in NS/tissue/ fecal samples is 2 min. Most of the α emitters can be detected in direct urine with a CT of 5 min, except Pu(α) which requires a minimum CT of 1h to achieve the required sensitivity. Following the above procedure for calibration of LSC, methodologies have been developed at BARC, for estimation of gross α/β in NS, excised tissue and fecal samples.

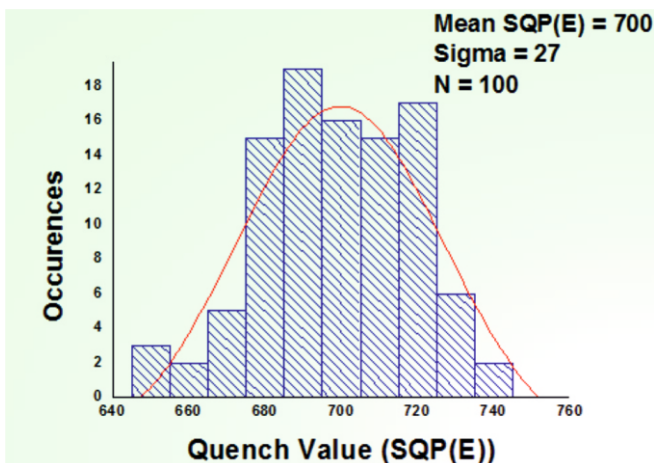


Fig.2: Observed quench levels of urine samples and overlaid Gaussian distribution curve.

Table 2: MDA for gross α/β in bioassay & NS samples.

Matrix	CT (min)	MDA (Bq)	
		Gross α	Gross β
NS/tissue	2	1.5	16.0
Urine (100 mL)	5	0.7	3.0
	60	0.1	0.8

NS is a best indicator of possible internal contamination by inhalation. Sawant et. al. reported the procedure for collection of NS [4]. The NS results are further confirmed by carrying out bioassay monitoring. The NS analysis is as follows: NS are wet digested using conc. HNO₃ and H₂O₂ and the solution is evaporated to dryness. The residue obtained is extracted using dilute HCl. 1 mL of this extracted sample was counted using LSC. MDA observed for gross α/β is shown in Table 2. The technique standardized is sensitive enough to detect gross α/β activity in NS samples significantly below derived CDG level (Fig.3).

Tissue samples excised from contaminated wound needs to be analyzed to know the radioactive contaminant(s) and their isotopic composition. This information is extremely essential for internal dose assessment as well as for decorporation treatment. Sawant et. al., reported the procedure for analysis of tissue samples [5] and gross α/β is estimated similar to that mentioned above for NS analysis.

Fecal samples collected from the internally contaminated individuals are dry ashed in muffle furnace at 450°C. Further wet digestion is done using conc. HNO₃ and

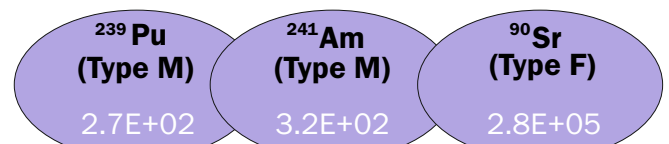


Fig.3: Derived CDG values (Bq) in NS for a few selected RNs [1-2].

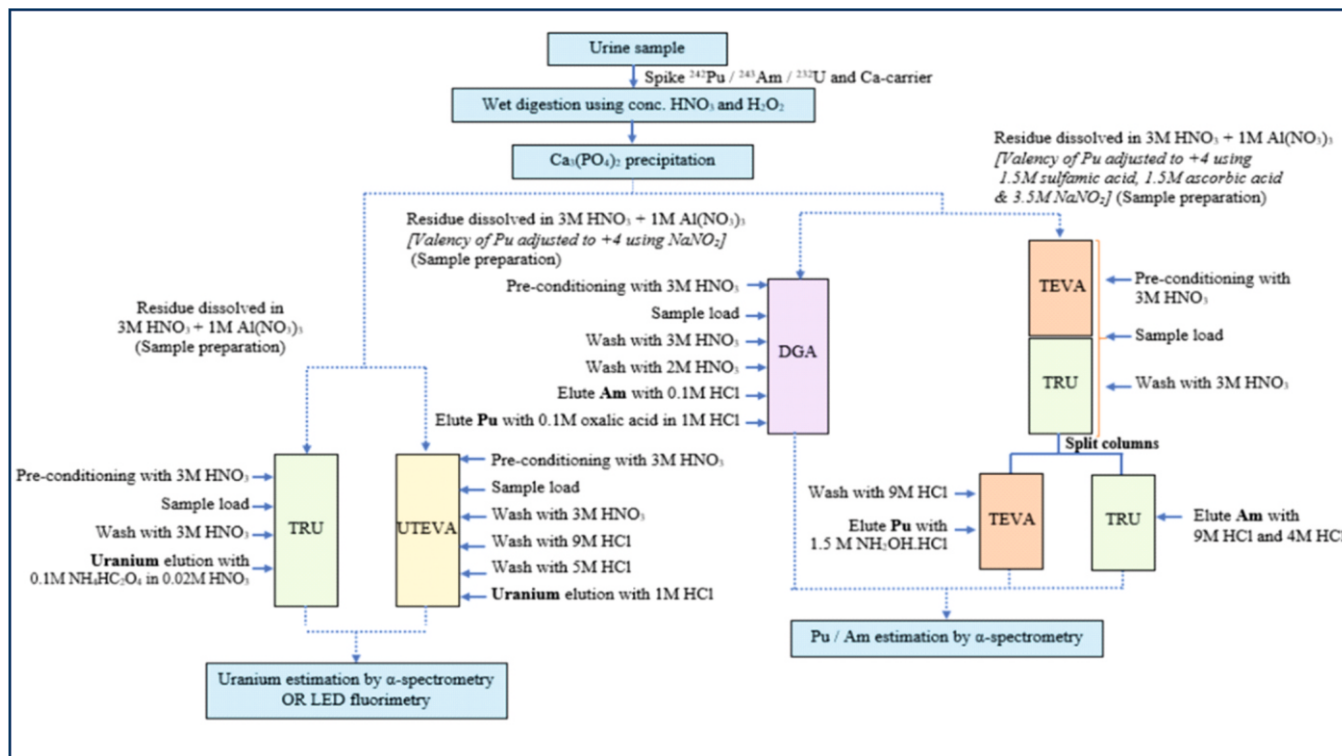


Fig.4: Radiochemical procedure for estimation of actinides in bioassay samples [8-10].

H₂O₂. The silica present in the sample is destroyed using HF and RNs present is extracted using dilute HCl. The procedure adopted for direct estimation of gross α/β in fecal samples is similar to that mentioned above for NS analysis.

Sequential Separation of Radionuclides

A rapid technique is developed for sequential estimation of Pu and Am in NS using extractive LSC [6]. MDA obtained for Pu(α), Pu(β) and Am(α) is 45.6, 522 and 72 mBq respectively for 5 min CT. The developed method is sensitive enough to sequentially separate and estimate Pu isotopes and Am in NS below derived CDG value within 10 minutes (Fig.3).

For concentrating and isolating uranium in urine, liquid-liquid extraction technique is applied [7]. The method standardized requires ~ 1 h for complete analysis of a single sample. MDA obtained is 240 mBq/100 mL for 5 min CT. This method is sensitive enough to detect soluble compounds of U in urine below derived CDG value, even in samples collected one month after the exposure (Table 1).

For separation of actinides in bioassay samples efforts have been made to reduce the overall analysis time using extraction chromatography resins (UTEVA, TEVA, TRU and DGA). The individual radionuclides are estimated using LSC, LED Fluorimetry (LF) for uranium and α-spectrometry techniques [8-10]. Further reduction in analysis time is achieved using micro-precipitation technique for source preparation for α-spectrometry [11]. The urine sample for analysis is prepared and loaded onto TRU / UTEVA columns for U estimation and DGA / stacked TEVA & TRU column for Pu and Am estimation as shown in steps described in Fig.4.

Activity of U, Pu and Am in eluted fractions are determined by α-spectrometry or LF in case of U. Estimation of U using LF is accomplished within 10 min for single sample analysis as against 24h required by α-spectrometry.

Radiochemical separation procedure is also standardized for estimation of Sr in urine samples using

Sr-spec resin [12]. MDA obtained is 1.1Bq/100 mL for 5 min CT. The method standardized is sensitive enough to detect radioactive Sr in urine below derived CDG value collected one month post exposure (Table 1).

Few international incidences have shown potential of ²¹⁰Po for malevolent purposes. Polonium in urine is usually estimated by chemical deposition onto a silver planchette followed by counting in α-spectrometry. In emergency situations, resourcing of silver planchette may be difficult and hence, a procedure is developed using SS planchette [13]. MDA of the technique is 12.8 mBq/100 mL for 1h CT. This method is sensitive enough to detect ²¹⁰Po in urine below derived CDG value collected one month post exposure (Table 1).

Quality Assurance (QA)

As part of QA, all the above methods are tested based on the performance criteria for radio bioassay according to ANSI N13.30 [14]. The methods developed and systems used are also validated by participation in inter-laboratory inter-comparison exercise for estimation of these RNs in emergency bioassay samples.

References

- [1] National Council on Radiation Protection and Measurements. Management of persons accidentally contaminated with radionuclides. NCRP report no. 161, 2008.
- [2] Birchall A., Puncher M, James A. C., Marsh J. W., Jarvis N. S., Peace M. S., Davis K. and King D. J., IMBA Expert: Internal Dosimetry Made Simple. Journal of Radiation Protection Dosimetry, 2003, 105, 421-425.
- [3] Curie L. A., Limit for qualitative detection and quantitative determination. Application to radiochemistry. Analytical Chemistry, 1968, 40(3),586-593.
- [4] Sawant P. D., Prabhu S. P., Rath D. P., Gopalakrishnan R. K. and Rao D. D., Nasal swab reference levels for plutonium based on aerosol

characteristics and breathing patterns of individuals. *Journal of Radiation Protection and Environment*, 2015, 38, 115-119.

[5] Sawant P. D., Prabhu S. P., Rath D. P., Rao D. D. and Pradeepkumar K. S., Estimation of ^{241}Pu and its contribution to internal dose. IARPNC-2014, 137, India.

[6] Panda S., Reddy P. J., Yadav J. R., Sawant P. D. and Kulkarni M. S., Development of a rapid technique for sequential separation of Pu/Am in nasal swab using solvent extraction and liquid scintillation spectrometry. *Journal of Applied Radiation and Isotopes*, 2022, 186, 110297.

[7] Reddy P. J., Wankhede S. M. and Sawant P. D., Estimation of Uranium in Water and Urine by Liquid Scintillation Spectrometry. ARCEBS-2018, 173-174, India.

[8] Wankhede S. M., Suja A., Chaudhary S., Prabhu S. P. and Rao D. D., Rapid Column Extraction Method for Uranium in Urine. *Journal of Separation Science and Technology*, 2013, 48, 2431–2435.

[9] Prabhu S., Kumar S. A., Sawant P. D. and Rao D. D., Solid extraction chromatography for estimation of uranium in urine. IARPIC-2016, 208, India.

[10] Prabhu S., Chaudhary S., Kumar S. A. and Kulkarni M. S., Rapid separation of Pu & Am from bioassay samples. IARPNC-2020, 130, India.

[11] Sawant P. D., Wankhede S., Kumar S. A., Chaudhary S. and Prabhu S. P., Alpha source preparation of actinides by micro-precipitation. *Journal of Radioanalytical & Nuclear Chemistry*, 2019, 319 (1), 109-113.

[12] Wankhede S. M., Chaudhary S. and Sawant P. D., Rapid bioassay method for estimation of ^{90}Sr in urine samples by liquid scintillation counting. IARPIC-2018, 221, India.

[13] Mandal P., Gondane S. and Sawant P. D., Cost effective estimation of Polonium using Stainless Steel planchette. IARPNC-2020, 76, India.

[14] Health Physics Society (HPS) Performance criteria for radiobioassay: American National Standard ANSI/HPS N13.30 American National standard Institute, 2011.

Industrial Hygiene

11

Overview of Activities Related to Industrial Hygiene and Safety

Munish Kumar, Garima Singh, Praveen Dubey, Nitin V. Choughule and Alok Srivastava*

Industrial Hygiene and Safety Section; Health, Safety & Environment Group, Bhabha Atomic Research Centre, Trombay - 400085, INDIA



Height pass facility

ABSTRACT

Industrial Hygiene Safety Section is responsible for Industrial Hygiene surveillance of wide spectrum of operations carried out at BARC as well as matters related to industrial safety. This includes providing Beryllium safety at PMD, Vashi, assessment of hazards associated with various plant activities, HAZOP studies, accident analysis, medical analysis, conducting accident prevention programme, training etc.

KEYWORDS: Industrial hygiene, Height pass facility, Safety awareness

Introduction

Industrial hygiene monitoring refers to the practice of measuring the extent of worker exposure and employing engineering, work practice controls, and other methods to control potential health hazards. It helps to determine whether ongoing worker exposure to a hazardous substance is within the occupational safety standards set by OSHA (Occupational Safety & Health Standards) / BIS (Bureau of Indian Standards) / Atomic Energy Factory Rules (AEFR) 1996 or recommended guideline values prescribed by American Conference of Governmental Industrial Hygienists (ACGIH). Periodic surveillance ensures that the potential hazards present in the workplace are within limits and checks effectiveness of existing hazard control methods. It also determines the need for additional safety measures, such as the use of engineering hazard controls (e.g. ventilation) or personal protective equipment (PPE). Furthermore, it can provide employers with protection against compensation claims and may be required by insurance agencies hired to guarantee an employer against losses due to occupational injury or illness. The measurement is conducted through combination of qualitative and quantitative procedures, depending on the purpose of the monitoring and the substance being monitored.

Steps involved in Industrial Hygiene Surveillance are:

- Preliminary Investigation
- Initial Survey
- Sampling Plan
- Industrial Hygiene Monitoring Data Analysis
- Corrective Action and checking effectiveness

A well-planned workplace industrial hygiene surveillance training program ensures protection against health hazards, avoids loss in productivity due to illness or injury, reduces worker compensation for medical leave due to work-related injuries and illnesses, ensures preparedness against liability lawsuits, gives employee satisfaction and prevents future incidents.

Monitored chemical and physical are:

- Exposure to high noise levels
- Exposure to ionizing and non-ionizing radiation
- Extremes of temperature
- Exposure to vibration
- Exposure to Chemicals
- Breathing Air Quality
- Appropriate illumination
- Appropriate ventilation & Air Changes

Development of height pass facility for qualification to work at height

Fall from height is one of the leading causes of injuries and death at workplace. It is the key requirements to enhance overall safety culture and educate the employees as well as contract workers involved in work at height in BARC. Industrial Hygiene and Safety Section, HS&EG took initiative to develop 'height pass test facility' to issue height pass certificate to the workers. The procedure certifies the suitability of a person to work at height thus reducing the possibility of fall accident while working at height. This is a mandatory requirement and the objectives of this facility is to protect employees from the hazards related to work at heights. This results in (i) managing work at height jobs being done under Permit-To-Work, (ii) controlling the incidents related to Work at Height, (iii) compliance to Regulatory requirements to make work place safety. The regulations recommend that a fall protection system be provided during working at height. As a part of qualification test, departmental person shall undergo medical test as per listed test in the prescribed format (height pass) by the Certifying Surgeon / Doctor at TOHC, Trombay. Contractor's personnel shall obtain the certificate in the format (height pass) from Certifying Surgeon / MBBS Doctor. Person medically fit to work at heights shall be given pep talk by Industrial Hygiene and Safety Section on various aspects of working at height. After undergoing medical examination, the worker has to go through Height Pass test which include three tests to understand the physical status of the workers.

*Author for Correspondence: Alok Srivastava
E-mail: aloksri@barc.gov.in

Structure for conducting physical test of Height pass

- Walking freely over a horizontal 6" narrow bar at 1 ft height.
- Walking freely over a horizontal bar at 9/12 ft height wearing a safety belt.
- Climbing a 12 ft high rope.



Fig.1: Physical test of Height pass.

Height Pass certificate will be issued once all the tests are successfully performed by applicant. The Height pass certificate is valid for 6 (six) months. In case the individual wants to continue the work at height beyond this period he has to obtain a fresh height pass certificate.

Safety Awareness Programmes Conducted in BARC

Safety is given the top priority and attaining zero incident status is a collective endeavor. Towards this, conducting safety awareness campaign plays an important role. A dedicated Accident Prevention Programme (APP) is introduced in BARC in the year 1962, and is still continued. The objective of APP is to prevent accidents through proactive measures. Industrial Hygiene and Safety Section is imparting the efforts in the promotion of industrial safety in the different activities. Safety awareness is one of the most important elements in promoting safety culture. Safety culture is a practice to observe safety in every activity and is an integral part of all the activities in BARC since inception. The various safety awareness programmes

aim at a single objective that is enhancement in safety culture through various techniques. The main role of training and awareness programmes at BARC is to spread awareness about work place hazards and take counter measures at all levels of employees. It is essential to motivate the personnel to adopt safe and right method of work. The safety awareness campaign is aimed at renewing the commitment of employees to perform their activities safely without meeting with accidents throughout the year.

Keeping this in view, the Industrial Hygiene and Safety Section organizes annually a two-week course on **Accident Prevention and Promotion of Occupational Health and Safety** every year for the benefit of all employees. This course has been designed to be a comprehensive programme providing an insight into various health, safety and environmental aspects. The programme includes a visit to the Safety Centre of Central Labour Institute, Sion and BARC facilities at Trombay. The programme is conducted with the faculty support of scientists from different Divisions of BARC, AERB, NPCIL, DGFASLI etc.

It is the enlightened human factor that plays a crucial role in planning, execution and maintaining a high safety standard in an organization. This course serves as a positive step to provide this enlightenment. As a part of safety awareness campaign Industrial Hygiene and safety Section organizes **National Safety Day** Programme within the Centre where individual abilities and skills in terms of participation in drawing safety posters, conveying meaningful messages through safety slogans and pinpointing workplace hazards are visualised. As part of safety promotional activities, Industrial Hygiene and Safety Section of HS&EG, BARC has introduced an Industrial Safety Award Scheme in the form of Director's Safety Shield for BARC units within Trombay as well as outstation units.

Applications received from facilities are scrutinized and assessed. Based on the scrutiny of the applications and records available with IHSS, an evaluation is carried out considering the different parameters in respect of Safety performance statistics and Safety Management Indicators followed by documents verification and assessment as suggested by the Committee.



Glimpses of various events held in BARC to mark safety culture among scientific community.

Industrial Hygiene

12

Beryllium: Associated Hazards, Safety Evolution & Safety Limits

Ankur Chauhan, Mahesh K. Kamble, Munish Kumar and Alok Srivastava*

Industrial Hygiene and Safety Section; Health, Safety & Environment Group, Bhabha Atomic Research Centre, Trombay – 400085, INDIA



(a) Beryl ore extracted in India (b) Lungs affected by chronic beryllium disease (c) & (d) Some Beryllium metal components manufactured by BARC

ABSTRACT

In addition to conventional industrial safety and associated hazards, Industrial Hygiene and Safety Section of Health, Safety & Environment Group have been providing safety surveillance as well as monitoring for BARC Beryllium facilities since inception. This includes regular air monitoring, surface swipe sampling as well as monitoring of waste effluent so as to comply the limits as stipulated by BARC Safety Council. As on-line detectors are not available for Beryllium, its surveillance is a challenge and engineering, medical & administrative controls are quite helpful in this regard. In addition, cautious and conservative approach along with use of personnel protective equipments, continued education, training and awareness plays an important role in ensuring beryllium safety of individuals as well as the environment.

KEYWORDS: Beryllium safety surveillance, Limits, Chronic and acute beryllium diseases, and estimation of beryllium

Introduction

Beryllium (Be) is one of the most remarkable element in the nature & is used in nuclear, space, defense as well as in many other household items of day-today use. It has very low density, high specific heat, high strength to weight ratio, good thermal conductivity and good dimensional stability over wider temperature range. It is lighter than Aluminium but more rigid than steel. Due to low atomic number, the K shell energy is ~218 eV (0.218 KeV), so poses little attenuation (via photoelectric effect) to X-ray photons and thin Be metal windows are used in X-ray machines as well as in synchrotron beam lines. Properties like low atomic weight, low absorption and high scattering cross section for neutrons, low photon neutron reaction threshold value and low mass absorption, favour Be as a nuclear material [1].

In combination with α emitters like Ra, Am etc., Be releases neutrons (neutron source) as α particles having energy of few MeV available naturally are capable to cause (α , n) reaction with Be nucleus i.e. easily overcome coulombic repulsion barrier. Further, Be or BeO is used as a neutron reflector in research reactors as well as in many reactor physics experiments. However, Be is one of the most toxic element in periodic table and was the first element to have environmental exposure limit.

Beryllium and its Prevalence in Environment

Beryllium occurs in rocks, minerals etc. and its average concentration in earth crust have been reported to be 1-10 ppm. Many minerals are known to contain Be, but Beryl ($3\text{BeO}\cdot\text{Al}_2\text{O}_3\cdot 6\text{SiO}_2$) and bertrandite ($4\text{BeO}\cdot 2\text{SiO}_2$) ores have been commercially exploited. The commercial grade Indian beryl ore (Fig.1) contains ~12 % BeO and fairly large deposits are found in Andhra Pradesh, Bihar, Rajasthan, Tamil Nadu and Chhattisgarh. Beryllium has many isotopes out of which ^9Be is a

stable isotope, whereas ^7Be and ^{10}Be are radioactive and are produced by cosmic rays in the upper atmosphere in trace amount. The typical concentration of ^7Be in atmospheric air is reported to be ~5 mBq/m³ and is being considered as a radioactive tracer for studying global atmospheric changes.

In addition to this, Be is present in air, soil, water and food. The typical concentration of Be in air is reported to be <0.05-0.30 ng/m³. However, coal combustion in thermal power plants and use of hydrocarbons further increases the ambient background levels to values >0.30 ng/m³.

The fly ash is reported to contain Be up to few hundreds ppm. Similarly, Be is prevalent in the soil and its concentration is reported to be few ppm although it varies from place to place and is the main contributor to the background levels in food, air and water. It needs to be mentioned that typical Be concentration in water is reported to be < 1 ppb whereas in fruits and vegetables, it is generally \leq 1-10 ppb; although many factors like uptake of Be from soil, water etc. influence these values [1].

Health Hazards Associated with Beryllium

Typical health hazards associated with Be exposures are mainly to lung and are classified as chronic or acute beryllium diseases. It is generally believed that Acute Beryllium Disease (ABD) occurs when human are exposed to Be air concentration normally exceeding 100 $\mu\text{g}/\text{m}^3$ and is characterized by irritation in respiratory system, chest pain, fever, dry cough with blood etc., whereas chronic beryllium disease (CBD) (Fig.2) is known to occur even after 20-30 years after cession of exposure and exposure response relationship is not much understood. Further, ABD is reversible (but it was found that many a times ABD causes CBD later), whereas CBD in neither curable nor reversible [2-4].

Comprehensive information on its chemical toxicity and other adverse effects on humans became available after the appearance of lung related diseases and deaths amongst

*Author for Correspondence: Alok Srivastava
E-mail: aloksri@barc.gov.in



Fig.1: Beryl ore from Jharkhand, India. (Courtesy: AMD's exhibition at AOCP-6, Mumbai)

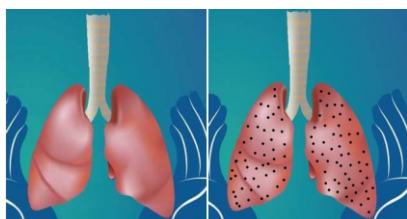


Fig.2: Lungs affected by CBD (formation of granules leading to problem of inflation/respiration).

fluorescent lamp (handling BeO_2SiZn (Beryllium Zinc Silicate)) manufacturing workers and the use of Be based compounds in lamp industry was later discontinued. Further, during end of second world war, production and use of Beryllium increased in USA and cases of chemical pneumonia in workers extracting BeO from Be based ores, continued to be reported. All this led to the requirement of some safety standards for protection of occupational workers and public environment.

Basis of Safety Standards for Beryllium

In view of chemical toxicity of Beryllium resulting in chronic and acute diseases arising from inhalation of dust, fumes or particles, the standard of $2.0 \mu\text{g}/\text{m}^3$ for Be in air ($\text{Be}_{\text{Air-Conc}}$) as particulate matter with time weighted average over 8 hours was defined by Department of Energy (DOE), USA in 1948 and were adopted in the end of 1949. This was the first standard which put regulations on allowable $\text{Be}_{\text{Air-Conc}}$ and was initially termed as **Occupational Exposure Limit (OEL)** at the time of its inception [5].

The notion behind adoption of $2.0 \mu\text{g}/\text{m}^3$ was based on the fact that during 1950s, $\sim 100 \mu\text{g}/\text{m}^3$ as air concentration was an established value for occupational safety at workplaces as far as chemical toxicity of heavy metals (Pb, Hg etc.) was concerned. Considering the fact that toxic heavy metals are of having atomic weight of ~ 200 whereas ${}^9\text{Be}$ is a light metal with a atomic weight of ~ 10 (ratio of mass number of heavy metal to lighter metal = $200/10 = 20$) and assuming atom for atom toxicity, the typical value for Be exposure limit comes to be $100 \mu\text{g}/\text{m}^3 / 20 = 5.0 \mu\text{g}/\text{m}^3$ as derived from heavy metals toxicity. In addition, an adjustment factor of 2.50 was further applied as the lung disease (CBD) associated with Be exposure is not only incurable but also irreversible and there was also not much epidemiological data or details about understanding of CBD during 1950s. This finally lead to Be standard of $5.0 \mu\text{g}/\text{m}^3 / 2.5 = 2.0 \mu\text{g}/\text{m}^3$ or $0.002 \text{mg}/\text{m}^3$ as a time weighted average over 8 hours/per shift (daily limits on $\text{Be}_{\text{Air-Conc}}$) for occupational Be workers/workplaces [5].

However, the questions on adequacy of $2.0 \mu\text{g}/\text{m}^3$ to eliminate CBD always remained and cases of CBD continued to be reported till recently and it was suggested by OSHA in 2017 that "maintaining Be exposures $< 0.20 \mu\text{g}/\text{m}^3$, 95% of the time may prevent CBD in workplace" i.e. daily 8-hour time weighted average should not exceed $0.20 \mu\text{g}/\text{m}^3$ [6]. In view of above, the overall philosophy behind Beryllium related guidelines/standards follow from the fact that acute beryllium disease which occurs at higher Be air concentrations is ruled out by selecting much lower levels i.e. limits much below the threshold value of ABD and CBD occurrence is further minimized to lowest acceptable level.

Indian Scenario on Beryllium Activities and Related Safety Standards

In India, Be related ore mining activities date back to pre-independence era and a survey of literature shows that ~ 281

Table 1: Be air concentration, surface level contamination & effluent discharge criteria as stipulated by BARC Safety Council (BSC).

Category	Type	Criteria/Levels/Limits	
Air concentration $-\mu\text{g}/\text{m}^3$	Occupational workplace*	Be air concentration $\mu\text{g}/\text{m}^3$	
		Previous (up to 2021)	Present
	Public/ambient area** at any ground level location around production facility	2.0 [§]	0.20
	STEL/Peak value***	0.01	0.01
Surface contamination $-\text{ng}/\text{cm}^2$	Occupational workplace	25	2.0
	Any equipment to be taken to public area from Be area or release of Be contaminated equipment to non-Be area	10.0	1.00
Effluent discharge-ppm	Maximum concentration of liquid effluents dischargeable to public sewers	0.10 ppm (100 ppb)	

* Average over an 8 hour time period, [§]Action level of $0.10 \mu\text{g}/\text{m}^3$ & PLE value of $0.20 \mu\text{g}/\text{m}^3$ with STEL of $2.0 \mu\text{g}/\text{m}^3$ is followed in DAE from February, 2021, As per Directorate General Factory Advice and Labour Institutes (DGFASLI), India, the value of $2.0 \mu\text{g}/\text{m}^3$ is stipulated. ** Averaged over 30 day period, *** Maximum peak exposure limit not defined in AEFR, 1996 but reported by various Indian researchers.

Ton beryl ore was mined in 1932 which raised to ~ 1500 Tons per year during second world war although whole of beryl ore was exported to Germany and USA. Post independence, because of strategic nature and associated applications of Be, export of beryl ore was banned [5]. From literature, it can be seen that the attempts for extraction of Beryllium from beryl ore were made during 1960s along with a proposal for establishing pilot plant for production of sintered Beryllium

Air sampling using dry vacuum pumps at prescribed flow rate is carried out and dust particles are deposited on 0.8 micron mixed cellulose ester filter by the air passing through it. The filter is chemically processed and Be is measured which gives information about concentration of Be in the breathing zone ($\mu\text{g}/\text{m}^3$) of the personnel working in the given area.

High volume air samplers having typical flow rate of 500 LPM are also used for Be measurements on short term basis and suitable for measuring instantaneous concentration of Be (STEL value) at a given location and such pumps can be operated for few minutes (3-15min).

Personnel air samplers are quite useful for measurement of Be concentration of individual workers and are suitable for knowing and assigning exposure in situations where high concentration gradients occur and workers may encounter higher air concentration during works. The only limitation associated with personnel air samplers is that the air flow rate is low i.e. up to 5 LPM or so and it may be difficult to get reasonable measurement signal especially for low concentration values.

Swipes are collected from floors, walls, equipment/items to check the surface contamination levels. In case of higher values, cleaning/decontamination, wet mopping of floors, equipment etc. is continued to bring the surface levels within the stipulated values.

Fluorometry is done in which Be or its compounds are leached in to the solution and this solution is capable of exhibiting fluorescence in visible in the presence of specific reagent (dye) when excited by ultra-violet (UV) rays. During measurements blank solution is prepared to adjust background/zero setting & blank is identical to various Be calibration standards or samples and after calibration, Be concentration from sub-ppm to few or higher ppm is estimated. Using this, Air concentration and surface contamination levels as low as $0.002 \mu\text{g}/\text{m}^3$ & $0.10 \text{ ng}/\text{cm}^2$ are measured.

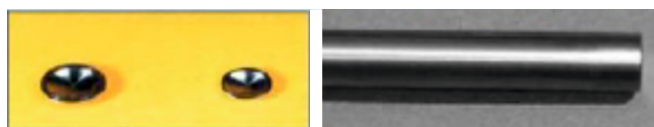


Fig.3: Beryllium metal window for X-ray tube and metal rod manufactured by BARC.

oxide from beryl ore by Department of Atomic Energy (DAE) [7]. Regarding Be protection related standards in India, survey of literature also shows that in DAE, the safety related guidelines were framed way back in 1960 by Soman and Kamath [8]. Although R&D activities about Be in DAE were started during 1960s but large-scale work in beryllium extraction/production and its applications started in 1982 with the establishment of Be plant at Vashi, Navi Mumbai by BARC prior to which the integrated flow sheet for extraction of beryllium from beryl and its consolidation by powder metallurgy was developed at a special laboratory set up for the purpose at Modular Laboratory, BARC in 1968. [9-11]. Some of the Beryllium metal components like windows for X-rays tubes and metal rod are shown in Fig. 3 [10-11]. As per the Atomic Energy Act, 1962, Be is categorized as a prescribed substance. Details about the Be safety procedures, operations and protocols can be had from Atomic Energy Factory Rules (AEFR), 1996 [12]. Historical details about various regulatory limits/levels pertaining to Be ($\text{Be}_{\text{Air-Conc}}$) for occupational workers and ambient air standards for public as adopted in India are given in Table 1 [2, 4-5].

Role of Industrial Hygiene Practices

IHSS, HS&EG plays an important role in ensuring Beryllium safety. All the processes being carried out at Powder Metallurgy Division, BARC, Vashi are under strict supervision of IHSS experts. Frequent sampling at every stage is carried out to ensure the safety limits for plant personnel and public are not exceeded.

Safety Provisions

Special provisions were made in the plant to handle toxic metal viz. negative pressure/ventilation at working areas, use of PPEs like boiler suits, hand gloves, comfo-respirator-half or full-facemask, goggles, airline breathing supply or SBCA as per requirement. These play an important role in prospective planning and minimizing Be exposures to occupational workers. Further, good and regular housekeeping practices keep spread of Be contamination in check. Personnel working

in Be plants are provided with change room, shower facility and lockers. In addition to all above, medical surveillance plays an important role and periodic medical tests are performed by the management. A minimum medical surveillance program should include skin examination, respiratory history, spirometry and periodic chest x-ray. Any abnormal observation may be helpful in taking necessary steps/cautions by the management.

Conclusions

In view of high toxicity of Be, utmost precautions need to be taken while handling Be related compounds during processing, manufacture and machining, including Be items bearing loose contamination. Continued education and training of workers and awareness along with engineering, medical, housekeeping and administrative controls can be helpful in maintaining Be exposures as low as reasonably achievable. Use of appropriate PPEs further helps in reducing the exposure as well as handling emergency situations. In the absence of any online/active detectors for Be, it is preferable to adopt a cautious and conservative approach while dealing with Be safety related affairs. IHSS is playing an important role in ensuring Be safety along with the plant management from 1970s or so.

References

- [1] Munish Kumar and Alok Srivastava, Beryllium Safety, Lecture notes of BSCS's 43rd training course on safety and regulatory measures for BARC Facilities, 94-103, June 22-25, 2022.
- [2] BSC Report - Safety in Extraction, Handling and Processing of Beryllium and its Compounds, BSC Safety Guide, BSC/SG/2018/5 Rev.-0, March 2018.
- [3] Munish Kumar, Mahesh K. Kamble and Alok Srivastava, Emergency preparedness during Beryllium handling Operations and associated challenges, 37th DAE Safety and Occupational Health Professionals Meet (DAESOHPM), 1-2, October, 2021.
- [4] S. Narayan and A. Ramamurthy. Health and safety aspects of Beryllium operations, Mineral Processing and Extractive Metallurgy Review: An International Journal, 14, 301-318, 1994.
- [5] Munish Kumar and Alok Srivastava, Evolution of beryllium safety standards over the last 70 years and challenges ahead, Radiat. Prot. Environ., 45(3-4), 7-20, 2022.
- [6] A. K. Madl, K. Unice, J. L. Brown, M. E. Kolanz, M. S. Kent. Exposure-response analysis for beryllium sensitization and chronic beryllium disease among workers in a beryllium metal machining plant. J. Occup. Environ. Hyg., 4(6), 448-466, 2007.
- [7] N. Srinivasan and G. S. Tendolkar. Proposed pilot plant for production of sintered Beryllium oxide from beryl ore, Proceedings of the Symposium on Pilot Plants in Metallurgical Research and the Development (National Metallurgical Laboratory, Jamshedpur), Paper No 14, page 1-6, 15-18 February, 1960.
- [8] S. D. Soman and P. R. Kamath. Toxicity and handling hazards of Beryllium, Report No. AEET/HP/SM/7, BARC, 1960.
- [9] C. V. Sundaram, C. M. Paul, B. P. Sharma, J. S. Nair, S. Saha, Pilot plant for production of beryllium and copper-beryllium alloys, Key Engineering Materials, 8, 251-271, 1985.
- [10] www.dae.gov.in/writereaddata/publ/saga/vol2/pdf2/Chapter%20-%202004.pdf
- [11] www.barc.gov.in/div/67_532.html
- [12] www.aerb.gov.in/images/PDF/Atomic-Energy-Act-1962.pdf

Academic Programs

13



Certification Courses on Radiation Safety

Valedictory of 59th Dip.R.P. course and inauguration of 60th DipRP course.

Address by Dr. Ajit Kumar Mohanty, Director, BARC. On the dias: Dr. S. D. Sharma, Head, MPS, RP&AD, Dr. D. K. Aswal, Director, HS&E Group, BARC and Dr. B. K. Sapra, Head, RP&AD (from left to right).

Dr. B. K. Sapra

bsapra@barc.gov.in

Introduction

Ionising radiation and radioisotopes are extensively used in the field of medicine, industry, agriculture and research for the societal benefit. Atomic Energy Act, 1962 by the Government of India, empowers Department of Atomic Energy (DAE) to promote safe use of ionizing radiation and radioisotopes for peaceful purposes. Hence, it is necessary that radiation sources are handled by the trained personnel with adequate knowledge in radiation safety and the certified personnel will ensure radiation safety for members of public, radiation workers, patients, and the environment. Atomic Energy Regulatory Board (AERB) is responsible to ensure the use of ionising radiation and nuclear energy in India does not cause undue risk to the health of people and the environment. Radiation Protection Rules (2004) and Safety Standards and Codes published by AERB for various applications emphasizes the mandatory requirement of trained and certified personnel in institutions handling radioisotopes.

Radiological Physics and Advisory Division (RP&AD), BARC is authorized by AERB for conducting various certification courses on radiation safety related to medical, industrial and research applications of ionizing radiation. The syllabi of various radiation safety training courses were approved by AERB in 2012 (AERB/RF/Training-Syllabi/2012). Recently, the syllabi have been revised in 2021 with an addition of few new courses. The syllabi describe the eligibility criteria, course content, course duration, examination pattern, passing criteria and reappearance for examination. RP&AD also conducts one-year post M.Sc. Diploma in Radiological Physics under the aegis of HBNI.

Post M. Sc. (Physics) Diploma in Radiological Physics

RP&AD is conducting the one-year post M.Sc. Diploma in Radiological Physics from 1962. Currently, 60th course is underway and will be completed by September 2023. Till 2006, this course was affiliated to University of Bombay and from 2007 it is conducted under the aegis of Homi Bhabha National Institute (HBNI), Mumbai. So far about 1096 candidates have successfully completed the course and majority of them are performing exceptionally well in India and abroad. Total allocated seat for this course is 25 (non-sponsored) plus 5 (sponsored).

The eligibility for admission to Dip.R.P. course is M.Sc. (Physics) with aggregate marks not less than 60%. The candidate should also have undergone B. Sc. course majoring in Physics and the aggregate marks shall not be less than 60%. The selection process of non-sponsored candidate included two steps, (i) Written test for screening, and (ii) Interview. Sponsored candidates are selected by interview only. There is no reservation of seats in admission, however, OBC, SC/ST, physically challenged and sponsored candidates are given relaxation in upper age limit by 3, 5, 10 and 10 years, respectively. Non-sponsored candidates are paid a monthly stipend of Rs. 25,000/- for 12 months whereas sponsoring institute takes care of the expenditures of sponsored candidates.

Dip.R.P. is an important programme of DAE to provide adequately qualified manpower for various institutions/facilities in the country including AERB and DAE establishments. The syllabus of Dip.R.P. course consists of

topics related to medical, industry and research applications of radiation. The course consists of about 430 lectures and 32 laboratory exercises. Field training is provided at TMH, RMC, AERB and various Divisions of BARC over the eight weeks. The facilities available at BARC, experienced faculty of DAE and therapeutic facilities available at TMC provide a model support system for the Dip.R.P. course. The knowledge assessment is done through written examination and viva-voce at the end of each semester (total two semesters). The knowledge acquired during 3 weeks visit to clinical facilities of RMC and TMC is evaluated through the student seminar. This Diploma course is perceived as a benchmark by medical physics community in the country and it has produced many eminent medical physicists practicing in India and abroad.

The Dip.R.P. qualified candidates are eligible to work as clinical medical physicist in the hospital on successful completion of one-year medical physics internship at AERB-recognized radiotherapy centres in the country. These candidates are also eligible for nomination as Radiological Safety Officer (RSO) in medical, industrial and research institutions. However, the working as clinical medical physicist, candidates shall undergo one-year medical physics internship. Over the years, there has been an increase in the number of medical radiation facilities in the country and hence there is an increased demand of Dip.R.P. qualified candidates.

Certification Courses on Radiation Safety

RP&AD conducts various short-term certification courses on radiation safety that are mandated by AERB either by itself or in association with governmental or non-governmental organizations for personnel from medical, industrial and research institutions. RP&AD also conducts certification courses for different government agencies such as Ministry of Defence, Ministry of Home Affairs and Customs House and Ports. For all these courses, the certification is done by RP&AD through evaluation as stipulated by AERB. The list of courses approved by AERB/BSC and duration of each course is given in Table 1. During the period 2017-2022, 209 courses were conducted and 5168 candidates were certified.



Fig.1: 59th & 60th batch Dip.R.P. course students with Dr. Ajit Kumar Mohanty, Director, BARC.

Sr. No.	Title of certification courses on radiation safety	Duration
1.	RSO Certification in Radiation Processing Facilities (Gamma and Electron Beam)	6 weeks
2.	Radiation Safety Certification of Operators for Radiation Processing Facilities (Gamma and Electron)	3 weeks
3.	Training cum Certification Course on Radiation Safety for Industrial Radiographer	9 days
4.	RSO Certification for Nucleonic Gauges and Well Logging Applications	7 days
5.	RSO Certification for Radiological Calibration Laboratories (RSO-RCL) - Radiation Monitoring Instruments and Personnel Monitoring Badges	10 days
6.	RSO Certification for Gamma Irradiation Chamber (Category-I Irradiator)	7 days
7.	RSO Certification for Research, Radiotracer and Column Scanning Applications of Ionizing Radiation	7 days
8.	RSO Certification for Scanning Facilities	7 days
^a 9.	RSO -NM Certification for DMRIT /M.Sc. (NMT)/DRM Nuclear Medicine courses conducted by Universities /Institutions	Only Certification
^a 10.	RSO - Med certification for M.Sc. (Med. Phy.)/DRP Courses conducted by Universities	Only Certification
11.	RSO Certification for Service Engineers/QA Service providers in Diagnostic Radiology (RSO- QADXE)	11 days
12.	Radiation Safety Certification for Service Engineers of Radiotherapy Equipment (RS- SRE)	7 days
13.	RSO Certification for Industries handling Naturally Occurring Radioactive Material (RSO-NORM)	7 days
14.	Radiation Safety Certification for Suppliers of Consumer Products, Analytical Equipment, Small Activity Sources, and Equipment Containing Small Activity of Sources	5 days
15.	RSO Certification for Gas Mantle Manufacturing Facility	5 days
16.	Radiation Safety Certification for Personnel in Medical Cyclotron Facility	4 weeks
^b 17.	RSO Certification for NDRF Personnel	7 days
^b 18.	RSO Certification for Defence Personnel	7 days
^b 19.	Training cum RSO Certification Course on Radiation Safety Aspects of Flash X-ray and Neutron Generator Facilities	10 days

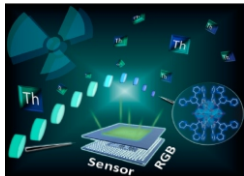
Sr. Nos. 1 – 16 (AERB approved courses)

a : Courses conducted by Universities and RSO certification done by RP&AD.

b : Devised jointly by RP&AD and BARC Safety Council (BSC) and approved by BSC, BARC

Reporting on latest global developments in health, safety and environment

Radiation detection based on a fluorochromic and piezochromic nanocluster

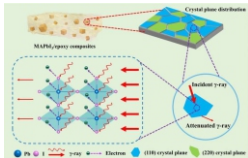


Th-101 is a Colorimetric ionizing-radiation-responsive material.

Integration of thorium cation and photoresponsive terpyridine carboxylate ligand gives rise to a thorium nanocluster, Th-101, which displays fluorochromic response and unprecedented piezochromic behavior among all actinide materials. The emission color of Th-101 exhibits a gradual transition from blue to cyan to green upon irradiation with accumulated dose, which renders colorimetric dosimetry of ionizing radiation based on a red-green-blue (RGB) concept.

Dong and Fang. Light: Science & Applications (2023) 12:8

Radiation Shielding: MAPbI3/epoxy composites exhibit superior performance



Metal halide perovskites (MHPs) have been increasingly gaining attention as high performance, yet low cost radiation shielding materials. MAPbI₃ –Epoxy composites prepared by a simple method, employing a crystal plane engineering strategy, showed a high shielding performance against gamma rays in terms of a larger mass attenuation coefficient and linear attenuation coefficient compared to commonly used shielding materials. The long term stability of this composite with respect to moisture, irradiation and temperature needs to be studied for its possible diverse applications. Futuristically, these may serve as lead free MHPs for reduced environmental toxicity.

Dong and Fang. Light: Science & Applications (2023) 12:8

Synthetic Hibernation: A tool to mitigate radiation induced toxicity?



In the recent times, hibernation has been proposed as possible mitigation against radiation based on studies that show that hibernators are resistant to acute high dose rate radiation exposure. Artificially induced hibernation, also termed as synthetic torpor was successfully demonstrated in rats with the results showing increased radio resistance. In an interesting study in arctic ground squirrels, it has been shown that radiation-induced genomic instability is avoided during torpor-arousal-cycles, by preventing DNA damage and promoting efficient DNA repair. Understanding this adaptive mechanism will be highly promising for future human space missions. Also understanding the mechanism of muscle preservation by hibernators might help astronauts to keep their strength and physical health.

Anggraeini Puspitasari, Matteo Cerri, Akihisa Takahashi, Y. Yoshida, K. Hanamura, and Walter Tinganelli. Life. (2021), 11(1): 54.

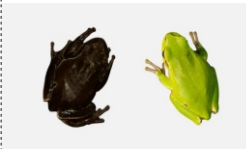
Blue carbon as a natural climate solution



The Blue Carbon concept was introduced as a metaphor aimed at highlighting that, coastal ecosystems, in addition to terrestrial forests (coined as Green Carbon), contribute significantly to the organic carbon sequestration. Oceans provide a long term, nature-based solution to reduce CO₂ concentrations in the atmosphere. This is done by carbon that can be stored long term in the soils and vegetation of marine ecosystems, such as mangrove forests, salt marshes and seagrass meadows. Using natural and artificial radionuclides to measure the rates and origin of sediment accumulation, one can determine accurate carbon storage rates – known as carbon sequestration in vegetated coastal areas, allowing scientists to determine which Blue Carbon habitats are more efficient carbon sinks.

P. Macreadie, M. Duarte de Paula Costa, T. B. Atwood, C. M. Duarte. Nature Reviews Earth & Environment, 2021, 2(12)

Unusual evolution of tree frog populations in the Chernobyl exclusion zone



More than ten generations of frogs have passed since the Chernobyl accident and a classic process of natural selection explains why the dark frogs are now the dominant type for the species within the Chernobyl Exclusion Zone. It is apparent that frogs with darker coloration, also present at the time of the accident, would have been favored by the protective action of melanin. Melanin's protective role extends to ionizing radiation too, as it has been shown with fungi. Melanin absorbs and dissipates part of the radiation energy. In addition, it can scavenge and neutralize ionized molecules inside the cell, such as reactive oxygen species. The dark frogs would have survived the radiation better and reproduced more successfully. Incidentally, Chernobyl has become a refuge for wildlife 3 decades after the nuclear accident. The diversity of wildlife has been documented by the TREE project of UK's centre for Ecology and Hydrology.

Clément Car, André Gilles, Olivier Armant, Pablo Burraco, Karine Beaugelin-Seiller, Sergey Gashchak, Virginie Camilleri, Isabelle Cavalié, Patrick Laloï, Christelle Adam-Guillermin, Germán Orizaola, and Jean-Marc Bonzom. Evol Appl. 2022 15(2): 203–219.

From Vision to Realization

The Success Story of 'APURVA'

(From Left to Right): Shri K.N. Vyas, Chairman, AEC & Secretary, DAE, Shri V.K. Mehra, Former Director, RPG and Dr. A.K. Mohanty, Director, BARC present for an event organized in BARC in April 2023.

Vivek Shrivastav, Harish, Rajit Kumar, P.K. Mishra and Joe Mohan

Reactor Projects Group, Bhabha Atomic Research Centre, Trombay - 400 085, India

An installation erected near Engineering Hall-11 BARC, christened APURVA, which stands for “Advanced **P**urified Reactor Vessel **A**lloy”, was inaugurated on 29th April, 2023 by Shri K.N. Vyas, Chairman, AEC & Secretary, DAE, in the august presence of Dr. A.K. Mohanty, Director, BARC. Shri V.K. Mehra, former Director, Reactor Projects Group, who had championed the vision of self reliance in nuclear reactor technologies for Compact Light Water Reactors (CLWRs), was the guest of honour for this special event. The event was hosted by the Reactor Projects Group (RPG), lead by Shri Joe Mohan, Associate Director, RPG.

The APURVA installation, built for inspiring the present and future generations of young scientists and engineers, symbolizes the successful indigenous development of reactor pressure vessel (RPV) forging technology for large-sized commercial Pressurized Water Reactors (PWRs). The project was executed with collaborative efforts of BARC and M/s. L&T Special Steels and Heavy Forgings (LTSSHF), Hazira. The forged steel developed through these efforts has been christened “APURVA” (अपूर्व), meaning “unprecedented”, or, “first time ever”.

Historical Background

The foundation stone for indigenous development of RPV forging technology in the country was laid down by Shri V.K. Mehra former Director of RPG and his team, way back in 1984, when the first attempt of manufacturing RPV forgings was undertaken in association with Heavy Engineering Corporation (HEC), Ranchi. The first breakthrough was achieved with the successful development of smaller size RPV forgings for Compact Light Water Reactors (CLWRs) in the year 2000.

Development of APURVA grade Steel Forgings

The main challenges associated with large size RPV forgings are, relatively higher thicknesses, maintaining the desired chemistry and purity level, controlling chemical segregation, achieving a favourable microstructure and high mechanical properties over the entire section thickness, along with good weldability and freedom from hydrogen induced micro-cracks. Realizing that this work called for special technological know-how to be developed through collaboration between R&D and the industry, a development contract was signed with LTSSHF in the year 2015 (Project XII-N-R&D-57).

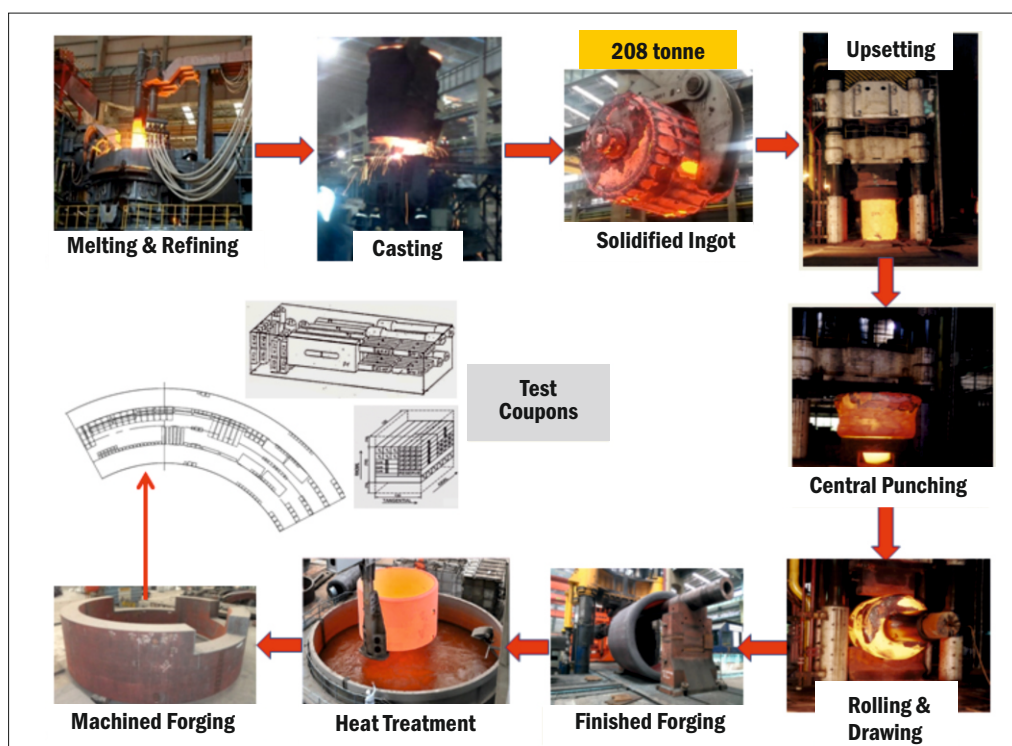


Fig.1: Schematic of Manufacturing Technology of APURVA Steel Forgings

Manufacturing Technology

A mix of specially selected pure steel scrap and direct reduced iron (DRI) are melted in a 100 t Electric Arc Furnace (EAF) followed by refining and alloying additions in a 100 t Ladle Furnace (LF). The chemistry adjusted molten steel is then degassed in a 100 t Vacuum Degassing (VD) unit operating at a vacuum of < 1.0 torr to remove hydrogen. Two such 100 t melts, after degassing, are cast sequentially in to a 200 t ingot mould placed inside a Vacuum Ingot Casting (VIC) set up under a vacuum of < 1.0 torr. This is followed by forging, heat treatment, machining and testing as shown in Fig.1.

Research & Development

Large shell & ring forgings (inner diameter ~ 4.0 m) of different thicknesses, 340 mm, 550 mm & 750 mm, were manufactured successively, with lab scale experiments, industrial scale trials and extensive testing, to progressively improve and optimize the manufacturing processes. Optimum chemical composition and technological process parameters were evolved for each forging. Cooling rates achievable during quenching treatment were determined by analysis for each thickness and validated through large scale quenching experiments.

Heat treatment, which largely governs the microstructure and mechanical properties, was developed specifically for each thickness. Reactor Projects Group developed an innovative technique for laboratory scale physical simulation of heat treatment of the actual forging, utilizing the facilities and support from the Atomic Fuels Division. The heat treatment parameters were optimized using this technique through a large number of lab-scale simulations (~300 nos., involving ~3000 test specimens) carried out at LTSSHF, followed by industrial-scale validation before implementing on the prototype forgings. Materials Group provided their laboratory facilities for extensive microstructural characterizations.

Results

The forgings developed were rigorously tested for ultrasonic soundness, chemical homogeneity, through-thickness mechanical properties, fracture toughness, low cycle fatigue, thermal endurance and weldability. The quality and properties of the forgings developed meet the acceptance norms of various international codes with high margins (see Fig.2 for typical test results). The project was concluded successfully in 2020.

Salient Features of APURVA Steel Forgings

- Si-modified Mn-Mo-Ni Low Alloy Steel grade, equivalent to KTA 20MnMoNi55 and ASME SA508 Gr3 Cl1
- Ultra-clean Steel P<0.004%, S<0.002%, Cu<0.05%, As, Sb, Sn<0.005% each
- Hydrogen ≤ 1.0 ppm
- RTNDT ≤ -25 °C for 340mm thick forging; ≤ -12 °C for 750mm thick forging
- High strength and toughness throughout section thickness
- High resistance to irradiation and thermal embrittlement



340 mm thick Shell Forging for Nozzle Area of RPV-OD4900 x ID4220 x 2000L



750 mm thick Ring Forging for Flange Area of RPV-OD5300 x ID3800 x 700L

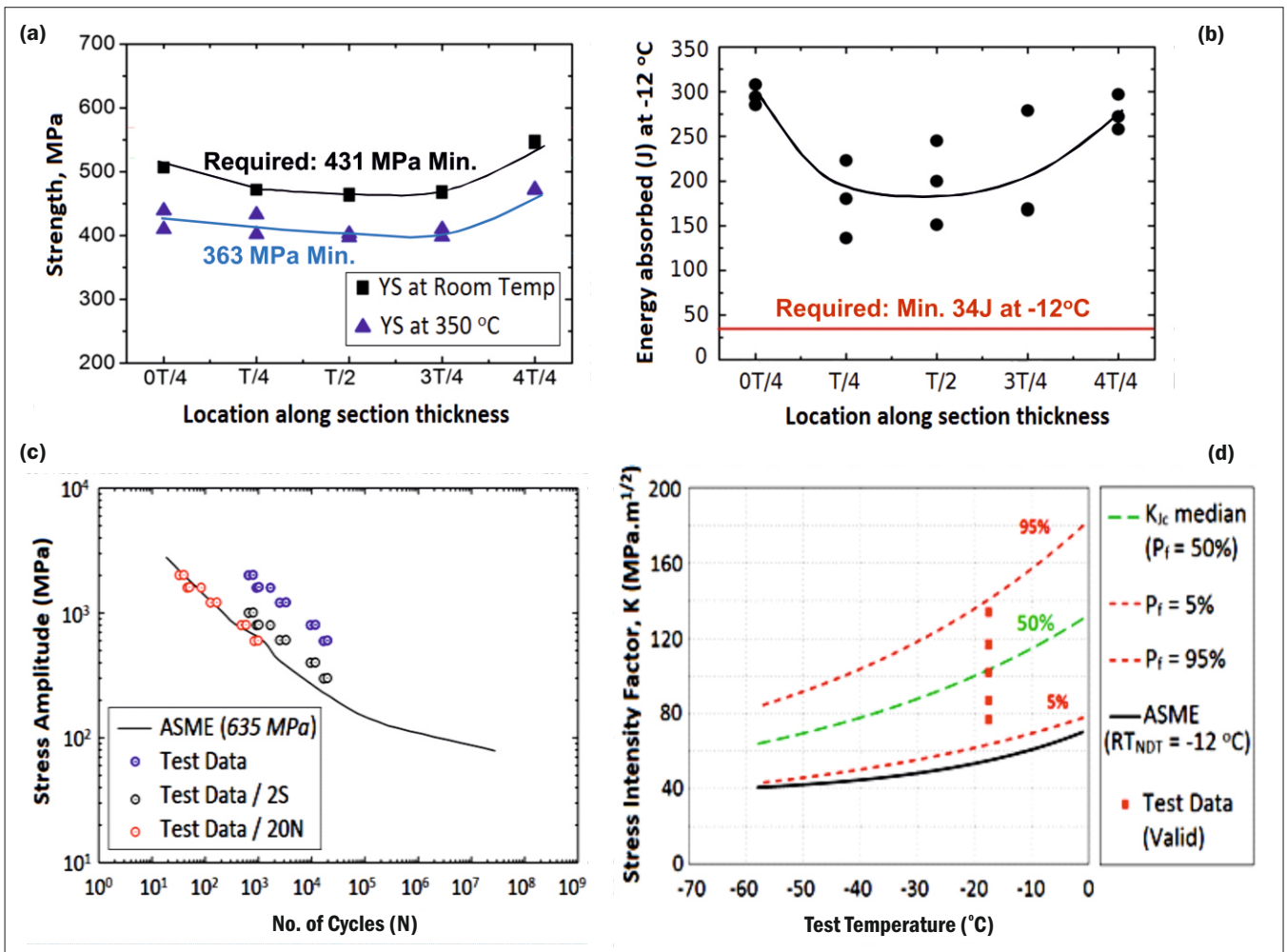


Fig.2: Typical test results of 750 mm thick APURVA grade Forging, (a) Yield strength, (b) Impact toughness, (c) Low cycle fatigue test as per ASTM E-606, and (d) Fracture toughness test as per ASTM E-1921.

Conclusion

The technology developed can be used for manufacturing of thick steel forgings for construction of RPV, Steam Generators and other such pressure retaining equipment of nuclear power plants of PWR, PHWR or SMR types for design temperatures of up to 350°C. The APURVA installation is built from the remnants of the 340 mm thick and 750 mm thick prototype forgings, to commemorate the achievement of this significant technological milestone in LWR technology. It also stands testimony to BARC's commitment towards the vision of self reliance through persistent efforts in partnership with the industry.

Tapping the Potential of Ionizing Radiations

- For synthesis of nanomaterials with biomedical and sensing applications

Apurav Guleria and S. Adhikari

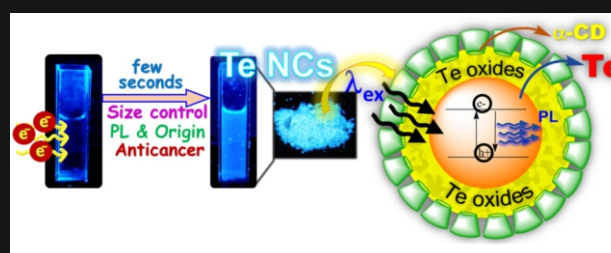
Considering the impending applications of nanomaterials, it is crucial to develop a sustainable and eco-friendly protocol for their synthesis with minimal use of corrosive, flammable reagents and toxic/hazardous chemicals (i.e., precursors, reducing and capping agents). In this perspective, ionizing radiation (e.g., e-beam, gamma-ray) assisted synthesis of nanomaterials is a well-known technique, and do not involve any stringent experimental conditions. More so, this strategy offers many advantages, such as time efficient, scale-up production, one-step approach and *in situ* generation of reducing species (i.e., solvated electron, e_{sol}^-). Additionally, the nucleation and growth processes of the nanoparticles can be conveniently controlled by the suitable choice of the experimental conditions such as absorbed dose, dose rate, host matrix, solvent environment, and capping agent.

Taking account of these advantages, radiation-chemical approach is being used to prepare nanomaterials with unique features which otherwise require complicated synthetic procedures in conventional routes. Some of the highlights of the recent works pertaining to radiation-assisted synthesis of nanomaterials are mentioned below.

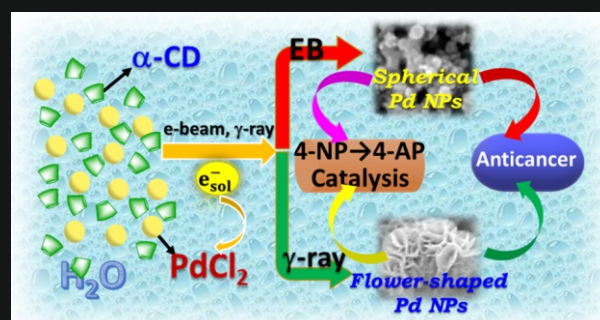
For the first time, blue light emitting amorphous Si-based nanomaterials were prepared in aqueous media using radiolytic method. It was revealed that the nanomaterials were formed via hydroxyl radical ($\cdot\text{OH}$) induced reaction. Usage of nanomaterials was demonstrated in anti-counterfeiting & fingerprinting. Further, post-functionalization with glutathione, these nanomaterials exhibited tumor selectivity at lower pH along with cell labelling capabilities and propensity to localize at the nucleus.

Te-based nanomaterials have found an enormous interest in biomedical applications recently. However, anisotropic property of Te makes it difficult to control phase and morphology of its nanomaterials. Radiolytic approach with high dose rate facilitated formation of photoluminescent size controlled, amorphous Te-nanocomposites (NCs). Formation of NCs proceeds through a solvated electron driven reaction. Remarkable concentration-dependent killing was observed only in the case of cancerous cells, while no such trend was seen in normal healthy cells.

The *in situ* generated solvated electrons were used for one-pot highly facile preparation of spherical and flower-shaped Palladium (Pd) nanoparticles (NPs) coated with cyclodextrin molecules. The nanomorphology varied considerably as a function of dose rate, wherein spherical-shaped nanoparticles NPs were formed in case of high dose rate electron-beam assisted synthesis, while nanoflakes self-assembled to form nanoflower-shaped morphologies in γ -ray mediated approach involving low dose rate. Implications of morphology control was observed from the superior catalytic and anticancer properties of flower-shaped Pd NPs as compared to spherical shaped ones. The interplay of dose rate along with soft matrix of molecular assemblies can facilitate morphology tuning of nanomaterials *vis-à-vis* their properties.



▲ Photoluminescent cyclodextrin coated tellurium nanocomposites.



▲ Ionizing radiation (EB and gamma-ray) mediated synthesis of α -CD coated Pd NPs with different morphologies.

(Dr. S. Adhikari, Outstanding Scientist, is currently heading Scientific Information Resource Division of BARC, Mumbai)



Dr. Apurav Guleria, Scientific Officer/F in Radiation and Photochemistry Division, Chemistry Group, BARC, works in the field of Radiation Chemistry and Nanomaterials. His research interests include radiation and photochemical studies of microheterogeneous media (microemulsions, room temperature ionic liquids, deep eutectic solvents) and ionizing radiation-assisted synthesis of nanomaterials with novel features for biomedical and sensing applications. He has published about 50 research articles in peer reviewed national and international journals. Dr. Guleria is a recipient of the "Young Scientist Award-2016" from the Department of Atomic Energy and the "Young Associate of Maharashtra Academy of Sciences (MASc)-2021."

THE SOURCE OF ENERGY FOR CREATION OF THE UNIVERSE

A new quantum-cosmological model

Biswaranjan Dikshit
bdikshit@barc.gov.in

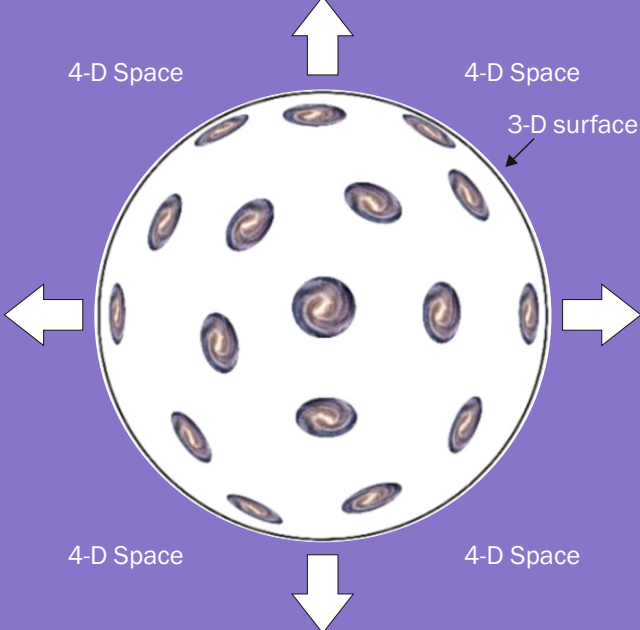
The law of conservation of energy is the most sacred law in the history of science as not a single experiment till date has reported violation of the law. Then, a natural question arises, what was the source of energy for creation of all the matter in the universe? (matter including the dark part is about $\sim 10^{54}$ kg). As per uncertainty principle, a quantum vacuum fluctuation can at most create energy of ~ 0.02 mg in a Planck time of $\sim 5.4 \times 10^{-44}$ s. To solve this problem, it has been proposed that the sum total of energy due to matter/vacuum and gravitational potential energy might be zero. This is possible as the sign of gravitational potential energy is negative, whereas that of other forms is positive. However, a mathematical proof for the zero-energy universe didn't exist yet.

In our recent paper [1] published in Canadian Journal of Physics, by quantizing the zero-point fields existing in the space, we have mathematically proved that the total energy of the universe could be zero right from the beginning of the universe and law of conservation of energy can be satisfied even during creation of the universe. A short description of the model and some additional merits as compared to standard inflationary cosmological model are given below.

To maintain isotropy of space, following the Einstein's model, we consider the universe to lie on the surface of a 3-sphere existing in a four-dimensional (4-D) space. Just like in a 3-D space, surface of a football (2-sphere) is two dimensional and isotropic, in a 4-D space, surface of a 3-sphere is three dimensional and isotropic. Even if our universe is closed, its spatial curvature cannot be detected by us as our space freely expands under gravitation (just as an observer freely falling in a gravitational field cannot detect the curvature of space-time). Since the space of our universe is closed and spherical, circumference must be integer multiple of wavelength of zero-point wave leading to quantization of the zero-point fields. So, counting all possible modes of zero-point field, we calculated the vacuum energy (or dark energy) to be, $u_{vac} = \frac{c^2 H^2}{4\pi G} = 5.2 \times 10^{-10} J/m^3$ which agreed well with the observational data. Thus, we solved the cosmological constant problem in which prediction for vacuum energy in standard cosmological model was $\sim 10^{123}$ times more than the observed value.

In addition, our new cosmological model theoretically predicts the matter energy density (including dark matter) of the universe to be, $u_{nonvac} = \frac{c^2 H^2}{8\pi G} = 2.6 \times 10^{-10} J/m^3$, which agrees well with the observation. But, modern inflationary cosmological model fails to theoretically predict the matter energy density. In the new model, ratio of dark energy to matter energy comes out to be equal to '2' irrespective of age of the universe. Thus, the new model explains the cosmic coincidence problem which questions why dark energy and matter energy are of the same order at present time. Standard Big-Bang model fails to explain the cosmic coincidence.

In our model, total energy density due to vacuum and matter comes out to be, $u = \frac{3c^2 H^2}{8\pi G}$ which is equal to the critical density required to explain the observed flatness of space. Thus, in contrast to conventional cosmological theory, our model doesn't need fine tuning or inflation field having a specific potential energy distribution to prove flatness.



The new quantum-cosmological model

Key highlights

- ▲ Overcomes the cosmological constant problem and cosmic coincidence problem.
- ▲ Satisfies the law of conservation of energy during creation of universe.
- ▲ Theoretically predicted dark (or vacuum) energy density, $u_{\text{vac}} = \frac{c^2 H^2}{4\pi G} = 5.2 \times 10^{-10} \text{ J/m}^3$
- ▲ Theoretically predicted matter energy density (including dark matter), $u_{\text{nonvac}} = \frac{c^2 H^2}{8\pi G} = 2.6 \times 10^{-10} \text{ J/m}^3$
- ▲ Explains flatness of space and predicts smallest possible wave length to be,
 $\lambda_{\text{min}} = l_p \sqrt{\pi/2} \approx 1.25 \times l_p \approx 2.0 \times 10^{-35} \text{ m}$ where l_p is Planck length

The mathematical treatment in the new model shows that magnitude of vacuum/matter energy (which is positive) and magnitude of gravitational potential energy (which is negative) can be exactly equal to each other resulting in zero net energy of the universe only if smallest wave length of zero-point field in space is taken to be $\lambda_{\text{min}} = l_p \sqrt{\pi/2} \approx 1.25 \times l_p \approx 2.0 \times 10^{-35} \text{ m}$ where l_p is Planck length. This minimum value λ_{min} bears significance in QED, quantum gravity and string theory as it gives an upper limit of momentum of any particle in nature. Thus, the zero-energy universe is mathematically possible and can lead to creation of the universe from empty space without violating law of conservation of energy.

To summarize, our new quantum-cosmological model not only satisfies the law of conservation of energy during creation of the universe but also correctly predicts the dark energy density, matter density and flatness of space.

Acknowledgements

Author is grateful to Archana Sharma, Director of Beam Technology Development Group, Bhabha Atomic Research Centre (BARC) and S. Kundu, Head, ATLAD, BARC for their encouragement and support during this research.

Reference

[1] Biswaranjan Dikshit, "A new cosmological model based on quantization of the zero-point field", *Canadian Journal of Physics*, 100, 218-225 (2022).



Dr. Biswaranjan Dikshit joined Laser & Plasma Technology Division, BARC in 1995 after passing out from the 38th batch of OCES (Electrical Engg.) program of BARC training school. He is presently working as Scientific Officer (H) and heads the Quantum Computing & Process Diagnostics Section, ATLAD, BARC. He is recognized as a Professor by Homi Bhabha National Institute, Mumbai. Dr. Dikshit has published more than 40 papers in international journals. He is a recipient of DAE Young Technologist Award, Outstanding Doctoral Thesis award from HBNI and Outstanding Reviewer Award from European Journal of Physics, IOP Publishing, London. His current fields of interest include Ion optics, Electrodynamics, Quantum physics and Cosmology.

Reports from conferences, theme meetings and workshops



SAAR-2023

Dr. D.K. Aswal, Director, HSEG, BARC speaking at the theme meeting SAAR-2023. Present on the dais (from right) are Dr. S. S. Bajaj, Former Chairman, AERB and Dr. B.K. Sagra, Head, RP&AD, BARC.

Theme meeting on

Severe Accident Aerosol Research – Investigations & Directions

Health, Safety and Environment Group, BARC organized a two-day theme meeting on “Severe Accident Aerosol Research – Investigations and Directions” (SAAR-2023) during March 20-21, 2023 at CT&CRS Auditorium, Anushaktinagar, Mumbai. The meeting was attended by about 50 participants from various DAE units and IITs, and was sponsored by Board of Research in Nuclear Sciences (BRNS), Department of Atomic Energy (DAE). Topics of the meeting included ongoing activities and the near-future insights on severe accident aerosol research in the context of Indian reactors.

Presentations from stakeholders from nuclear aerosol facilities viz., Nuclear Aerosol National Test Facility at RP&AD, BARC, National Aerosol Facility at IIT Kanpur and High Temperature Aerosol Facility at IIT BHU emphasized the importance of large scale experimentation and the associated interpretations. Discussions were held on severe reactor accident aerosol research aspects for existing and futuristic reactor designs, recent developments in experimentation and modelling and the ongoing work at experimental facilities. It was concluded that gaining predictive power of aerosol behavior ultimately helps to get a more reliable prediction of the potential radiological source term.

A panel discussion during the concluding session was attended by experts from AERB, DAE, BARC and NPCIL, which focused on the linkage of the progress made so far and the need for the future. Members, during the panel discussions, provided their inputs on different aspects of roadmap for the future of research in this direction. This included the need to continue research at laboratory as well as facility scale, to perform validation of in-house developed codes and to arrive at database essential for assisting the regulators. Overall, the meeting provided a directional flow for severe reactor accident related aerosol research activities of national importance and for international recognition.

Reports from conferences, theme meetings and workshops



AdMet-2023

8th National Conference on Advances in Metrology

Health Safety and Environment Group, Bhabha Atomic Research Centre (BARC), Trombay in association with Metrological Society of India, New Delhi, Institute for Design of Electrical Measuring Instruments (IDEMI), CSIR-National Physical Laboratory, New Delhi and National Accreditation Board for Testing and Calibration Laboratories, Gurugram organized a workshop-cum-national conference on “Advances in Metrology” (AdMet-2023) during March 23-25, 2023 at DAE Convention Centre, Anushaktinagar, Mumbai. The focal theme of the workshop and the conference was “Radiation Metrology for Nuclear Medicine & Industries” and “Metrology for Science and Industrial Growth”, respectively.

The main objective of the Admet Series Conference was to provide a common landing platform for metrologists, technocrats, researchers and students of various NMI's, laboratories and institutes to participate and share their knowledge and experience, identify the thrust R&D areas and foster collaborations with fellow scientists in the domain of metrology. AdMet-2023 saw participation of experts, researchers, students, technocrats, bureaucrats, manufacturers, vendors, suppliers etc. Demonstration of radiation technologies, application of nuclear medicines & radioisotopes in all industrial sectors was the new dimension of the conference. More than 250 delegates from various institutes and industries participated in this maiden conference on radiation metrology. Two hundred and eight original research works were presented at the conference. 10 best papers were awarded by the Springer India and MSI. The “Handbook of Metrology and Application”, authored by Dr. D.K. Aswal et al. of BARC and published by Springer nature, was released during the conference.

11 invited talks were delivered in the pre-AdMet workshop and 29 invited talks were delivered during the conference. The invited talks covered a wide range of topics ranging from metrology in testing and calibration laboratories, healthcare, medical, pharmaceutical and clinical devices, human machine interface (HMI) and internet of things (IoT), radiation metrology, environmental metrology, digital transformation, electrical, mechanical to electronics and digital metrology. The major thematic area of discussion included new development on metrological aspects of accreditation and certification, industrial and legal metrology, quality assurance and quality control in metrology, uncertainty and traceability, development of reference material, process control instrument, renewable sources and environmental metrology.

Photo caption: Key dignitaries attending the conference on Advances in Metrology (AdMet-2023) share the dais. Conference chief guest Shri. R.K. Singh, Secretary, Ministry of Consumer Affairs, Government of India (seen in the background) participated in the event through virtual mode. Inset: Dr. D.K. Aswal, Director, HSEG, BARC (2nd from right) and other eminent individuals released the Handbook of Metrology and Application during the inaugural day.

Reports from conferences, theme meetings and workshops



5th Asian Congress of Radiation Research

The 5th Asian Congress of Radiation Research (ACRR 2022) was organized by the Bio-Science Group, Bhabha Atomic Research Centre (BARC) in association with the Society for Radiation Research-India (SRR-India) and Asian Association for Radiation Research (AARR) at DAE Convention Centre during November 17-20, 2022.

The program of the 5th ACRR included 22 scientific sessions comprising a special session of panel discussion on Linear-No-Threshold (LNT) model of radiation protection, fifteen plenary lectures, five special lectures, one eye-opening lecture, six AARR award recipient lectures, 38 invited talks and proffered oral and poster sessions.

The proceedings of the entire program have been covered in detail in a souvenir and a special issue of Journal of Radiation and Cancer Research, which were released by Dr. Ajit Kumar Mohanty, Director, BARC during the inaugural event. About 300 delegates from several reputed institutes of India and abroad including Canada, Germany, Japan, Republic of Korea, The Netherlands, and the United States of America have attended the 4-day program.

Many overseas eminent scientists in the field of Radiation Research/ Radiobiology namely Prof. Yoshiya Shimada (President, IARR and Director, Institute of Environmental Sciences, Japan), Prof. Gayle Woloschak (Northwestern University, USA and Editor-in-Chief, Intl. J. Radiation Biology), Prof. Satoshi Tashiro, (Director, Research Institute for Radiation Biology and Medicine, Hiroshima University, Japan), Prof. George Iliakis, (University of Essen, Germany), Prof. E. J. Calabrese (University of Massachusetts, USA), Dr. Zhanat Carr (WHO, Geneva), Dr. Nils Cordes (Onco Ray National Centre, Dresden, Germany), Dr. Hans Crezee (University of Amsterdam, The Netherlands), Prof. Sung-Kee Jo (KAERI, R. P. Korea), Dr. Sharmila Bhattacharya (NASA, USA) and Dr. Rebecca J. Abergel (Lawrence Berkeley National Laboratory, Berkeley, USA), Dr. Madan Rehani (MIT, USA) have presented their research work in the congress. Prof. Gayle Woloschak has delivered third SRR AR Gopal Ayengar Oration Lecture during the conference.

Senior Scientists from various Indian Institutes/Universities have also delivered their invited talks namely, Dr. Avinash C. Pandey (Director, IUAC, New Delhi), Dr. Sandeep Basu (RMC-BARC, Mumbai), Dr. Sanjay Gupta (ACTREC, Mumbai), Dr. Teerthraj Verma (RMLIMS, Lucknow), Dr. Krishna Sharan (MAHE, Manipal), Dr. Damodar Gupta (INMAS-DRDO, New Delhi), Dr. Tapas Das (BARC, Mumbai), Dr. S. D. Sharma (RPAD, BARC), Dr. Hema Rajaram (MBD, BARC), Dr. Birajalaxmi Das (RB&HSD, BARC), Dr. Bhavani Shankar (RB&HSD, BARC) and Dr. Anu Ghosh (RB&HSD, BARC). A full list of speakers of 5th ACRR is available in Oct-Dec 2022 issue of *Journal of Radiation and Cancer Research* available at www.journalrcr.org. All the abstracts of the 5th ACRR have also been published in this issue.

Reports from conferences, theme meetings and workshops



Participants of the one-day workshop pose for a group photograph on the sidelines of the event at Multipurpose Hall in Training School Hostel facility in Anushaktinagar.

Workshop

on BARC Technologies for Swachhata Mission

A one-day workshop focussed on BARC technologies available for deployment in activities of *Swachhata Mission* was organized by Bioscience Group on 16th February 2023. Around 100 delegates participated in the workshop offline, and more than 100 students and delegates took part in it through online mode. Dr. Tapan Kumar Ghanty, Director, Bioscience Group, BARC briefed the participants about the background of the workshop, which was started in 2019. Dr. A. P. Tiwari, Director, Knowledge Management Group, BARC was the program chief guest.

The workshop was conducted in two sessions – technical presentations followed by field visit to working facilities. The technical session comprised presentations on Nisargruna technology for processing different types of biodegradable waste (by Dr. S. T. Mehetre); Composting technology for dry leaves and garden waste management (by Dr. Poulomi Mukherjee); Waste water treatment process by SBR technology (by Dr. Y. V. Nancharaiyah); Work on Sludge Hygienisation Research Irradiator facility at Vadodara (by Dr. Naresh Kumar); Plasma incineration technology for solid waste disposal (by Dr. S. Ghorui); Electron beam technology for waste water treatment (by Dr. Asavari Dhavale); Technologies for clean drinking water (by Dr. Soumitra Kar); Role of radiation technology for enhancing shelf life of food commodities (by Dr. Sudhanshu Saxena); Chemical waste disposal and legacy waste management (by Dr. R. K. Singhal). The technical session was chaired by Dr. S. Gautam, Head, Food Technology Division, BARC.

In the second session, participants visited various waste processing sites near Anushaktinagar, including BARC Training School Hostel and Homi Bhabha Centre for Science Education. Technologies relevant to *Swachhata Mission* were demonstrated for the benefit of the participants. It must be noted that the Swachhata technologies are being promoted in the incubation program of BARC for the benefit of young entrepreneurs.

This page intentionally left blank

This page intentionally left blank



BARC Central Library

Edited & Published by

Scientific Information Resource Division

Bhabha Atomic Research Centre, Trombay, Mumbai-400 085, India

BARC Newsletter is also available at URL:<https://www.barc.gov.in>